PRE-CLINICAL IN VIVO AND IN VITRO ASSESSMENT OF HEMOSTATIC EFFECTS OF CONTINUOUS-FLOW VENTRICULAR ASSIST DEVICES

BY

DANIEL CRANDALL

DEPARTMENT OF BIOMEDICAL ENGINEERING

Submitted in partial fulfillment of the
requirements for the degree of
Doctor of Philosophy in Biomedical Engineering
in the Graduate College of the
Illinois Institute of Technology

Approved _____
Adviser

Chicago, Illinois
07/2011

ACKNOWLEDGEMENT

To my advisors I owe my deepest gratitude: Dr. Vincent Turitto, Dr. Constance Hall, and Dr. Setsuo Takatani. Throughout my doctoral studies each has proved invaluable. I thank Dr. Turitto for welcoming me as an advisee with guidance and support. I thank my committee: Dr. Eric Brey, Dr. Georgia Papavasiliou, and Dr. Jialing Xiang. It is their expertise that helped overcome the many obstacles of this endeavor. I thank Dr. Megan Francis-Sedlak for her inspired assistance and boosts of momentum. For the many hands-on learning opportunities he afforded, I thank Dr. Paul Fagette.

The work presented in this thesis would not have been possible without the assistance of my colleagues at the Illinois Institute of Technology and the Tokyo Medical and Dental University: Dr. F. Zaman, Y. Lee, Shuo Yang, Jeff Larson, and Michael Turturro; and Dr. E. Nagaoka, Dr. T. Kitao, Dr. T. Kimura, H. Shibasaki, Y. Anzai, R. Sakamoto, S. Machida, S. Ota, Y. Yokoyama, D. Sakota, H. Osawa, and N. Yokoyama. It is through their efforts that I have learned the lessons and reaped the benefits of teamwork. The fruitfulness of my Japanese adventure is largely due to the generosity of the Shibasaki family of Tokyo.

It is my intent that this body of work be the tangible validation of the values constructed within me by my family. To my mother and father who have provided me with opportunities; to my partner who has helped me improve myself in countless ways; to my grandparents to whom I live up to; and to my sisters who have provided warmth and love – thank you. Contributions from others of time, knowledge, and imagination fueled this accomplishment. I am in their debt.

TABLE OF CONTENTS

LIST OF TABLES

LIST OF FIGURES

LIST OF FIGURES

LIST OF FIGURES

LIST OF SYMBOLS AND ABBREVIATIONS

Symbol	Definition
p	p-value (Statistical Significance)
[P]	Concentration of Particle of Interest
E_t	Number of Events from the Test Sample
E_p	Number of Events from Control Particles
N_p	Lot Specific Number of Particles per 50µL
V_t	Initial Volume of Test Sample
M	Molar (Concentration)
V_x	Velocity in X-direction
V_h	Velocity of Moving Wall for Couette Flow
y	Variable in Height Direction for Couette Flow
h	Height of Gap in Couette Flow
τ	Shear Stress
µ	Viscosity (non-prefix)
R	Specific Radius
NIH	Normalized Index of Hemolysis
ΔfreeHb	Change in Plasma Free Hemoglobin (g/L)
Hct	Hematocrit (%, Volume Percent Erythrocytes)
Q	Flow Rate
T	Sampling Time

ABSTRACT

Heart failure results in significant morbidity and mortality for those afflicted. The current gold standard treatment is allogenic heart transplantation, however insufficient supply of donor organs limits the effectiveness of this treatment to ideal candidates. This has led to interest in mechanical circulatory support. The most recent generation of devices are smaller, continuous-flow devices with increased durability compared to their predecessors. However, these new devices exhibit increased rates of hemostatic events – both thromboembolic and hemorrhagic. This thesis details an *in vivo* evaluation of hemostatic parameters in a bovine animal model to evaluate the effect of the ventricular assist device (VAD), and compares these results to what has been seen clinically. Most importantly this thesis has found that bovines do not experience pathophysiologic degradation of high molecular weight Von Willebrand Factor (VWF) as a result of VAD placement, whereas this complication is well documented in humans. This is due to a decreased sensitivity to shear stress induced cleavage of VWF in bovines when compared to humans, as demonstrated in this thesis. Due to the inability to replicate clinical conditions with the bovine animal model, this thesis develops an alternative methodology using an in vitro flow loop using the same human donor blood on all pumps tested. This methodology eliminates the need for interspecies extrapolation; allows for more direct comparisons by eliminating donor variation; and is both cheaper and faster than animal models. This methodology could provide an invaluable option for evaluating hemostatic effects of various pump design parameters.

CHAPTER 1

INTRODUCTION

Heart failure affects over five million Americans resulting in mortality for approximately 300,000 Americans yearly. Direct cost estimates are over 35 billion dollars per year [51]. Cardiac transplantation is the only treatment that provides substantial individual benefit, however less than 3000 heart transplants occur per year worldwide lending little epidemiological impact to the therapy [62]. The success of transplantation as a therapy, coupled with the limited supply of donor organs and overabundance of patients not meeting transplantation criteria (due to age or other underlying disease), has prompted great interest in alternative approaches to cardiac replacement including ventricular assist devices and total artificial hearts. Furthermore, these blood pumps provide additional uses within mechanical cardiac assistance for cardiopulmonary bypass, femoral bypass, or extracorporeal membrane oxygenation [35].

1.1 Heart Failure

Heart failure is the disease state resulting from any condition that reduces the ability of the heart to sufficiently pump blood to the body. When the heart is unable to satisfy the needs of the body, termed cardiac decompensation, heart failure can occur. The cause of cardiac decompensation is usually decreased contractility resulting from the damage to the myocardium. Diminished coronary perfusion (i.e. myocardial infarction) causes myocardial damage, which results in increased cardiac decompensation further diminishing coronary perfusion leading to a feedback loop and a steep decline in overall patient health.

While decreased contractility due to myocardial dysfunction is typically the cause of heart failure, other causes include damaged heart valves, external pressure around the heart, vitamin B deficiency, primary cardiac muscle disease, any other abnormality resulting in ineffectual pumping [31], severe hypertension, infection, pulmonary emboli, and renal failure [28]. A single risk factor is frequently insufficient to trigger heart failure. It is a multi-factorial, long-term, progressive disease. Risk factors for heart failure include hypertension, diabetes, kidney dysfunction, cardiotoxic substances (i.e. chemotherapy agents, some diabetes medication), cardiac dysfunction (i.e. myocardial infarction, conduction irregularities), and genetic propensity.

Despite advances in medical treatment for heart failure, 30-day, 1-year, and 5-year mortality rates for patients hospitalized with heart failure are 10%, 22% and 42% respectively [52]. Patients with early stage heart failure, before the onset of structural or functional heart disease, have the best prognosis. However diagnosis of early stage heart failure is difficult as the pulmonary congestion due to increased venous pressure is often misdiagnosed as pneumonia, bronchitis or asthma.

Tests of cardiac function are used to diagnose and classify heart failure. Electrocardiograms (ECG) may show the presence of ventricular hypertrophy, atrial abnormality, arrhythmias, conduction abnormalities, previous myocardial infarction or active ischemia. Echocardiography determines valvular abnormalities, decreased ejection fraction, ventricular cavity size/function, and wall motion abnormalities. Stress testing allows for characterization of coronary

ischemia, functional cardiac capacity, decreased residual cardiac capacity, and helps differentiate cardiac and pulmonary limitations as well as the potential for cardiac transplant. Such testing is frequently used as the primary indicator for classification of patients. Pharmacological stress testing can be performed for patients unable to exercise [28].

These tests allow for information to help stratify patients based on severity. A common classification schemata utilized in the clinic is the New York Heart Association (NYHA) classification system, detailed in table 1.1 [17]. Patients are classified based on symptomatic presentation; namely, exercise tolerance based on the presence of symptoms, such as dyspnea (shortness of breath) and angina, and the presence of physical activity limitations.

Table 1.1 New York Heart Association Classification System

NYHA classification	Physical activity limitations	Symptoms: fatigue, angina, palpitations, dyspnea	Discomfort at rest
I	None	None with normal activity.	Absent
II	Slight	Mild with normal activity.	Absent
III	Marked	Mild to severe with moderate activity.	Absent
IV	Severe	Severe with mild activity. May be present at rest.	Present

1.2 Device Treatment for Heart Failure

While there have been many pharmacological therapies to treat heart failure, recent advancements have targeted many of the structural and

mechanical aspects of heart failure. Specific emphasis has been placed on those conditions not addressed by pharmacologically based therapies, including electrical conduction abnormalities, coronary artery and valvular architecture changes, and alterations in ventricular size, shape and strength.

Electrical conduction abnormalities are frequently addressed with the implantation of a cardiac pacemaker or defibrillator. Changes in coronary artery architecture can be addressed with stenting. Valvular abnormalities can be corrected with artificial valves. Abnormalities of ventricular size and shape can be addressed with ventricular restraints or surgical restoration [78]. **The primary focus of this thesis is related to problems with ventricular strength due to heart failure, its treatment with novel blood pumps, and the extent to which such treatment can cause unwanted secondary effects associated with thrombosis/hemostasis.** The optimal treatment for refractory heart failure is cardiac allo-transplantation. However, because of the current lack of donor hearts, cardiac transplant therapy is unavailable to many patients. The unavailability of hearts for transplant therapy has lead a growing interest in mechanical circulatory support, either as an acute support mechanism while the heart recovers or as a bridge to transplant. Recently, new technologies have allowed the ventricular strength to be augmented with the placement of various types of ventricular assist devices (VAD) [15].

Most commonly, the left ventricle requires assistance, and the term VAD is frequently used interchangeably with left ventricular assist device (LVAD). However, in the event of right or total heart failure, devices can be used to

augment pulmonary circulation or used for bi-ventricular (both left and right) support. These technologies employ mechanical pumps to augment the function of the ventricle and restore a more normal blood circulation; this enhanced circulation improves end-organ perfusion. From the earliest pumps to the current technologies, many challenges have been overcome, however many challenges remain. The earliest pumps utilized biomimetic pulsatile displacement pumps that have more recently been supplanted by continuous flow devices. Such devices show much promise relative to previous generation pumps; however, this is a rapidly developing field and much is not known about the effect on the cellular and proteinacous elements involved in hemostasis and thrombosis. The current thesis looks at several pump designs and measures their effect on blood elements.

1.3 Evolution of Assist Devices

Landmark events in the evolution of assist devices and treatment of heart failure are summarized in table 1.2, adapted from Goldstein et al. Briefly,

1964 – the National Heart, Lung, and Blood Institute began sponsoring the development of short- and long-term circulatory support devices;

1967 – the first human heart transplantation was performed and this became the gold standard therapy for heart failure;

1994 – the Food and Drug Administration (FDA) approved the first left ventricular assist devices (LVADs) as a bridge to transplantation.

The table demonstrates the long road to clinical use of VAD therapy, and with increased FDA approval the therapy has become increasingly available to patients.

Table 1.2 Evolution of VAD Technology – Landmark Events [29]

Year	Event
1954	Cardiopulmonary-bypass machine developed
1964	Artificial Heart Program chartered
1966	First generation device used as bridge to recovery
1967	First human heart transplantation
1969	First generation total artificial heart implanted as bridge to transplant
1984	First generation total artificial heart implanted as destination therapy
1985	Multicenter Evaluation of LVADs as bridge to transplant
1991	Moratorium on total artificial heart
1993	New Investigational Device exemption for total artificial heart
1994	First generation LVAD as bridge to transplantation approved by FDA
2002	First generation LVAD as destination therapy approved by FDA
2010	Second generation LVAD as bridge to transplantation approved by FDA

First generation ventricular assist devices were pulsatile displacement-type devices (often pneumatically driven) that attempted to mimic the normal function of the heart. They required large-diameter percutaneous leads and had large pump diameters, limiting their use to larger, usually male, patients. These devices required moving diaphragms and valves, increasing their complexity and limiting their durability and miniturizability. These problems have led to near discontinuation of first generation pump usage [1]. However, patients treated with this generation of pumps were only required to have anti-platelet therapy

with aspirin, whereas later generations required more aggressive antiplatelet therapy with aspirin combined with anticoagulation to abate risk of thromboembolic events [10].

The second generation of pumps has moved away from pulsatility to continuous flow devices. The multiple moving parts of the previous generation of pumps have been reduced to a single moving part – the internal rotor. This change in the device resulted in increased durability and decreased size of both the pump and the percutaneous leads (see figure 1.1). This figure demonstrates the different sizes of Thoratec's HeartMate VE and HeartMate II and their positioning within the patient. The reduction in size and potential for longer support times increased the therapeutic population. Furthermore, these pumps resulted in decreased pump pocket infections in comparative studies with first-generation pulsatile-flow pumps (see section 1.4.3 – HMII DT Trial).

However, these pumps present challenges as well. Basically, there has been little improvement in the rates of hemostatic complications compared to first-generation devices – hemorrhagic stroke continues to be the most frequent cause of mortality (see section 1.4 – Ventricular Assist Device Clinical Trials). Also, the rates of bleeding complications are increased, particularly gastrointestinal bleeding (see section 1.7 – Ventricular Assist Devices and Acquired Von Willebrand Disease). In addition, the durability of these bearing-type devices was projected to be 5 years due to wear in the mechanical contact bearings [48]. The HeartMate II (HMII, Thoratec, Pleasanton, CA) is the most

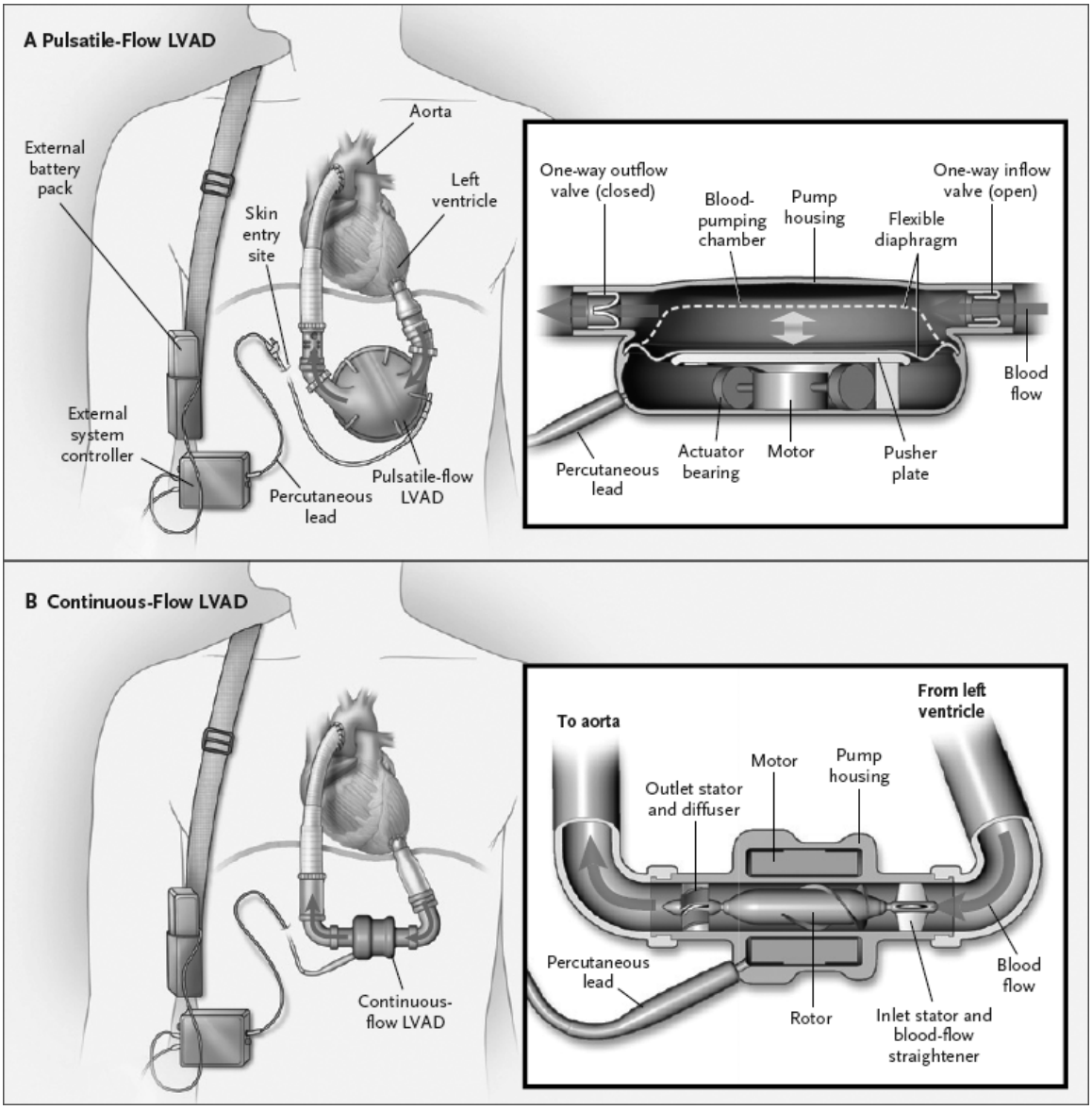

Figure 1.1. Pulsatile-Flow and Continuous-Flow Devices. The larger pump pocket required for HMVE (A) is clearly evident. The pump inlet is connected to the apex of the heart in the left ventricle. The outlet is anastomosed to the ascending aorta. Reprinted with permission from Thoratec Corporation.

successful FDA-approved second-generation pump with over 2,500 implantations worldwide as of 2009 [45].

The third generation pumps that have evolved are similar to second generation devices except they employ non-contact bearings using either hydrodynamic or magnetic levitation [1]. The non-contact nature is expected to

decrease mechanical wear, increase durability and possibly decrease thromboembolic complications[36]. The first report of the clinical use of the third generation of pumps was in a prospective, nonrandomized study of 11 patients undergoing coronary artery bypass grafting with the beating-heart technique and extracorporeal circulatory support in 2004 [58]. Low-level (insignificant) hemolysis was observed in the device. No internal thrombus formation was seen on the pump housing or connectors upon inspection. This study provided justification for continued research with and employment of non-contact bearing pump designs.

The design of second and third generation pumps can be separate into two categories – axial and centrifugal. In axial pumps, the rotor is centered along the axis of the lumen of the device. In centrifugal pumps, the inlet is centered on the rotor and the outlet is on the side of the rotor at 90º to the inlet. As the rotor turns, the fluid is propelled radially; flow exits through the outlet or is recycled in a secondary flow path. The secondary flow path follows the underside of the rotor then through a washout opening in the center of the rotor.

Clinical trial data are forthcoming and survival rates are beginning to rival that of cardiac transplant. There are several investigational devices that have promising early results for a wide variety of applications. As noted, Thoratec (previously Thermo Cardiosystems Inc.) is currently the industry leader with the FDA approved HeartMate II. They also have the HeartMate III under investigation. The HeartMate III is a third-generation centrifugal device. Heartware Inc. is also producing a device (HVAD), which is implanted under an

investigational device exemption in clinical trials with data forthcoming. As of March 2011, Heartware Inc has applied for pre-market approval from the FDA based on the initial results of the ADVANCE trial (see section 1.4.4 – ADVANCE Trial). The HVAD is a third-generation centrifugal device, whereas the HMII is a second-generation axial flow device.

1.4 Ventricular Assist Device Clinical Trials

Clinical trials have demonstrated benefits primarily to severely ill patients (NYHA class IV) with respect to survival, quality of life and improvement in NYHA classification due to ventricular assist device therapy. However, several barriers to successful long-term intervention remain, including device durability, infection and thromboembolic and hemorrhagic complications.

1.4.1 REMATCH Trial. The landmark REMATCH (Randomized Evaluation of Mechanical Assistance for the Treatment of Congestive Heart Failure) study demonstrated the efficacy of left ventricular assist device (LVAD) therapy over optimal medical management using the HeartMate VE (Thoratec Corporation, Pleasanton, CA) [62]. This study demonstrated a 48% reduction in death from all causes for the LVAD therapy group and an average extension of life of 8 months compared to the optimal medical therapy (OMT) group.

The medical committee has developed optimal medical therapy guidelines to optimize organ perfusion and minimize symptoms of congestive heart failure. The committee provided specific guidance for management with angiotensin converting enzyme inhibitors and encouraged the discontinuation of intravenous inotropic infusions. Patients were monitored monthly when not hospitalized.

Table 1.3 REMATCH Trial – Causes of Death

Cause of Death	OMM Group	LVAD Group	Total
	Number of Patients		
Left Ventricular Dysfunction	50	1	51
Sepsis	1	17	18
Failure of LVAD	0	7	7
Misc. Non-cardiovascular	0	5	5
Cerebrovascular Disease	0	4	4
Misc. Cardiovascular	1	2	3
Pulmonary Embolism	0	2	2
Acute Myocardial Infarction	1	0	1
Cardiac Procedure	1	0	1
Perioperative Bleeding	0	1	1
Unknown	0	2	2
Total	54	41	95

The HeartMate VE (see figure 1.1) was a first generation displacement pump with a moving diaphragm that could be run on bearings or if the bearings failed, the pump could be hydraulically operated. The surgical management committee developed guidelines, which included antimicrobial prophylaxis, intraoperative measures (e.g. drive-line placement), and post-operative care.

This study noted a stark disparity in the causes of death and incidence of serious adverse events for both groups summarized in Tables 1.3 and 1.4 respectively. Most patients in the medical therapy group died as a result of left ventricular dysfunction, whereas patients in the LVAD group died due to sepsis, LVAD failure, thrombotic complications, and to a variety of other reasons. The

Table 1.4 REMATCH – Incidence of serious adverse events

Event	OMT Group Rate/Patient-year	LVAD Group Rate/Patient-year	Rate Ratio (95%CI)
All	2.75	6.45	2.35 (1.86-2.95)
Non-neurologic Bleeding	0.06	0.56	9.47 (2.30-38.90)
Neurologic Dysfunction	0.09	0.39	4.35 (1.31-14.50)
Peripheral Embolic Event	0.06	0.14	2.29 (0.48-10.80)
Sepsis	0.30	0.60	2.03 (0.99-4.13)
Local Infection	0.24	0.39	1.63 (0.72-3.70)
Renal Failure	0.18	0.25	1.42 (0.54-3.71)
Hepatic Failure	0.00	0.02	–
Misc. Adverse Events	0.98	1.37	1.41(0.93-2.12)
LVAD related Events			
Malfunction	–	0.75	–
Perioperative Bleeding	–	0.46	–
Infection of driveline tract or pocket	–	0.41	–
Infection of Pump interior, inflow or outflow tract	–	0.23	–
Failure of LVAD System	–	0.08	–
Thrombosis in LVAD	–	0.06	–

majority of serious events were characterized by an increase in infection and coagulation related events.

1.4.2 INTrEPID Trial. The Investigation of NonTransplant-Eligible Patients who are Inotrope Dependent (INTrEPID) trial was a prospective, non-randomized clinical trial comparing LVAD therapy with optimal medical therapy (OMT). The trial investigated the Novacor LVAD as a destination therapy in patients ineligible for cardiac transplant [61].

The LVAD group had increased survival rates at 6 months (46% vs. 22%; p=0.03) and at 12 months (27% vs. 11%; p=0.02). Furthermore, 85% of LVAD

patients experienced an improvement in NYHA functional class, whereas the OMT patients experienced no improvement.

OMT group causes of death were comparable to the REMATCH trial - patients in this cohort died of cardiovascular dysfunction. Also in keeping with the REMATCH trial results, incidences of stroke, transient ischemic attack, and bleeding were increased in the LVAD group – indicating the presence of pump-induced coagulopathies.

1.4.3 HMII DT Trial. Recently the HeartMate II destination therapy (HMII DT) trial compared the HMII continuous-flow ventricular assist device with the HeartMate XVE (HMXVE – a HMVE with improved durability), pulsatile-flow ventricular assist device (both from Thoratec, Pleasanton, Ca)[71]. The study demonstrated increased rates of patients reaching the primary composite end point (two years free of disabling stroke or re-operation to replace the device) with continuous-flow devices versus pulsatile-flow devices. Figure 1.2 shows the comparison of this study with the REMATCH trial[19]. This figure demonstrates the similarity in survival course for the patient groups receiving the pulsatile-flow LVAD (HMVE or HMXVE) and the significantly improved survival course with the continuous-flow LVAD (HMII) patient group ($p=0.008$).

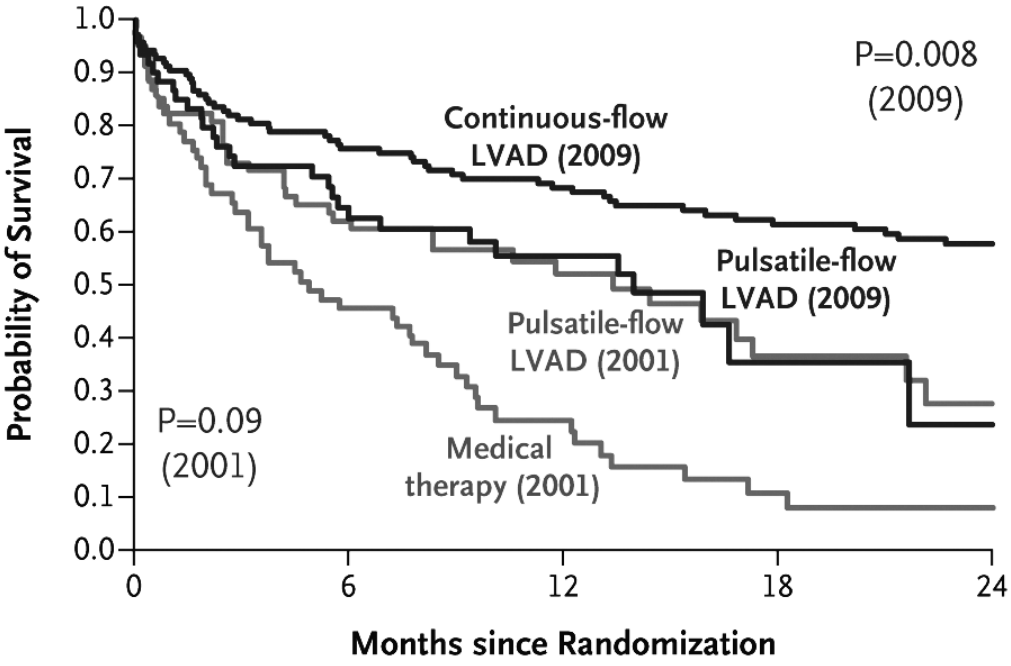

Figure 1.2. Survival Rates of Two Destination Therapy Trials [19]. REMATCH (gray lines) and HMII DT (black lines) survival rates are shown. Treatment with LVADs offer improved survival over optimal medical therapy. Furthermore, continuous-flow LVADs offered improved survival over pulsatile-flow LVADs.

This study reported decreased frequencies of adverse infection-related events (sepsis, LVAD related, and non-LVAD related infection) in patients with the continuous-flow devices. However, stroke (both hemorrhagic and ischemic) and bleeding events indicated a decrease that was not statistically significantly between the two groups. The leading cause of death in both patient populations was hemorrhagic stroke (9% with continuous-flow, 10% with pulsatile-flow). Furthermore, hemolysis and intra-device thrombosis were reported with the continuous-flow device, both in 5 patients (4% of the total patient population) at a rate of 0.02 events per patient-year, while there were no reports of intra-device thrombosis or hemolysis with the pulsatile-flow device. Such findings indicate

that the interactions with the device, specifically related to blood trauma and thrombosis, may not be present in the pulsatile-flow device.

1.4.4 ADVANCE Trial. Recently, at the 2010 American Heart Association Congress, the results of a bridge-to-transplant trial of the HeartWare left ventricular assist device (HVAD) (Heartware International Inc., Framingham, MA), a third generation centrifugal pump, were presented [25]. The results of this study have yet to be published in a peer-reviewed journal.

Survival, transplant or recovery rates at 180 days were 92% and were compared to a control of patients on a nationwide list (INTERMACs registry) receiving commercially available devices (90%). While not a “head-to-head” comparison, the reported rates of infection, bleeding and ventricular arrhythmias were decreased with the HVAD. Furthermore, the design of the HVAD results in a decreased pump size allowing it to be implanted within the pericardial space, further increasing the availability of assist device therapy to smaller patients. Indeed, in an attempt to further increase the availability of this pump to smaller patients, experimental surgery in a bovine animal model has been performed in which the left ventricle is resected, leaving the right ventricle intact, in order to create a space for the HAVD [22].

1.4.5 Summary. These studies demonstrate the immense progress that has been made in the field of ventricular assist devices over the preceding two decades. Indeed, it may be possible for ventricular assist devices to eclipse cardiac allo-transplantation as the primary treatment for patients with heart failure due to both the limited availability of hearts for transplant and the complications

of life-long immunosuppression therapy. Recent studies with third generation pumps demonstrate improvements in survival outcomes, device durability, and infection rates. However, the presence and prevalence of coagulation dysfunction remains clearly evident. Understanding of the mechanisms related to thrombotic and hemorrhagic events in such devices is incomplete.

1.5 Complications in Device Therapy

Because the primary end point of the clinical studies described above was increased survival, it is clear that the benefits of restoring cardiac output (by means of a ventricular assist device) outweigh the surgical risk and the subsequent device-related complications. There are distinct secondary problems to LVAD placement when compared with other forms of cardiac surgery as demonstrated in the clinical trials. The trials demonstrate three areas where blood pumps can be improved – infection control, durability, and blood trauma/coagulation dysfunction.

Infection control is being addressed in a multifaceted way. The decrease in size of pumps has lead to decreased pocket infections. Furthermore, there are devices under investigation that do not require percutaneous leads, thus keeping the skin barrier intact [18]. However the internal power supply does not last very long with a 30-minute charge and a 1-year lifespan, which limits the acceptance of the technology. Durability is also increasing with a reduction in moving parts as detailed in the evolution of assist devices (section 1.3 – Evolution of Assist Devices).

Besides line infection and durability, the major complications of third generation pumps are related to bleeding and thromboembolism [4]. The pump designs have exacerbated problems with coagulation dysfunction (see section 1.7 – Ventricular Assist Devices and Acquired Von Willebrand's Disease). The increased shear stresses in the new LVADs are thought to play a primary role in increased coagulation dysfunction. Because of the continued presentation of coagulation dysfunction in patients with VADs, this thesis examined the effect of ventricular assist device therapy on hemostasis both *in vivo* and *in vitro*.

1.6 Hemostasis

Hemostasis is a complex physiological process that results in the cessation of bleeding. In the normal hemostatic response, the endothelial monolayer is disrupted and the underlying constituents, including tissue factor (TF), basement membrane von Willebrand factor (VWF), and collagen, are exposed to flowing blood. Exposed tissue factor initiates the extrinsic coagulation pathway; exposed basement membrane VWF and collagen recruit platelets from the blood to the site of injury. At the site of injury a wide variety of agonists, including collagen and products of the coagulation pathway, induce platelet activation; additional platelet adhesion and aggregation results by granular release of secreted agonists and up-regulation of adhesion receptors on the activated platelets. Platelet activation causes changes in the membrane, which provides an additional surface for coagulation to occur [31].

1.6.1 Blood Coagulation. Coagulation is the transformation of liquid phase blood to a solid phase through a cascade of enzymatic reactions that results in

the formation of a cross-linked fibrin mesh (figure 1.3). The activation process can be separated into an intrinsic and extrinsic pathway. The intrinsic pathway is also known as the contact pathway because it is primarily responsible for fibrin formation due to the presence of exposure of blood to artificial surfaces. The extrinsic pathway is also known as the TF pathway. The only known endogenous initiator of the extrinsic pathway is TF. TF initiated coagulation feeds back into the extrinsic pathway for amplification.

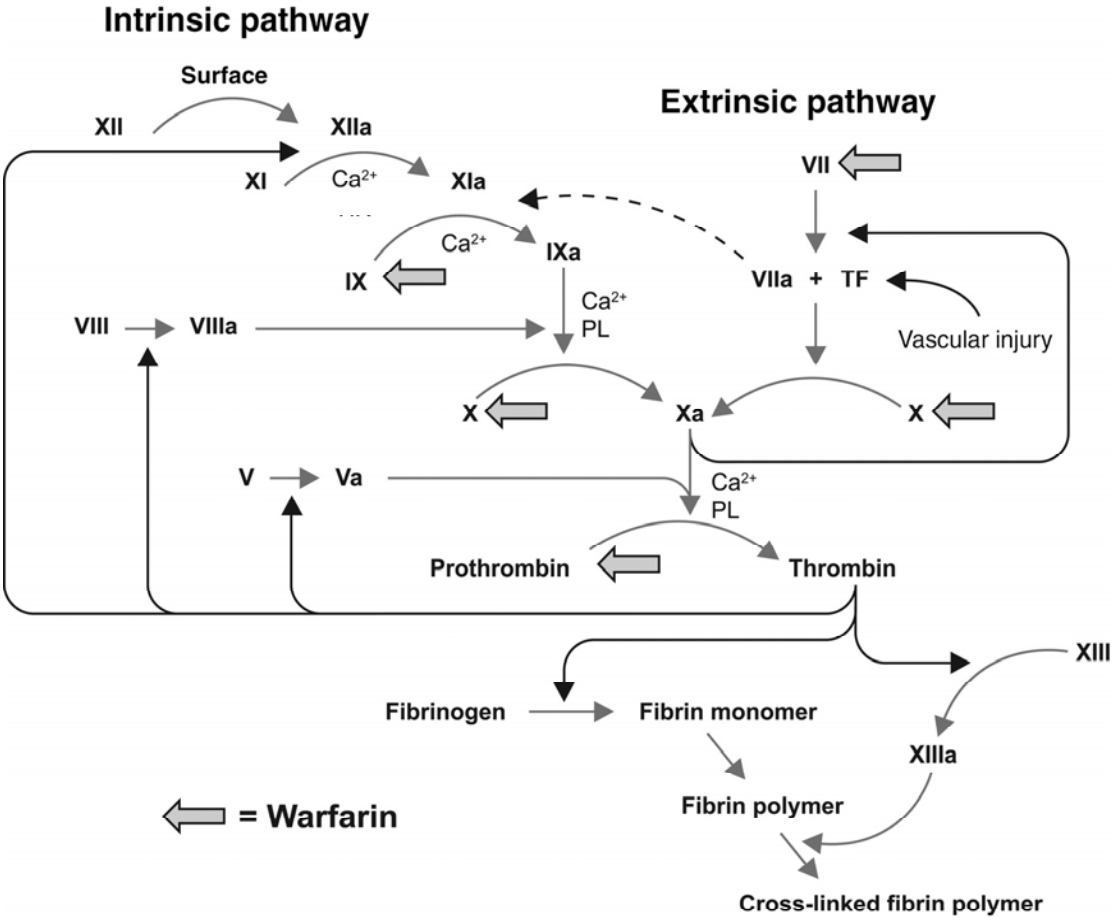

Figure 1.3. Coagulation Cascade [49]. The intrinsic (contact) pathway and extrinsic (TF) pathways are shown. Zymogens activation requiring calcium ion (Ca2+) and negatively charged phospholipid (PL) are shown. Inhibition of vitamin K dependent zymogen synthesis (by the anticoagulant Warfarin) is shown.

The extrinsic pathway is initiated with exposure of subendothelial surface tissue factor to flowing blood and the formation of a tenase complex. TF and FVIIa combine to form the tenase complex, which in turn activates factor X (FX) to form FXa. FXa combines with factor Va (FVa) to form the prothrombinase complex. The prothrombinase complex cleaves prothrombin of its F1 and F2 regions, resulting in the formation of thrombin. Thrombin has many roles in hemostasis including activation of FV to FVa, activation of factor VIII (FVIII) to form FVIIIa (which is also involved in the contact pathway), platelet activation, and conversion of fibrinogen to fibrin. The half-life of thrombin *in vivo* is very short and direct measurement is difficult. Antithrombin III binds thrombin forming the inactive thrombin-antithrombin III complex (TAT). Cross-linked fibrin formation is the end product of the coagulation cascade. Upon degradation, a peptide, d-dimer, along with additional fibrin degradation products, are released as fibrinolysis occurs.

Because of the highly reactive and transitory nature of many of the constituents of the coagulation system, it is not always possible to measure them directly. Frequently indirect measurements are used as a substitute – such as measurement of d-dimer, prothrombin fragment F1+2, TAT, or the generation of FXa to measure TF activity.

1.6.2 Platelet Aggregation. Platelets (also known as thrombocytes) are formed by thrombopoiesis in bone marrow by budding from megakaryocytes. The average healthy adult human normally has between 150 - 300 x 10^6 platelets per mL. The average healthy adult Holstein cow has 152-1,229 x 10^6 platelets

per mL [67]. The circulating lifespan of platelets is 1-2 weeks. Old platelets are cleared from circulation in the spleen or by Kupffer cells in the liver. The spleen also serves as a reservoir for additional platelets, which can be released by splenic contraction [31].

Platelets are recruited to site of injury in flowing blood in a shear dependent manner. Platelets are more heavily involved in the hemostatic response at high shear stresses and form what are known as a 'white' thrombus. At lower shear stresses, fibrin is more heavily involved and red cells are more easily incorporated in the thrombus forming 'red' thrombi.

In normal hemostasis, exposure of subendothelium presents substrates for platelet adhesion to flowing blood. After initial adhesion, most likely to subendothelial collagen or VWF, autocrine and paracrine mediators are released from platelets granular contents to amplify and sustain the platelet response. These mediators result in increased expression and activation of integrin $\alpha_{IIb}\beta_3$. It is the main receptor for adhesion and aggregation of platelets [12].

Significant advancement has been made in understanding platelet thrombus growth with specific emphasis on mechanistic interactions of adhesive proteins/receptors, effects of soluble agonists, signaling pathways, and rheological factors [39]. Multiple adhesive ligands and receptors are involved in platelet adhesion and aggregation and their involvement is dependent on shear rate, as demonstrated in figure 1.4. An important ligand in platelet adhesion is von Willebrand factor (VWF), which is particularly critical at high shear rates.

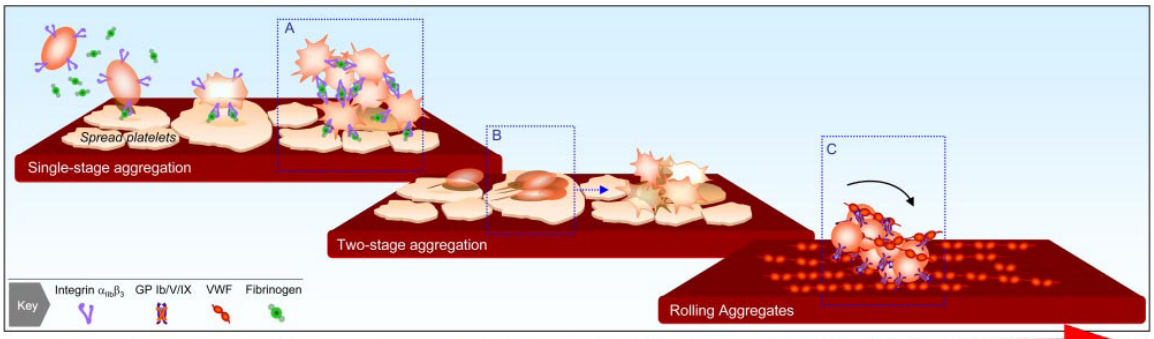

Characteristic Features:	A	B	C
Adhesion Receptor	Integrin $\alpha_{IIb}\beta_3$	Integrin $\alpha_{IIb}\beta_3$, GP Ib/V/IX	GP Ib/V/IX
Activation-dependent	Yes	Yes	No
Tether formation	No	Yes	Yes
Ligand	Fibrinogen	VWF, Fibrinogen, Fibronectin	VWF
Platelet Morphology	Sphere and filopodia	Discoid	Smooth Spherical

Figure 1.4. Platelet Aggregation as a Function of Wall Shear Rates – Dark red shows the surface upon which platelets are aggregating. Different adhesive ligands/receptors involved are shown in the key. As shear rate increases interaction mechanism and presentation changes [38].

VWF has two major receptors on platelets – GPIb/V/IX and integrin $\alpha_{IIb}\beta_3$. Furthermore, VWF can act as a bridge between subendothelial collagen and platelets at high shear rates with the A3 domain on VWF binding to collagen. The adhesion receptors GPIb and integrin $\alpha_{IIb}\beta_3$ on platelets bind to the A1 domain and the RGD binding site C1 domain of VWF respectively (see section 1.6.3 for more detailed information about VWF).

Granular release by activated platelets creates a cloud of soluble agonists, which aids in the recruitment of platelets from within the flowing blood. Platelet granular contents include ADP, ATP, serotonin, and calcium from the dense granules and soluble vWF, fibrinogen, FV and FXIII from the alpha granules. Activation also initiates shape change in resting discoid platelets, transforming them from a discoid to a stellate morphology. Formation of stellate activated

platelets results in increased membrane tethers and up regulation in both the amount and the activity of binding integrins including integrin $\alpha_{IIb}\beta_3$ [38].

Platelets response to ADP is a weak response when compared to collagen and results in a reversible aggregation reaction [23]. ADP stimulation results in transition to a stellate morphology, but not release of granular contents, which is thought to be a determinant in non-reversible aggregation [47]. Platelet response to collagen occurs in two steps – initial adhesion mediated by GPIb-V-X, which is followed by firm adhesion mediated by release of granular contents. Platelet response to collagen is thought to be most important at moderate and high shear stresses and be mediated through the initial action of the GPIb-V-X complex with VWF.

1.6.3 Von Willebrand Factor. Von Willebrand factor (VWF) is a large multimeric glycoprotein constitutively expressed by endothelial cells and megakaryocytes in a range of molecular weights (250-20,000 kDa) [63]. The VWF monomer has multiple binding sites for a variety of antigens including FVIII, GPIb, integrin $\alpha_{IIb}\beta_3$, collagen, botrocetin, and heparin as shown in figure 1.5. Normal plasma concentrations of VWF are widely varied (100 ± 56 %) with a half-life of ≈12 hours [5]. VWF is regulated by an enzyme known as A Disintegrin And Metalloproteinase with a ThromboSpondin type 1 motif, member 13 (ADAMTS13), which cleaves VWF at the A2 domains [69]. Both the normal physiological function and enzymatic processing of VWF into smaller molecular weight multimers have been shown to occur in a shear dependent manner.

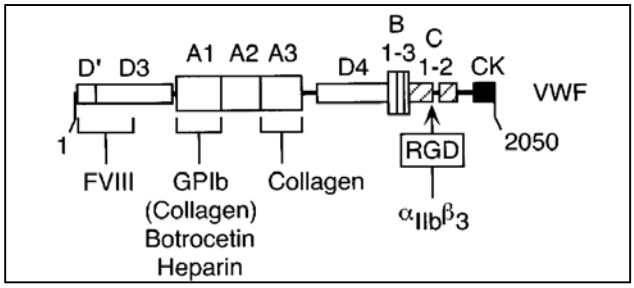

Figure 1.5. Binding Sites of Monomeric VWF. Binding sites on monomeric VWF of various antigens including GPIb and integrin $\alpha_{IIb}\beta_3$ on platelets and coagulation zymogen FVIII [63].

When not under flow, VWF assumes a globular conformation, which elongates under flow (figure 1.6) [68]. Under flow the VWF chain lengthens and, with increasing force, the A2 domains, normally inaccessible in the globular form of VWF, become increasingly exposed [2]. The unfolding of the A2 domain is required for ADAMTS13 to cleave the A2 domain [84]. Larger molecular weight multimers of VWF will experience higher tensile forces, which will concentrate towards the center of the chain, under the same flow conditions (figure 1.7). In this way shear stress and the mechanoenzymatic cleavage of VWF work together to regulate the molecular weight range *in vivo*. VWF is most physiologically active with respect to platelet function (adhesion and aggregation) at high molecular weights (HMW) and high shear stresses. It is required for platelet binding to subendothelium in arteries [65], and this binding (adhesion) is increased at high shear stresses [66]. In patients with von Willebrand disease (VWD), HMW VWF is either decreased or absent leading to bleeding diatheses. Alternatively, loss of enzymatic degradation of the largest molecular weights results in spontaneous clumping of ultra large molecular weight VWF (ULVWF) and platelets, characteristic of thrombotic thrombocytopenic purpura (TTP),

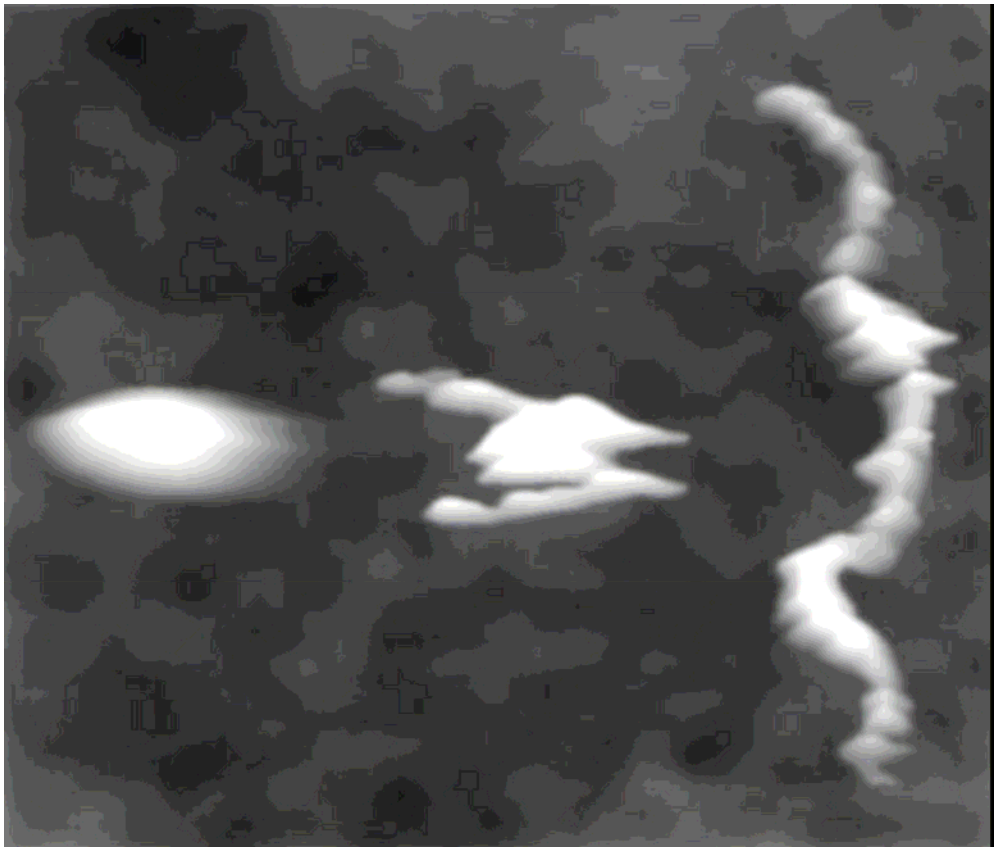

Figure 1.6. VWF in Globular and Elongated Forms. Atomic force microscopy image of VWF as a globular protein (left) and elongated with the AFM tip (center) or with shear stress (right) [68].

which has been directly linked to ADAMTS13 functionality [20]. When taken together the pathological clotting that results with increased ultra large molecular weight fractions and the bleeding diathesis with decreased high molecular weight fractions demonstrates that the activity of VWF is correlated to its molecular weight. Because VWF is secreted constitutively and has a short half-life, 12 hours, it is the balance between secretion rate and degradation rate that may regulate the concentration and activity of VWF *in vivo*.

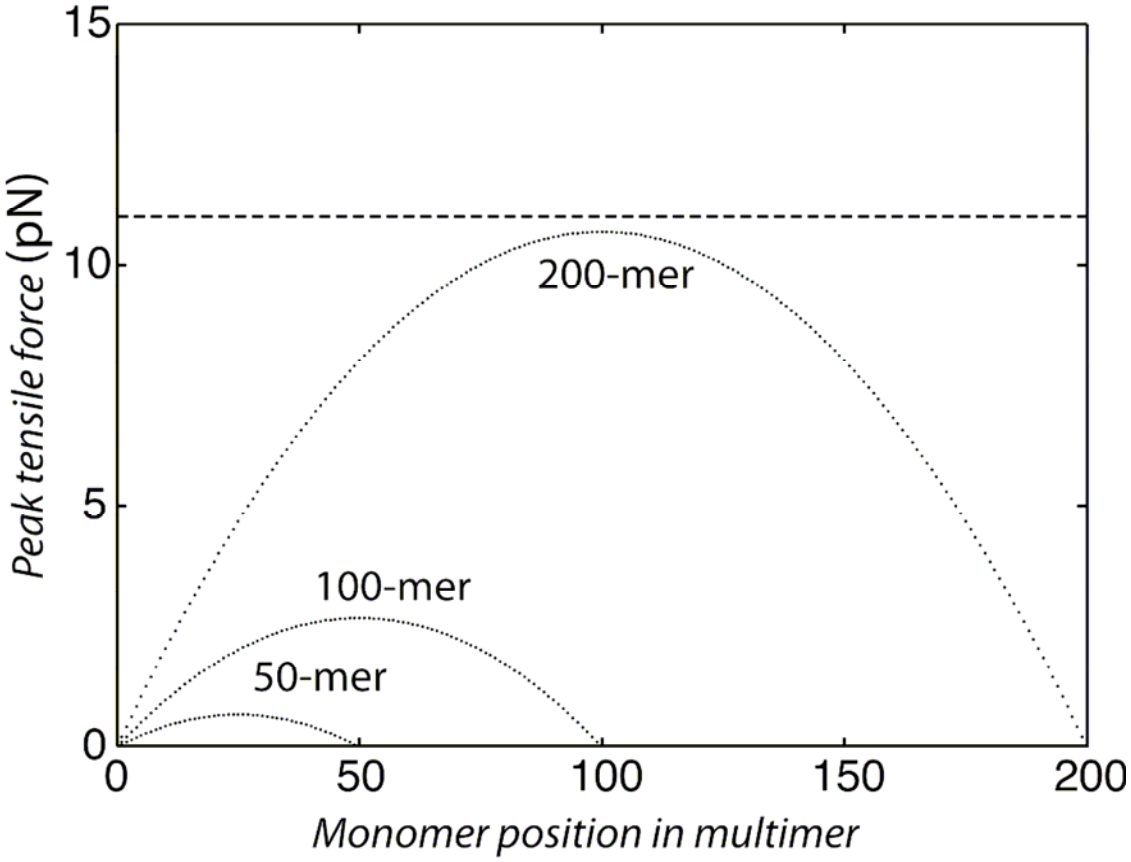

Figure 1.7. Peak Tensile Force Experienced Under Applied Shear Force. The peak force experienced by monomers is shown as a function of the position of the monomer within the VWF multimer. The dashed line represents the force most likely required for unfolding when the multimer is loaded at 24pN/s [84].

A decrease in high molecular weight multimers has been demonstrated in patients with second- and third-generation ventricular assist devices and these patients have been diagnosed with acquired von Willebrand's Disease (aVWD) as discussed in section 1.7.

1.6.4 Interactivity of Platelets, Von Willebrand Factor and Coagulation. The interactions between the proteins of the coagulation cascade and activated platelets are summarized in figure 1.8. Dashed magenta arrows represent activation processes of platelets or coagulation zymogens. Blue arrows

represent transport of species. Green segments with dual arrowheads represent binding and unbinding surface interactions. Rectangular boxes delineate species bound to the platelet surface. Black lines are enzymatic reactions. Solid black lines indicate forward reactions, whereas dashed black lines indicate feedback mechanisms. Red disks are inhibitors of the associated reaction.

Platelet activation results in up-regulation of scramblase-mediated transport of negatively charged phospholipids to the surface of the platelet, which provides a negatively charged surface required for the maximal function of the tenase complexes (TF:FVIIa in the extrinsic pathway and FIXa:FVIIIa in the intrinsic pathway) and the prothrombinase complex (FXa:FVa). Thrombin, a product of the coagulation reactions, is a potent activator of resting platelets.

Furthermore, constituents of the subendothelium effect both coagulation reactions and platelet activation. Subendothelial TF is a potent initiator of coagulation. In addition, subendothelial collagen and VWF provide surfaces for activated platelet binding and collagen is a platelet activator. Upon activation of platelets, numerous granular contents are secreted; these include ADP, a soluble platelet activator, and high molecular weight VWF, which can serve as a bridge strengthening platelet-platelet interactions. All of these interactions serve to propagate thrombus growth, while various inhibitors such as antithrombin III (ATIII), ADAMTS13 and tissue factor pathway inhibitor (TFPI) regulate thrombus growth under normal circumstances.

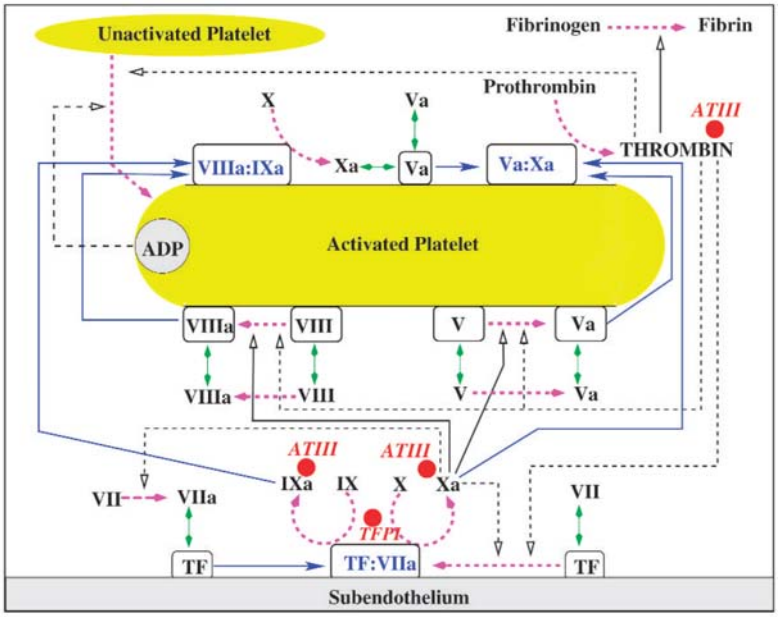

Figure 1.8. Coagulation Reactions with Platelets [46]. Dashed magenta arrows are activation processes. Blue arrows are species transport. Green lines are binding/ unbinding surface interactions. Boxes are surface bound species. Black lines are enzymatic reactions. Red disks are inhibitors.

If the procoagulant interactions overpower anticoagulant regulation, thrombosis can occur. Thrombosis is the pathological correlate of hemostasis, generally occurring in larger vessels. It is a major underlying cause of myocardial infarction and ischemic stroke. If there is insufficient hemostasis, bleeding diatheses may occur which can result in hemorrhagic stroke or gastrointestinal bleeding. Both thrombosis and bleeding diatheses are seen in patients receiving VADs. Recent interest has focused on VWF mediated bleeding complications and this thesis presents evidence that VWF multimer size is directly affected by shear conditions.

1.7 Ventricular Assist Devices and Acquired Von Willebrand's Disease

The rates of gastrointestinal (GI) bleeding are increased in patients receiving continuous-flow rotary-pump-type devices, such as the HeartMate II, when compared with those receiving pulsatile-flow displacement-type devices, such as the HeartMate XVE [32] [10]. The results of these studies may

potentially be confounded due to the varying anticoagulant regimens used with each pump. Continuous-flow recipients often receive warfarin (of varying dosage) and aspirin, whereas pulsatile-flow patients normally receive only aspirin. However, when comparing bleeding in continuous flow devices to mechanical valve implants, where comparable anticoagulant regimens are used, the GI bleeding rate in patients with continuous-flow devices was much greater than all types of bleeding in patients receiving mechanical valves (63 events per 100 patient years versus 4.6 events per 100 patient years) [10] [8]. Thus, the increased incidence of bleeding cannot be fully explained by the differences in anticoagulant.

This complication has lead to a growing interest in acquired von Willebrand's Disease (VWD) in patients implanted with high shear, continuous-flow VADs. GI bleeding is a major complication of VWD. A decrease in HMW VWF, which is sufficient for acquired VWD diagnosis, has been demonstrated by multimer analysis (figure 1.9) [81] [33] [44] [11] [9] [56]. A decreased response to ristocetin-induced platelet aggregation has also been demonstrated [44]. Furthermore, Malehsa *et al*. reported a case wherein the exchange of a pulsatile-flow first-generation HeartMate XVE assist device with a continuous-flow second-generation HeartMate II assist device resulted in acquired VWD [54]. The loss of high molecular weight multimers of VWF was attributed to the high shear continuous-flow device. Furthermore, in bridge-to-transplant studies, the plasma VWF multimeric structure has been shown to return to normal after heart transplantation [81] [56].

These studies indicate that the new high shear continuous-flow devices may result in a loss or dysfunction of high molecular weight multimers of vWF. Potentially, the lack of pulsatility could effect endothelial expression of VWF, thereby leading to a decrease in the amount of circulating HMW VWF. However, Slaughter reports that some pulsatility remains under most clinical conditions, and use of continuous-flow devices should not strictly be termed “non-pulsatile” [70].

Alternatively, the cause could be increased degradation of VWF, which has been shown to occur in response to elevated shear stress (for details on mechanoenzymatic cleavage of VWF see section 1.6.3). Increased GI bleeding associated with aortic stenosis, which alters hemodynamics and exposes blood to increased shear forces, has been linked to a loss in HMW VWF multimers. This occurrence reinforces the concept of increased degradation due to the nature of the shear forces because pulsatility is retained in this condition [53]. Also, patients with continuous-flow devices have decreased HMW multimers despite increased antigenic concentration of VWF [81] [54], which may be indicative of an increased production rate as opposed to a decreased production rate or increased consumption rate. Furthermore, in the previously mentioned case report by Malehsa *et al*, triplet structure, a product of enzymatic processing by ADAMTS13, was normal [54], indicating enzymatic processing in blood. The association with a previously described disease etiology, an increase in antigenic concentration of VWF and evidence of normal enzymatic processing may

suggest that decreased HMW VWF is due to increased degradation, rather than a decreased production.

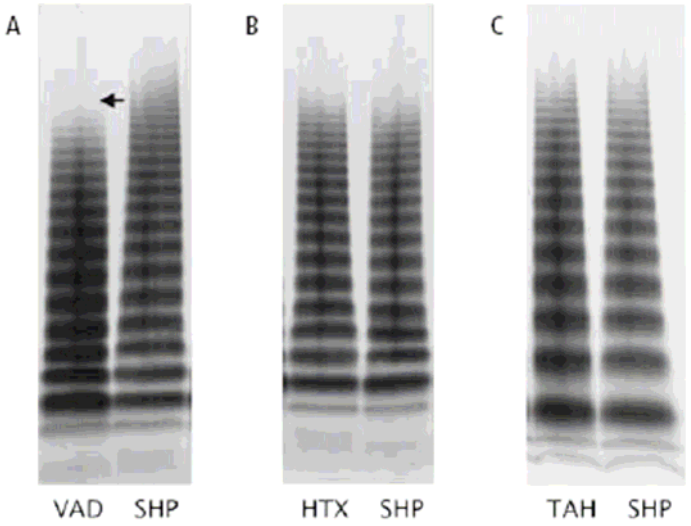

Figure 1.9. Acquired VWD in Patients with VADs. HMW VWF is decreased in patients with ventricular assist devices (VADs), but not patients undergoing heart transplant (HTX) or with displacement-based total artificial heart (TAH) as compared to Standard Human Plasma (SHP) [33].

1.8 Microparticles

Microparticles are small, lipid vesicles that have been shown to contain a number of physiologically active integral membrane proteins, among them tissue factor (TF) [3] [13] [59]. Blood-borne MP populations, present even under normal, non-diseased conditions, become elevated in many diseased states including obesity, diabetes, hyperlipidiemia, and cardiovascular disease [59] [77] [16] [55]. These disease states are associated with increased rates of heart failure (see section 1.1). Therefore, it is hypothesized that microparticle populations are elevated with VAD placement and may be an indicator of blood trauma due to the high shear forces within the VAD.

There is evidence associating TF-bearing MPs in thrombus propagation [3]. Platelet microparticles have been shown to adhere to a collagen, fibrinogen and VWF-coated surfaces [43] and monocyte microparticles have been shown to

deposit in growing thrombi to perpetuate fibrin deposition *in vivo* [30]. Therefore, it is possible that the increased microparticle populations could contribute to the hypercoagulable state experienced by patients on VADs.

1.9 Thesis Overview

This thesis is primarily concerned with the bleeding and thromboembolic complications associated with VADs. These complications are a significant barrier to effective therapy with these devices and a broader acceptance of their use. Chapter 2 and 3 will discuss two different sets of experiments aimed at developing and testing blood pumps. Chapter 2 is a novel blood pump being developed in Japan that has been implanted in a bovine animal model. The author spent ½ year working with this group and developing testing methodologies related to thrombosis and hemostasis, which continued after my departure. I present an evaluation of the parallelism of the bovine animal with what is seen clinically. Chapter 3 involves studies with a clinically developed VAD (for proprietary reasons the pump cannot be identified). This chapter is a presentation of an alternative *in vitro* methodology to stratify VAD designs and evaluate their potential to cause hemostatic and thrombotic complications.

The first set of experiments was conducted in Tokyo, Japan with the assistance of Dr. S. Takatani et al, in a bovine animal model over the course of a two-week survival experiment. The primary endpoint of the experiment was survival at two-weeks at which point necropsy was performed and the experiment concluded. In this set of experiments, platelet function was analyzed with aggregometry as a function of time on pump support; subsequently, the effects of

the pump on VWF multimers were analyzed. Microparticle populations were also analyzed as an additional measure of blood trauma induced by the pump. These experiments were fraught with many of the same complications experienced clinically, including thromboembolic/bleeding complications, infections, and pump malfunctions.

The second set of experiments offers an alternative method to compare pump function with respect to hemostatic and thrombotic effects. These experiments examine three different blood pump designs in a novel low-volume *in vitro* flow loop using human blood from the same donor for all three pumps. This allows for a more direct comparison of the effects of the different pump designs on the blood than can be obtained either clinically or through *in viv*o experiments.

CHAPTER 2

PRECLINICAL IN VIVO EVALUATION

In this chapter I will describe a novel blood pump being developed in Japan that has been implanted in bovines. I spent one-half year working with this group and developed various testing methodologies related to determining the nature of thrombotic and hemostatic alterations due to the pump implantation. These methodologies were compared with previously published results to assess the appropriateness of the bovine animal model for the evaluation of thrombotic and hemostatic alterations.

The MedTech Dispo is a magnetically levitated, disposable, centrifugal rotary blood pump intended for 1-month extracorporeal circulatory support. It is being developed for bridge-to-decision, bridge-to-recovery, or bridge-to-bridge treatment. It was designed in collaboration between the Tokyo Medical and Dental University (Takatani S; Tokyo, Japan) and the Tokyo Institute of Technology (Shinshi T; Yokohama, Japan). The unit is composed of a novel magnetically levitated pump head, which can be separated from the drive unit. This design dramatically reduces costs as all non-blood contacting surfaces can be reused and the non-reusable pump head can be manufactured at a very low cost (~20,000JPY or ~250USD).

2.1 Introduction

The pre-clinical feasibility studies of various VAD designs are frequently performed in a calf animal model [72] [76]. This chapter details pre-clinical feasibility studies of the MedTech Dispo and an additional study into the

hemostatic effects of the MedTech Dispo in a calf animal model with the primary endpoint of two-week survival. This chapter also compares the results to previously published results from clinical studies evaluating the fitness of the bovine animal model for hemostatic studies.

Previous studies have assessed hemostatic compatibility in pre-clinical animal feasibility studies in an attempt to better understand and predict the thromboembolic and bleeding complications associated with these devices in humans [79] [74] [73] [50] [42]. However, while these studies note the difficulty of interspecies extrapolation, reference literature assessing the fitness of the bovine animal model for this type of analysis is lacking. Recent clinical studies have established acquired VWD (altered protein composition) in patients receiving VAD therapy population (see section 1.7 Ventricular Assist Devices and Acquired Von Willebrand's Disease). Additionally, there is some clinical data published assessing platelet aggregation in response to collagen and ADP [44]. This study assesses platelet aggregation and VWF multimeric content to evaluate the bovine animal model's tendency toward bleeding and thromboembolic complications and the appropriateness of the interspecies extrapolation with humans with regards to these complications. Additionally, the microparticle (MP) population in plasma was assessed as an additional measure of blood trauma.

2.2 Materials and Methods

This study utilized a bovine animal model with a primary endpoint of survival at two weeks. The MedTech Dispo pump was implanted in the bovine animal model on the operation day and each subsequent day was enumerated

(i.e. the day after the operation day was the first post-operative day). The animal was euthanized and necropsy was performed on the 14th post-operative day. Various tests were conducted, including platelet aggregometry and flow cytometry in order to assess the effect of the pump on the blood. These techniques are described below.

2.2.1 Theory of Turbidimetric Aggregometry. Aggregation is the most commonly investigated of all the functional responses of platelets. Platelet to platelet interactions resulting in aggregate formation occurs as part of the normal hemostatic response to vessel injury and also as a pathological response to prothrombotic conditions. Therefore, the aggregation of platelets is clinically relevant to both bleeding and thrombotic conditions. Aggregometry is a simplified *in vitro* technique that has been developed to measure of the ability of platelets to aggregate in response to a variety of agonists.

The most common form of aggregometry utilizes the turbidimetric method, whereby light diffraction by the individual platelet particles is decreased as the particles clump together (aggregation) resulting in increased light transmission; i.e., optical density decreases with increasing aggregation. The plot of optical density (OD) of a platelet suspension versus time is a graphical representation of platelet aggregation. To normalize for any changes in the optical density of the plasma solution, typically percent aggregation is plotted, instead of OD, as shown in figure 2.1.

Experimentally, platelet poor plasma (PPP) is used to set the 100% aggregation; this accounts for any opacity in the plasma itself. Before the addition of the

agonist, the device records the optical density and sets this reading as the 0% aggregation reference point. As platelets aggregate, in the presence of agonist, the OD of the solution varies between these two preset points resulting in a trace that is independent of the plasma OD. The OD of the plasma, itself can vary for a wide variety of conditions, such as increased free hemoglobin due to hemolysis or due to lipids from a recent meal.

After the addition of the agonist there is a small increase in the percent aggregation, which is not related to platelet aggregation, but due to the dilution of the platelet suspension with the agonist. Subsequently, there is a slight decrease in the percent aggregation that is thought to be related to platelet shape change; i.e., the transition of platelets from discoid to a more spherical

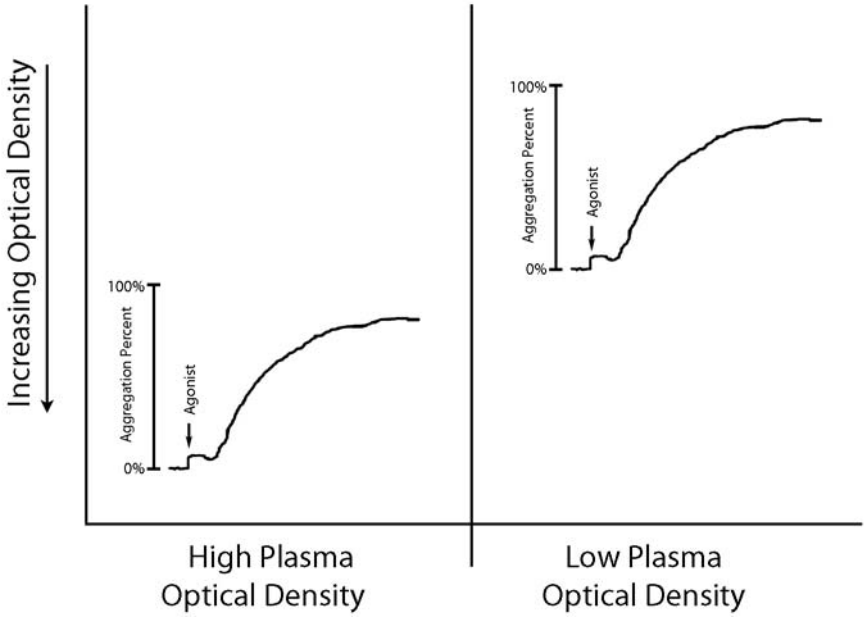

Figure 2.1. Normalization of OD to Percent Aggregation. The normalization of the optical density measurement to percent aggregation results in a measurement that can be compared without influence from changes in the optical density of the plasma (i.e. from changes in free hemoglobin or opacity of the plasma).

shape produces a larger cross-sectional area that blocks the passage of light through the suspension [41]. As the platelets aggregate due to the effect of the agonist, there is a continuous increase in the optical density indicative of the aggregation of the platelets.

2.2.2 Theory of Flow Cytometry. Flow cytometry is a technique that measures specific characteristics of a large number of cells or particles rapidly. The technique employs photo detectors positioned to detect forward and side scattering of light as cells pass through a focused light beam. Forward scatter is the amount of light diffracted at a small angle around the periphery of the cell; this measurement is considered to be an approximate measure of the size of the cell. Side scatter is the amount of light diffracted at a large angle due to the internal structure of the cell. Additionally, further optics can be utilized for immunofluorescence staining such as detection of changes in surface receptor expression.

2.2.3 MedTech Dispo Ventricular Assist Device System. The system consists of a disposable head unit; a reusable magnetic levitation and motor drive unit; and a computerized magnetic levitation control and drive system as shown in figure 2.2. The pump is capable of producing flow of 5 liters per minute against a head pressure of 800mmHg.

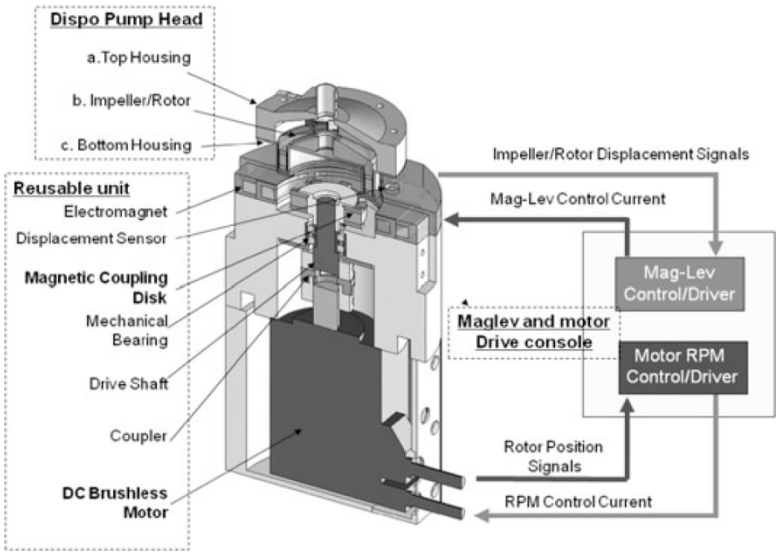

Figure 2.2. The MedTech Dispo Ventricular Assist Device. Shown here is a schematic of the MedTech Dispo VAD system including the disposable pump head, the reusable drive unit, and the drive console.

2.2.3.1 The Disposable Pump Head. The disposable pump head consists of a top and bottom housing and an impeller/rotor with an imbedded permanent magnetic ring. Blood contacting surfaces are coated with 2-methacryloyloxyethyl phosphoryl-choline (MPC) polymer to increase biocompatibility. The pump head is 37.5 millimeters in height and 75 millimeters in diameter. The total priming volume of the pump head is 23 milliliters.

The magnetic levitation creates a secondary flow path beneath the rotor against the flow of the centrifugal pumping due to the pressure gradient. Flow through the secondary flow path begins on the periphery of the pump head, travels under the rotor and up through a center washout hole within the rotor.

2.2.3.2 The Reusable Drive Unit. The drive unit is reusable and non-blood contacting, which greatly reduces use-costs. It contains two pairs of electromagnets to levitate the impeller/rotor from the exterior of the pump head

by the permanent magnetic ring embedded in the impeller/rotor. The impeller/rotor is rotated using a radial magnetic coupling disk on the interior of the permanent magnetic ring through the wall of the pump head. The disk is mounted on the drive motor shaft. The drive unit is 162mm in length and 108 mm in diameter.

2.2.3.3 The Control/Drive Console. The magnetic levitation and drive motor systems are controlled by a digital signal processor-based system. Two paired eddy current gap sensors control the magnetic levitation. Motor speed is controlled using a commercially available AC servo motor driver (Oriental Motor Co., Ltd., Model NXD20-A, Tokyo, Japan). The drive console provides continuous monitoring of power consumption, rotor displacement, and rotational speed.

2.2.4 Animal Model. The two-week survival study was performed on Holstein calves. Calves were transported to the lab and acclimatized to the laboratory, staff, and enclosure. All experiments were carried out in accordance with the Guideline for Animal Experimentation of Tokyo Medical and Dental University (TMDU) and approved by the Institutional Animal Care and Use Committee of Tokyo Medical and Dental University.

2.2.5 Surgical Procedure. Upon arrival and acclimatization, all calves were examined for physical condition. Animals were prepared for surgery with a 12-hour fast and fur removal at the surgical site. All control values for assays performed during the experiment were taken before the start of the fast using a

14-gauge in-dwelling catheter cannula (NIPRO Cat# NSL-140C4x1.1) via the right jugular vein.

Calves were anesthetized with isoflurane and maintained with an isoflurane/oxygen mixture delivered with an endotracheal tube. Surgery was performed with the calves in the right decubitus position (lying on the right side). The left carotid artery and jugular vein were exposed for insertion of arterial and venous catheters. The arterial line was used for drug infusion, blood sampling, and arterial pressure monitoring. The venous line was used for central venous pressure monitoring. In the case of left carotid artery catheter obstruction, the jugular vein catheter or a port distal to the outlet of the pump was used.

A left thoracotomy was performed through the fifth intercostal space followed by exposure of the descending aorta for clamping and pericardiotomy. Following initiation of heparin (infusion rate of 200-300 U/kg to achieve an activated clotting time (ACT) of over 450s), the inflow cannula was inserted through the left atrial wall and mitral valve into the left ventricle as shown in figure 2.3-A. The outflow graft was anastomosed in an end-to-side fashion to the aorta as shown in figure 2.3-B. The inflow and outflow cannulae were tunneled through the seventh intercostal space to connect to the disposable pump head extracorporeally. The chest was closed when stable pump performance and hemostasis were confirmed.

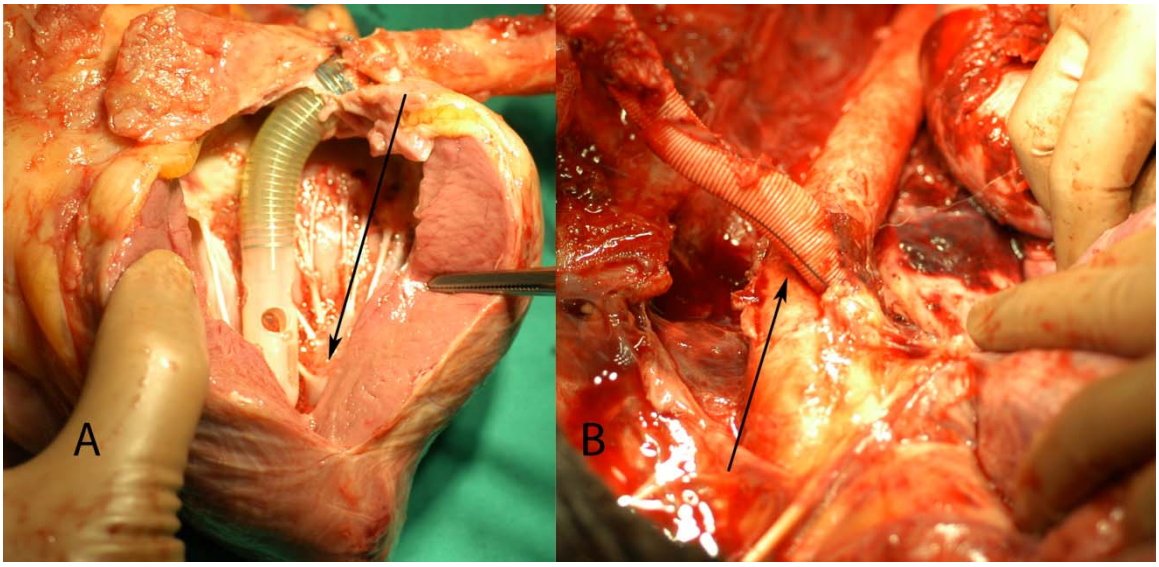

Figure 2.3. Pump Connections to Native Circulatory System. The inflow cannula (A) was inserted through the left atrial wall and mitral valve resting near the apex of the heart within the left ventricle. The outflow cannula (B) was anastomosed with descending aorta in an end-to-side fashion (arrow in the direction of blood flow).

2.2.6 Post-Operative Recovery. Calves were placed in sternal recumbency (lying with the legs beneath the body) in the operating room until cessation of anesthesia and the endotracheal tube was removed. Spontaneous swallowing and resumption of self-controlled head positioning indicated sufficient cessation.

Calves were then returned to the care facility for post-operative recovery and physiologic monitoring. The pump head and driver were fixed to a saddle mounted on the back of the calf, which was counterbalanced by two spring-loaded tensioners used to stabilize the pump during normal calf movement. Calves were encouraged to stand as soon as possible post-operatively – typically within several hours of waking. Food and water were provided immediately and regularly for the duration of the experiment.

Cephazolin or ampicillin was given for prophylaxis of infection initially (1-3 days post-operatively) and continued if signs of infection (e.g. increased temperature) presented. Heparin flow was adjusted to maintain an ACT value within limits established by the attending physician, Dr E Nagaoka. Generally, these limits were 200-250 seconds and adjusted as needed – increased heparin and longer times in the presence of potential thrombosis or decreased heparin or shorter times in the presence of potential hemorrhage.

2.2.7 Monitoring. Physiological conditions were assessed every two hours including respiratory rate, rectal temperature, oral intake (food and water), neurological status (behavior and mobility), breathing rate, and heart rate. Hemodynamic and pump performance was continually assessed using a computerized data acquisition and analysis system (National Instruments, LabVIEW, Austin, TX). Parameters assessed with this device included arterial pressure, central venous pressure, pump flow, rotational speed of pump rotor, motor current, and rotor displacement. Furthermore, blood samples were taken for analysis at least daily, with increased frequency early in the experiment. Analysis included hematological parameters (RBC, PLT, WBC, Hb, HCT, MCV, free Hb); blood biochemistry (TP, GOT, GPT, BUN, Cr, ALP, LDH, CPK); arterial blood gas (ABG; pH, pO2, pCO2, ABE, K, Na, Ca, Cl, Glu, Lac); and various coagulation markers (ACT, APTT, PT, FDP, D-dimer, TAT, Fbg). Full descriptions of all blood tests, including their physiological significance, are shown in table 2.1.

Table 2.1. Summary of Blood Tests (Page 1 of 3)

Full Name	Abbreviated Name	Clinical Significance
Erythrocyte Count	RBC	Anemia/bleeding
Platelet Count	PLT	Hemostasis
Leukocyte Count	WBC	Infection
Total Hemoglobin	Hb	Anemia/bleeding
Hematocrit	HCT	Anemia/bleeding
Mean Corpuscular Volume	MCV	Anemia/bleeding
Mean Corpuscular Hemoglobin	MCH	Anemia/bleeding
Mean Corpuscular Hemoglobin Concentration	MCHC	Anemia/bleeding
Free Hemoglobin	Free Hb	Hemolysis
Total Protein	TP	Liver Function, Infection
Glutamate-Oxaloacetate Transaminase	GOT	Liver Function

Table 2.1. Summary of Blood Tests (Page 2 of 3)

Full Name	Abbreviated Name	Clinical Significance
Glutamic Pyruvic Transaminase	GPT	Liver Function
Blood Urea Nitrogen	BUN	Kidney Function
Alkaline Phosphatase	ALP	Liver Function
Lactate Dehydrogenase	LDH	Cell damage, Hemolysis, Myocardial Infarction
Creatine Phosphokinase	CPK	Muscle Damage (e.g. Myocardial Infarction)
Activated Clotting Time	ACT	Heparin Monitoring
Activated Partial Thromboplastin Time	APTT	Coagulopathy, Heparin Monitoring
Prothrombin Time	PT, PT(%)	Liver Function, Coagulopathy
Fibrin Degradation Products	FDP	Thrombosis
Creatinine	Cre	Kidney Function
D-dimer	D-dimer	Thrombosis

Table 2.1. Summary of Blood Tests (Page 3 of 3)

Full Name	Abbreviated Name	Clinical Significance
Thrombin Anti-Thrombin	TAT	Thrombosis
Fibrinogen	Fbg	Coagulopathy
pH	pH	Acid-Base Control
Partial Pressure of Carbon Dioxide	pCO2	Lung Function
Partial Pressure of Oxygen	pO2	Lung/RBC Function
Arterial Base Excess	ABE	Acid-Base Control
Potassium	K	Critical Electrolyte
Sodium	Na	Critical Electrolyte
Calcium	Ca	Critical Electrolyte
Chloride	Cl	Critical Electrolyte
Glucose	Glu	Metabolism
Lactate	Lac	Metabolism

2.2.8 Necropsy. Upon completion of the experiment, calves received a bolus injection of heparin prior to euthanasia. Euthanasia was performed with pentobarbital anesthesia and lethal potassium chloride dose. The pump was disconnected, rinsed with normal saline, and disassembled to inspect for thrombus formation and mechanical/functional integrity. Necropsy included gross inspection of the surgical sites, heart, aorta, cannulae, lungs, liver, kidneys, spleen and digestive tract. Whole or portions of inspected organs along with all blood-contacting portions of the pump assembly were fixed in 5% formalin solution.

2.2.9 Turbidimetric Aggregometry. Samples of PRP were prepared by spinning blood at 500 rpm and obtaining platelet rich plasma which as then diluted with autologous PPP to a normalized count of $89 \pm 3.6 \times 10^9$ platelets per liter using complete blood count (Cell Tacα, Nihon Kohden, Tokyo, Japan). Normal platelet counts In bovine are 152-1,229 x 10^9/L [67]. A low platelet concentration was used due to the wide variance in overall platelet numbers that occurred post-surgery (see section 2.3.2 figure 2.6). The platelet count was chosen to be lower than the PRP platelet count at all time points so that results could be compared at the same counts. Increasing low counts would have required significant processing of the platelets enhancing the likelihood of inadvertent activation.

Platelet aggregation was measured on a HemaTracer 712 (MCMedical, Tokyo, Japan). Adenosine diphosphate (ADP, Sigma Aldrich, Cat# 01905-250MG-F, St Louis, MO) at 1, 5, 10, and 20 µM and collagen (MCMedical Cat#

HTR210105, Tokyo, Japan) at 5, 10, 15, and 19.8 µg/mL were used as agonists. Additionally, due to intra-pump thromboses, cuvettes coated with MPC were tested to assess changes in platelet reactivity to the surface of the pump head due to the surgery, anesthesia, or pump.

A typical trace of the platelet aggregation response to ADP is shown in figure 2.4. The rate of aggregation was expressed as the slope of the aggregation versus time curve or the angle of the trace over time in degrees. The reversibility was the percentage of the extent of aggregation at 20 minutes after the addition of the agonist normalized by the maximum response. For example, if the maximum response was 60%, and at 20 minutes the percent aggregation was 15%, the reversibility was 75%. The reversibility is only measured in response to ADP, which is a reversible reaction. Platelet response to collagen is not a reversible reaction.

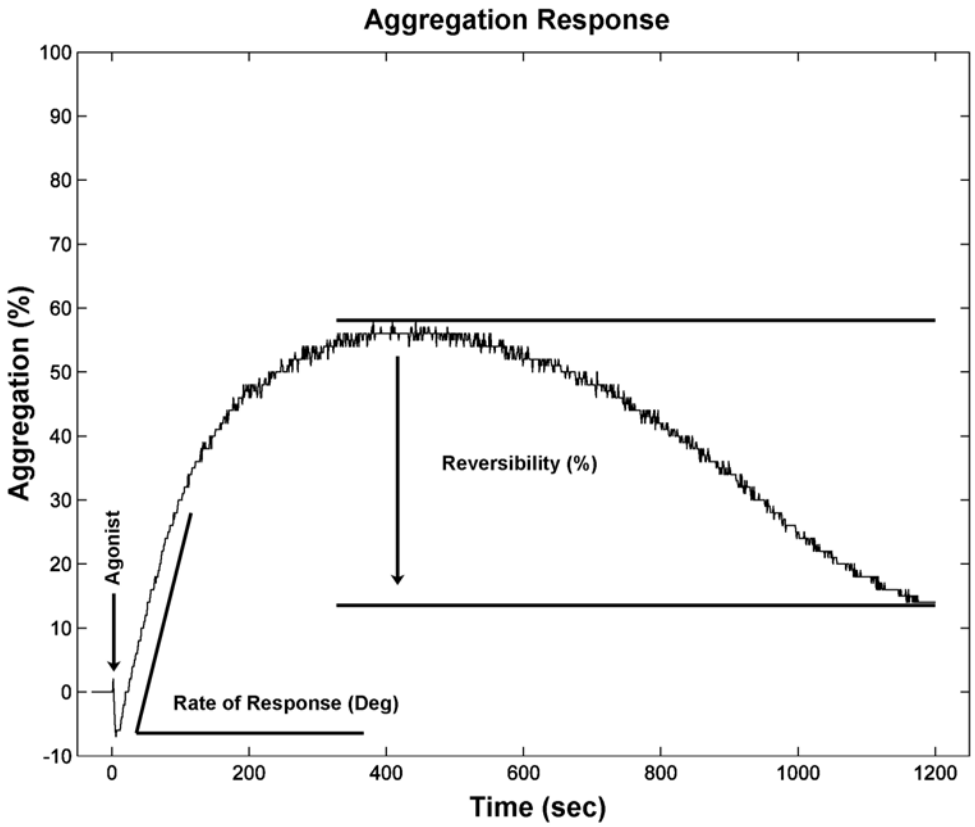

Figure 2.4. Aggregometry Trace in Response to ADP. The typical aggregometric can be reduced to many parameters highlighting different aspects of platelet aggregation. This study summarized the aggregometry results as the rate of the platelet response to the agonist (collagen) and the reversibility of the response (ADP).

2.2.10 Flow Cytometry. Counts of microparticle total population were analyzed in PPP using carboxyfluorescein succinimidyl ester (CFSE, Invitrogen cat # C34554) stained samples. Samples were measured using a FACSCalibur flow cytometer (Becton Dickinson, Franklin Lakes, New Jersey). Population concentrations were quantified by use of AccuCount Fluorescent Particles (SpheroTech Cat# ACFP-70-5, Lake Forest, IL). Calculation of final population concentration, [P], was performed using the provided calculation:

$$[P] = \frac{E_t E_p}{N_p V_t} \qquad \text{(Eqn 3.1)}$$

where Et is the number of events in the test sample, Ep is the number of AccuCount Fluorescent particle events, Np is the lot specific number of particles per 50 µL, and Vt is the volume of test sample initially used.

2.2.11 Von Willebrand Factor Multimer Analysis. Von Willebrand Factor multimer analysis was performed by western blot. Stacking and resolving electrophoresis gels were prepared with SeaKem® HGT(P) (high gel temperature (protein)) Agarose (Lonza Cat# 50050, Basel Switzerland) supplemented with Tris and sodium dodecyl sulfate (SDS). The stacking gel was held constant at 0.8% agarose, whereas the resolving gel was adjusted as needed to resolve either additional high molecular weight bands as in normal samples (low percentage – 1.5%) or low molecular weight bands as with more degraded samples (high percentage – 2.0%). Gels were run at 50V for 16 hours with a recirculating water bath at 16˚C.

The proteins were transferred at 250 mA to an Immobilon-P PVDH transfer membrane (Millipore Cat# IPVH-202-00, Billerica, MA) for 3 hours with a recirculating water bath at 4˚C. Completeness of transfer was confirmed with coomassie protein stain (Carolina Biological Supply Company Cat #21-9784, Burlington, NC).

The transfer membrane was blocked with non-fat dry milk in PBS prior to immunolabeling with polyclonal rabbit anti-human VWF primary antibody (DakoCytomation Cat# A0082, Glostrup, Denmark) and polyclonal donkey anti-rabbit IgG horseradish peroxidase conjugated secondary antibody (Abcam Cat# ab6802, Cambridge, United Kingdom). Gels were developed using

SuperSignal® West Pico chemiluminescent substrate (Thermo Scientific Cat#34080, Waltham, MA) and exposed twice for twenty minutes on a Kodak Digital Science Image Station CF440 (Eastman Kodak Company, Scientific Imaging Systems, Rochester NY).

2.2.12 Shear Stress Degradation of VWF. Specimens of bovine plasma that were removed periodically from calves with implanted heart pumps were measured for the effect of the pump on multimer size. Additional in vitro studies were conducted with both human and bovine plasma at precisely controlled flow conditions. To compare the degradation response of humans to the bovine animal model used in this study, both human and bovine platelet poor plasma was exposed to controlled shear stresses. Platelet poor plasma samples were loaded into a specially designed viscometer with a geometry that applies shear stress approximately evenly throughout the volume of the fluid. The geometries of the viscometer were a combination of Taylor-Couette (rotating coaxial cylinders) and cone-and-plate. By controlling the revolutions per minute, various shear stresses could be applied to the fluid for varying times. Plasma samples were sheared at 12.3 dynes/cm^2 for 10, 20 and 40 minutes and 54.2 dynes/cm^2 for 30 and 60 seconds. Multimer degradation was assessed by VWF multimer analysis (see section 2.2.11).

2.2.13 Statistical Analysis. Repeated measures analysis of variance (RM ANOVA) was used for all statistical analyses unless data failed normality or equal variance tests. In this case, Friedman RM ANOVA on ranks was used. For post-hoc analysis comparing all groups to one-another, Student Newman-Keuls (SNK)

was used. For post-hoc analysis of multiple comparisons to a control, Bonferroni t-test was used. Data is presented as mean ± standard deviation (SD) in the text and mean ± standard error on the mean (SEM) in the tables and figures except for error bars on the abscissa wherein mean ± SD was used. In all statistical methods, $p<0.05$ was considered statistically significant.

Clinical thrombosis/hemostasis markers used in this study, normal published reference values for bovine animal models were used whenever possible. When not possible, reference intervals were constructed using one-sided 95% confidence intervals based on pre-operative data. When construction of 95% confidence intervals was not possible, as in the case for d-dimer due to a variance of zero, a normal human reference interval was substituted.

2.3 Overall Feasibility Study Results

The overall pump feasibility studies experienced complications similar to those discussed in the introduction. Specifically, infection, thrombosis, and bleeding complications were frequently observed. Additionally, complications due to the investigational nature of the device resulted in pump stoppages and functional instability. All identified causes of stoppages or functional instability were remedied.

2.3.1 Pre-operative Conditions. Pre-operative results are summarized in table 2.2. Upon arrival at the care facility, animals were a mean age and weight of 2.4 ± 0.5 months and 86.2 ± 5.2 kilograms respectively. Blood tests were performed prior to the start of surgery. Two animals were admitted to surgery presenting with diarrhea. Furthermore, one of the two animals also exhibited elevated LDH

Table 2.2. Pre-Operative Conditions and Control Values

Experiment Number	Age (Months)	Weight (kg)	Hematocrit (%)	Platelet ($x10^9$/L)	Leukocyte ($x10^2/\mu L$)	Pre-Op Condition
0906	2	88.9	33.2	783	85	Normal
0907	3	92.2	28.7	388	68	Normal
0908	2	81.1	23.5	364	38	↑ LDH (1347), ↑ CPK (2688), Diarrhea
0909	2	89.6	25.0	415	67	Normal
0910	3	80.9	28.7	802	92	Diarrhea
Mean ± SD	2.4 ± 0.2	86.5 ± 2.3	27.8 ± 1.7	550 ± 99.2	70 ± 9.3	

and CPK values indicating muscular damage – likely incurred in transport to the care facility. Values of hematocrit, platelet count and leukocyte count were within the normal range in adult bovine - hematocrit (22-33% [27]), leukocyte (49-120 x 10^2/µl [27]), and platelet (152-1,229 x 10^9/L [67]) with the exception of a low leukocyte count in animal 0908. Values are listed in table 2.2.

It should be noted that, variations between healthy juvenile bovine hematology and healthy adult bovine reference ranges have been reported [7]. The reference range for platelet count was reported from calves, whereas the leukocyte and hematocrit reference range was that of adult cows.

2.3.2 Post-operative Course. Plasma samples were taken for various times after implantation of the pump, as shown in figure 2.5. Spikes in hemolysis were seen in all of the experiments for up to about 300 hours post surgery (figure 2.5). The platelet concentrations in each experiment showed a consistent decrease during surgery but stabilized at a lower level by the second postoperative day (Fig. 2.6). Two experiments exhibited platelet counts that were below the lower reference value; however, these normalized by the third post-operative day. The decrease below the reference value was not indicative of a problematic postoperative course. Hypoxia and/or anemia were present in two experiments. Hypoxia was determined by ABG and treated with infusion of oxygen up to 10 liters/minute. Anemia, an indication of possible bleeding complications, was determined by hematological analysis and treated with transfusion of autologous blood taken prior to surgery (see table 2.3).

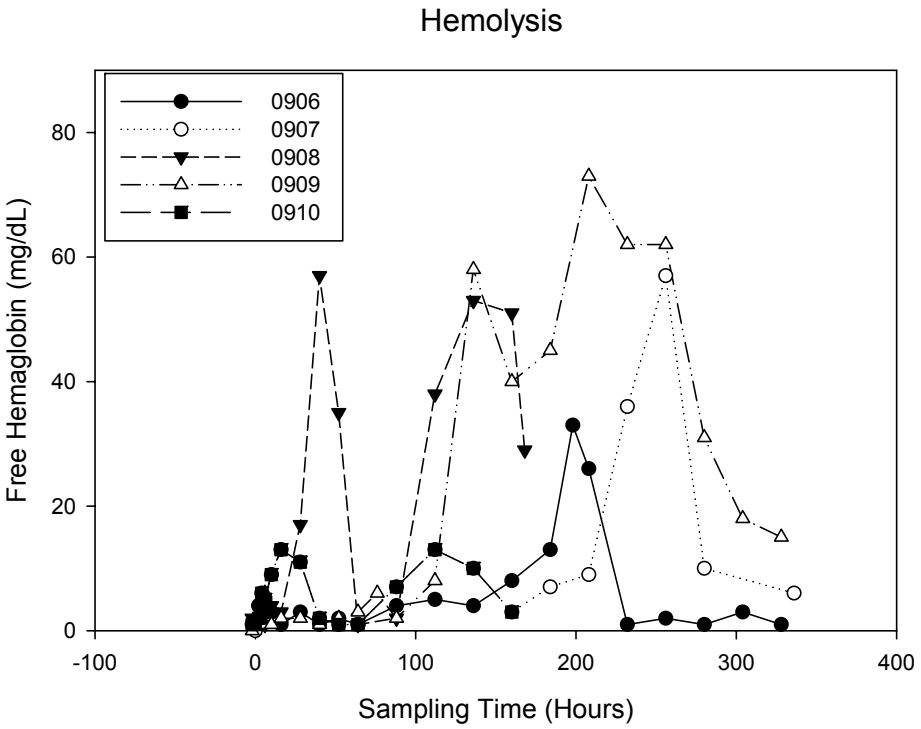

Figure 2.5. - Hemolysis – Hemolysis was seen in all animals to some degree throughout the course of experimentation.

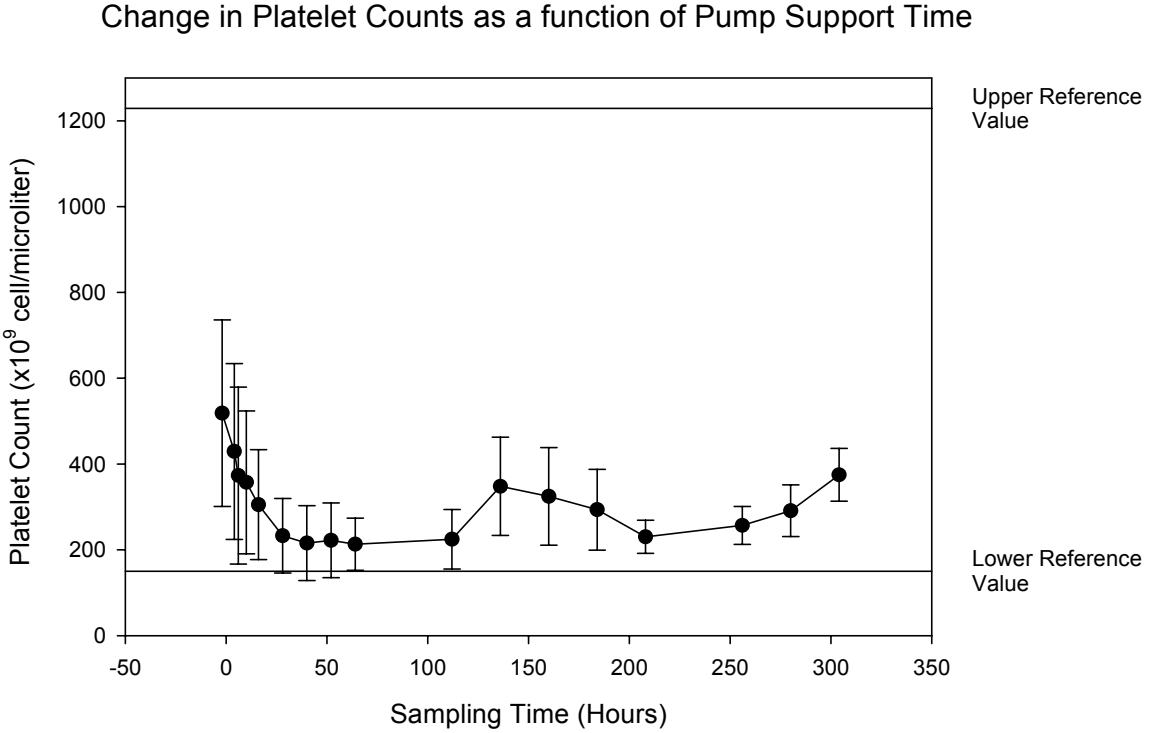

Figure 2.6. Platelet Counts as a Function of Time on Support. Platelet counts were shown to during the surgery and shortly thereafter stabilizing on the by the second postoperative day. Two experiments exhibited platelet counts below the lower reference value on the second and third postoperative day.

Table 2.3. Post-operative Course

	Anemia	Hypoxia	Termination Method	Termination Cause	Duration (Days)
0906	X	X	Euthanasia	Pump Malfunction	9
0907			Euthanasia	End of Experiment	14
0908			Euthanasia	Poor Health	12
0909	X		Euthanasia	End of Experiment	14
0910		X	Hypoxia	Poor Health	5

2.3.3 Malfunctioning of the Pump. The implanted pump is an experimental device and as such experimental failures occurred during the procedures. In the event of a pump stoppage, a bolus injection of heparin was administered, followed by a restart protocol (rebooting the control system). If the pump did not restart, the pump head was replaced and inspected. The extracorporeal positioning and disposable pump head facilitated ease of replacement. If the pump failure continued, the experiment was terminated and a necropsy commenced. Causes of stoppages were identified and rectified. Mechanical failures included separation of the rotor from the magnetic drive ring, which was rectified by manufacturing the drive ring and rotor in a single piece. Electrical failures included blown fuses and short circuits due to a loose wire connection. Stoppages are summarized in table 2.4.

Table 2.4. Pump Malfunctions

POD	1	2	3	4	5	6	7	8	9	10	11	12	13	14
0906									T*			T(2)	T	
0907														
0908														
0909	M/E*				M									
0910	E(3)		E		E									

"M" – refers to stopping of the pump due to mechanical complications (e.g. separation of rotor from permanent magnetic drive ring)
"*" – refers to replacement of the pump head
"(#)" – refers to the number of times the pump stopped on a specific post-operative day.
"T" – refers to stopping of the pump due to thrombus
"E" – refers to stopping of the pump due to electrical complications(e.g. blown fuse)

2.3.4 Assist Device System Thrombosis. Some amount of thrombosis was seen in all experiments as summarized in table 2.5. Outlet graft thrombosis was seen in one of five experiments (figure 2.7-A). Non-occlusive intrapump thrombi in the secondary flow path were seen in three of five experiments (figure 2.7-B). Occlusive thrombus in the secondary flow path was seen in one of five experiments (figure 2.7-C). Thrombi were observed in the two pump heads that were replaced mid-experiment (see section 2.3.3) and in the replacement pump heads at the time of the necropsy.

Table 2.5. Thrombi within the Pump or Connectors

POD	1	2	3	4	5	6	7	8	9	10	11	12	13	14
0906									H					H
0907														O
0908				H*								HC		
0909														H
0910					H									

"H" – refers to thrombus located within the pump head
"O" – refers to thrombus located within the outlet graft
"C" – refers to thrombus located in the tubing adjacent to the tubing connectors on the inlet and out let of the pump head.
"*" – refers to suspected thrombus

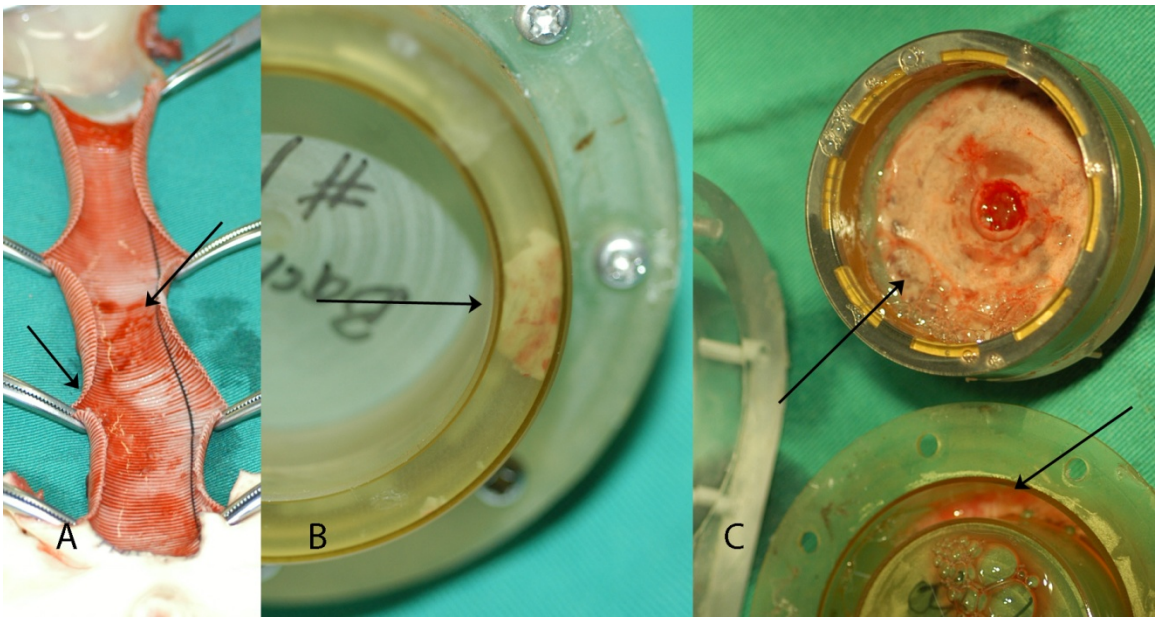

Figure 2.7. Thrombi Examples. Examples of an outflow graft thrombus (A), a non-occlusive thrombus (B), and the occlusive thrombus (C) from experiment 0909 are shown.

2.3.5 Hemostasis Markers. Thrombin anti-thrombin (TAT) complex concentration remained low for the first four post-operative days (see figure 2.8). There was a spike on the 6th post-operative day; however, this spike is heavily influenced by one experiment. At longer times all of the experiments demonstrated elevated TAT concentrations.

Plasma fibrinogen levels decreased post-operatively but remained within the normal reference range (see figure 2.9). By the second post-operative day, the fibrinogen levels increased greatly and remained elevated throughout the course of the 2 week experiment. Also, d-dimer plasma concentration (figure 2.10) and fibrin degradation products (FDP) concentration in plasma (figure 2.11) were increased by the second post-operative day. The spike in TAT complex concentration on the sixth post-operative day was paralleled by a similar spike in the d-dimer levels and in FDP on the 8th post-operative day.

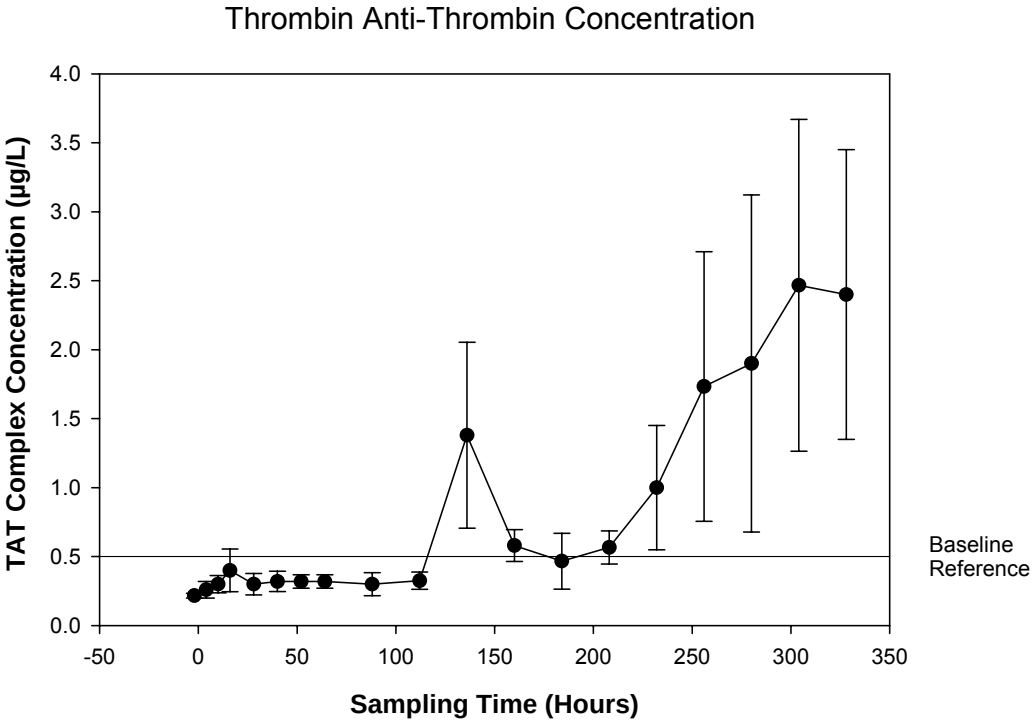

Figure 2.8. Thrombin Anti-Thrombin. Concentration of circulating TAT complex increases as a function of time on pump support above the reference interval before 150 hours and then again after 200 hours.

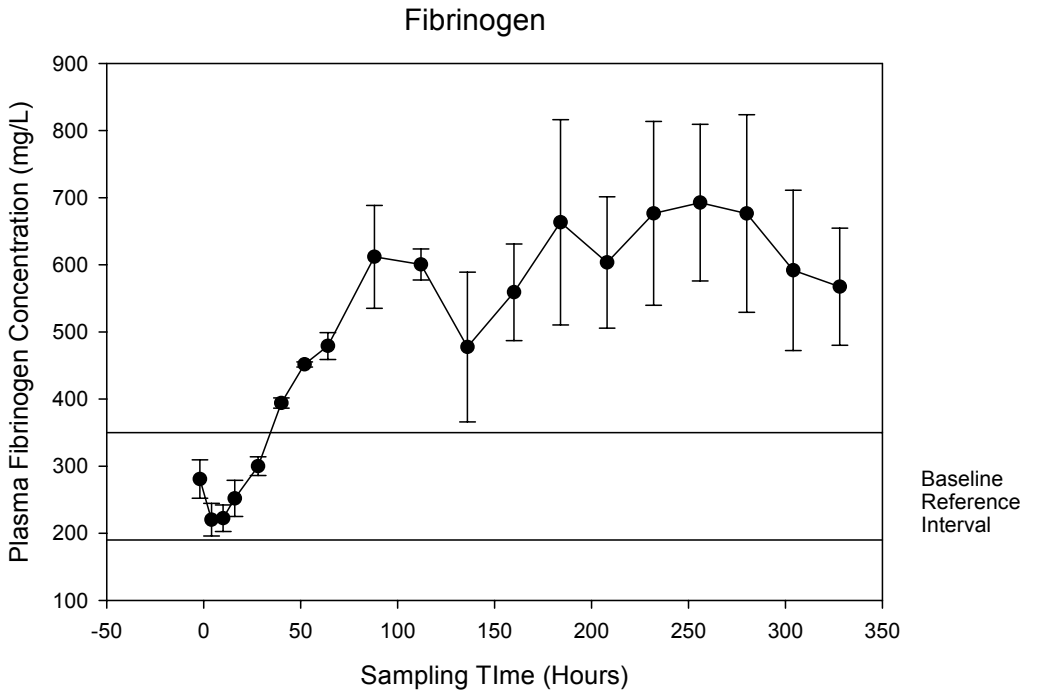

Figure 2.9. Plasma Fibrinogen Concentration. The concentration of plasma fibrinogen is shown to increase above the baseline reference interval on the second post-operative day. Concentrations remain elevated for the remainder of the experiment.

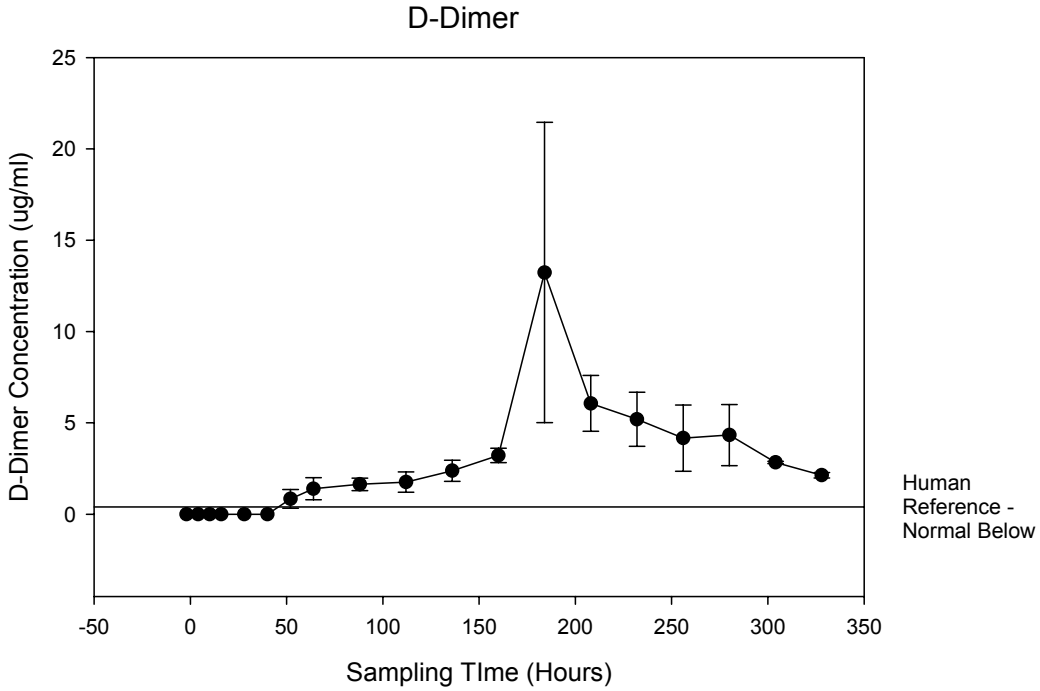

Figure 2.10. D-dimer Concentration. D-dimer concentration is shown to increase by the second post-operative day with a spike on the eighth post-operative day, followed by a decrease but not below the normal human reference interval.

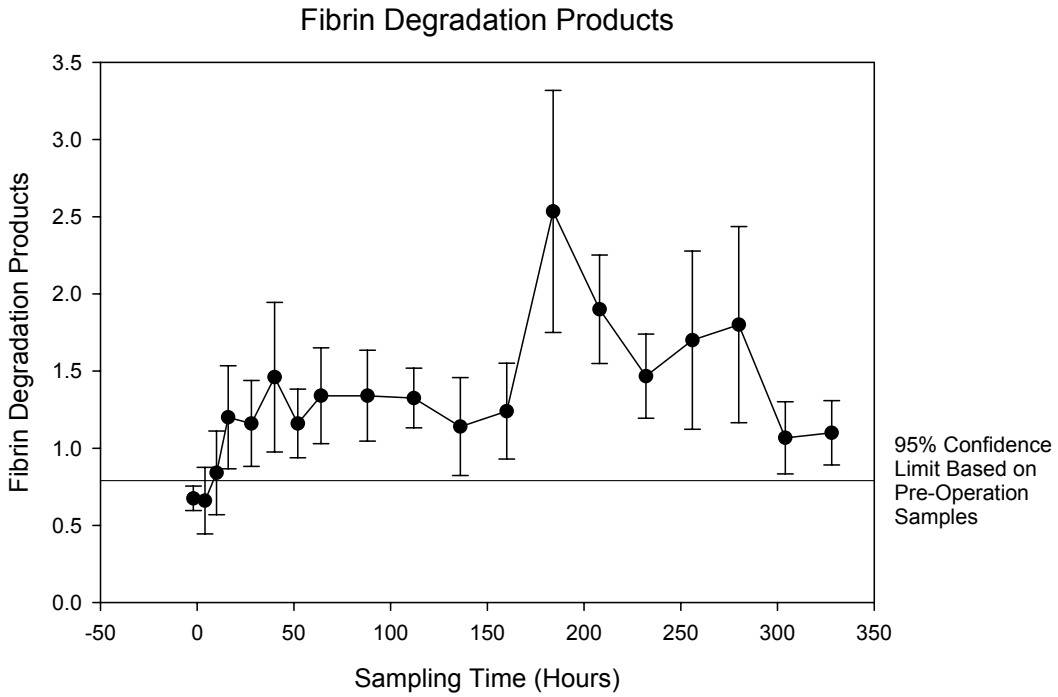

Figure 2.11. Fibrin Degradation Products. Fibrin degradation products are shown to be elevated above the confidence interval very quickly, within the first 24 hours, and remain elevated throughout the course of the experiment.

2.3.6 Necropsy Results. Necropsy results are summarized in table 2.6. One animal exhibited no symptoms of infection whereas two animals exhibited severe infection. Severe infection was characterized by driveline infection leading to sub-dermal sepsis covering a large area exposed during necropsy and/or massive lung infection. Massive subdermal sepsis is shown in figure 2.12-B with a normal subdermal tissue shown for comparison in 2.12-A. The attending physician determined presence of minor infections. One animal presented with a cardiac hemorrhage in two locations (figure 2.13). Lung dysfunction of was present in four of five experiments. One animal presented with massive lung infection with the appearance of tuberculosis (figure 2.14-A). One animal experienced a collapsed lung as a result of ventral hematoma (figure 2.14-C). Ventral hematoma was present in three of the five experiments (figure 2.14-B).

Table 2.6. Necropsy Results

Experiment Number	Infection	Ventral Hematoma	Organ Condition			
			Heart	Lung	Liver	Kidney
0906	None	X		Pneumonia		Infarct
0907	Minor					Infarct
0908	Suspected	X	Hemorrhage	Collapsed Lobe	Infarct	
0909	Severe			TB	Dysfunction	Infarct
0910	Severe	X		Pneumonia	Dysfunction	Infarct

Liver dysfunction was present in two of five experiments characterized by a jaundiced liver presentation (figure 2.15). Infarcts in the kidney (figure 2.16-A) or liver (figure 2.16-B) were present in all experiments.

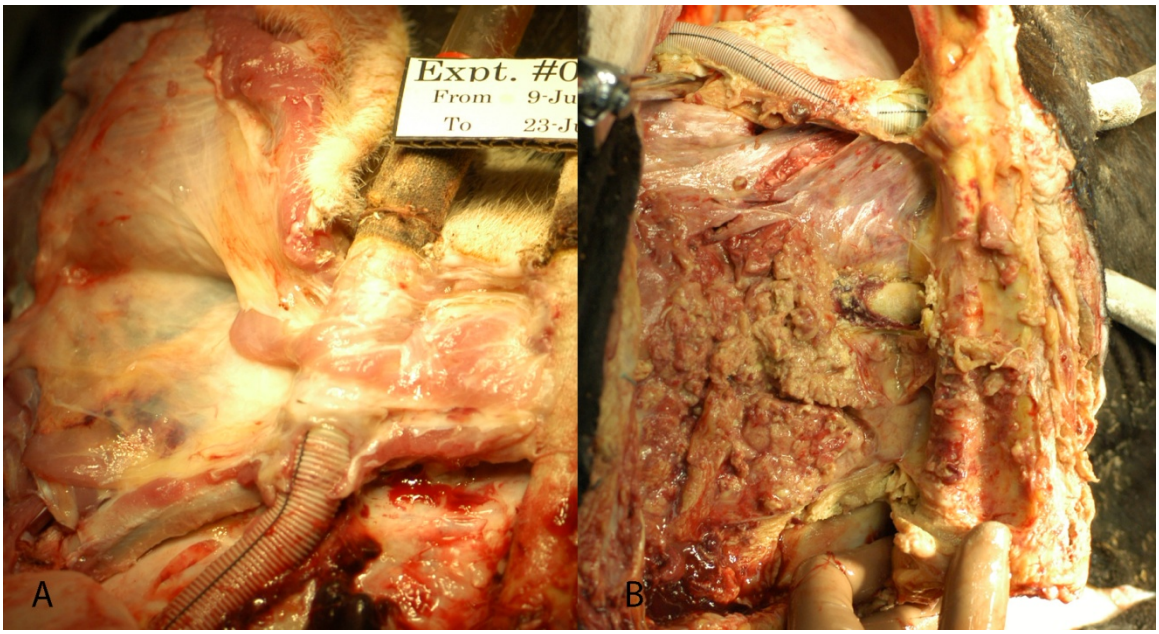

Figure 2.12. Subdermal Infection. Normal subdermal tissues (A) are contrasted with the massive infection (B) from experiment 0909.

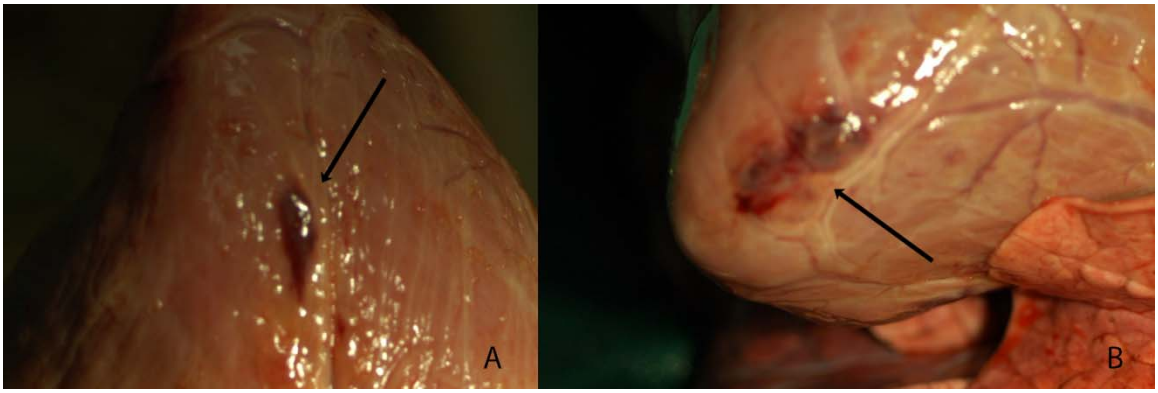

Figure 2.13. Cardiac Hemorrhage. Two cardiac hemorrhages were observed in experiment 0908.

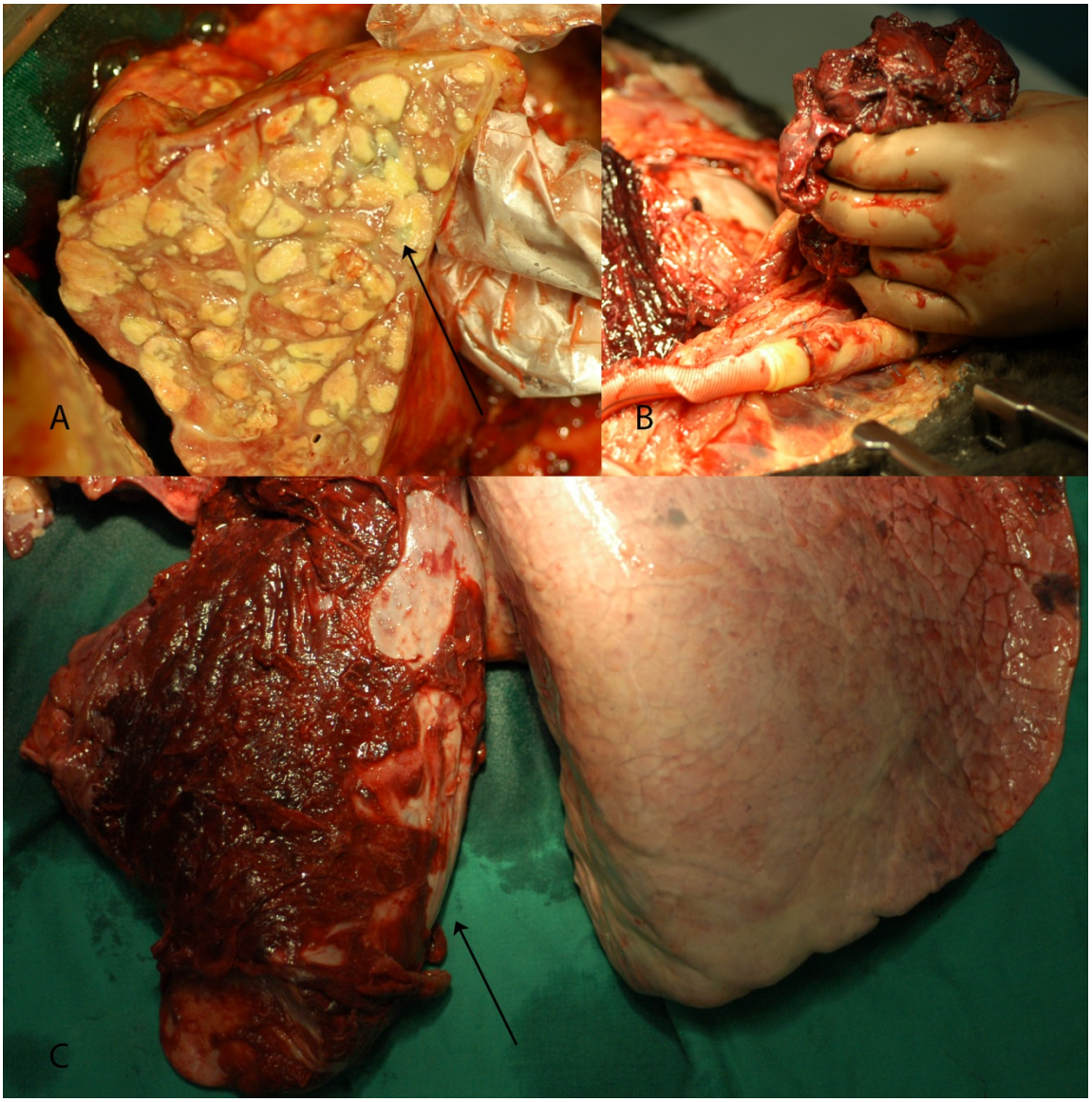

Figure 2.14. Lung Dysfunction and Ventral Hematoma. Massive lung infection with the appearance of tuberculosis is shown in A. Panel C shows a collapsed lung due to ventral hematoma, which is highlighted in B.

Figure 2.15. Liver Dysfunction. Liver dysfunction was observed as a jaundiced (yellowed) appearance.

Figure 2.16. Kidney and Liver Infarcts. Infarcts were seen in all experiments in either the kidneys (A) or the liver (B).

2.4 Effect of Rotary Blood Pump on Hemostasis In Vivo

As delineated in the introduction (chapter 1), thrombosis and bleeding complications have proven problematic in assist device therapies. In the feasibility study, four of the five animals demonstrated intra-pump-head thrombosis. Additionally there were ongoing markers of coagulation and thrombolysis indicating active hemostatic pathways.

2.4.1 Aggregometric Response. The response of platelets in plasma to adenosine diphosphate (ADP) and to collagen was measured as a function of

time on pump support. ADP is a soluble agonist that is released from the platelet upon degranulation. ADP has been shown to form a cloud around growing thrombi to help recruit additional platelets [37]. The aggregation that it produces is reversible – platelets activated with ADP can return to a resting state [6]. Collagen is a component of the vessel wall and is located in the basement membrane; this molecule provides an adhesive substrate for platelet binding in normal hemostasis.

As seen in Fig. 2.17, a statistically significant change in the percent of aggregation reversibility was observed with 20μM ADP. A slight decrease was also observed at 10μM ADP; however, this was not statistically significant. No significant changes in the percent reversibility were observed at 1 and 5 μM ADP (figure 2.17). Examining the time course of the statistically significant decrease in the percent reversibility (20μM ADP), it is evidently a short-lived phenomenon. The increase is significant on the first ($p<0.01$), third ($p<0.01$) and fifth ($p<0.05$) post-operative days. However, while a decrease may persist, it is no longer a statistically significant difference from baseline (figure 2.18).

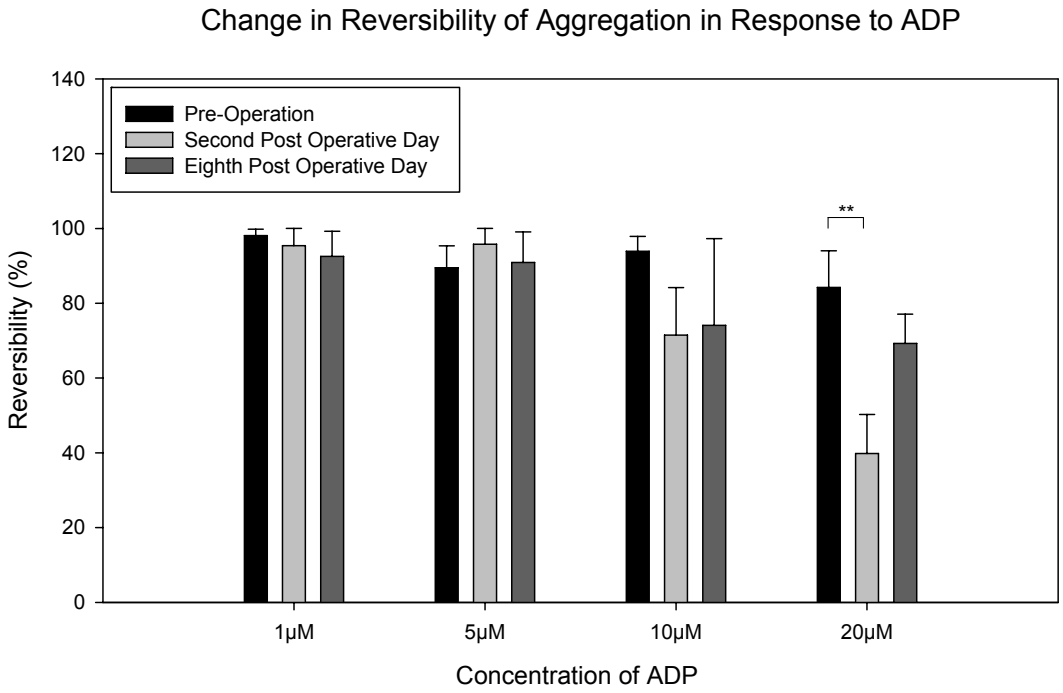

Figure 2.17. Reversibility of Aggregation Response to ADP as a Function of Concentration. Data presented as mean ± SEM. (** p<0.01)

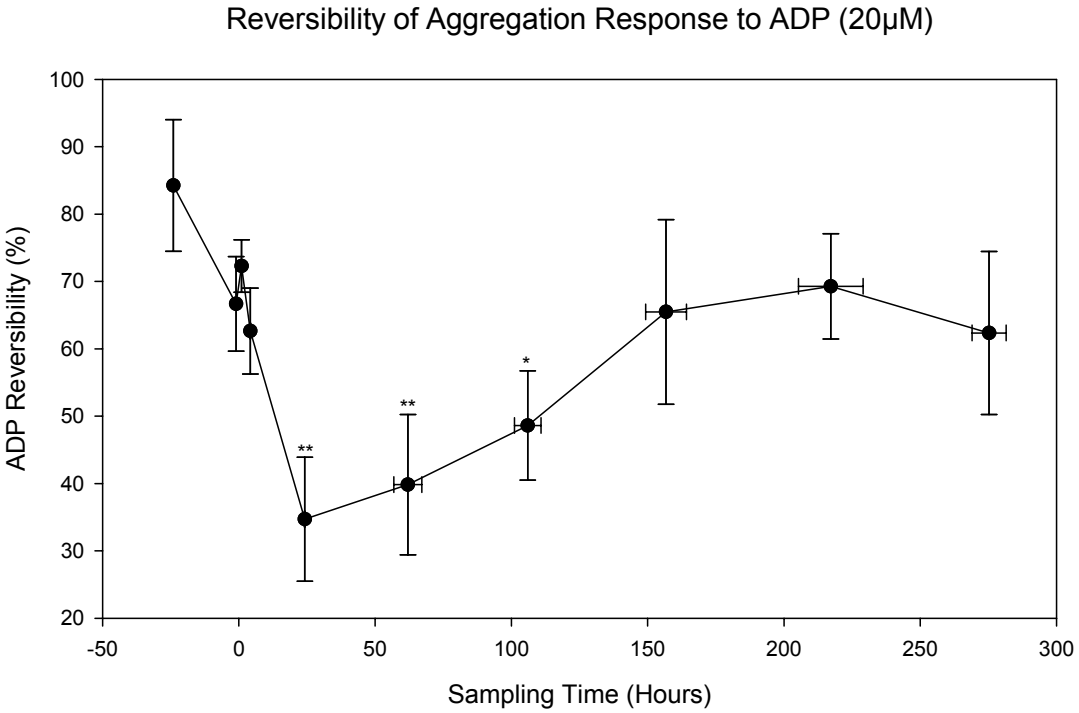

Figure 2.18. Reversibility of Aggregation Response to ADP as a Function of Time Post-Implantation. Negative hours are before the pump is started: –24 is before the operation, –1 is during the operation before the pump is started. Significance from –24 time-point noted. Mean ± SEM (ordinate), SD (abscissa). (* p<0.05, ** p<0.01)

Rate of aggregation response was monotonically increasing with increasing collagen concentrations prior to the operation with statistical significance between all of the rates. This statistically significant monotonic increase was lost in the acute phase after the operation. However the response trended back towards monotonically increasing as a function of time post-operation resulting in statistically significant monotonic increase by the sixth post-operative day (figure 2.19). No statistically significant changes in aggregometric response were seen with time after procedure at any of the concentrations of collagen studied.

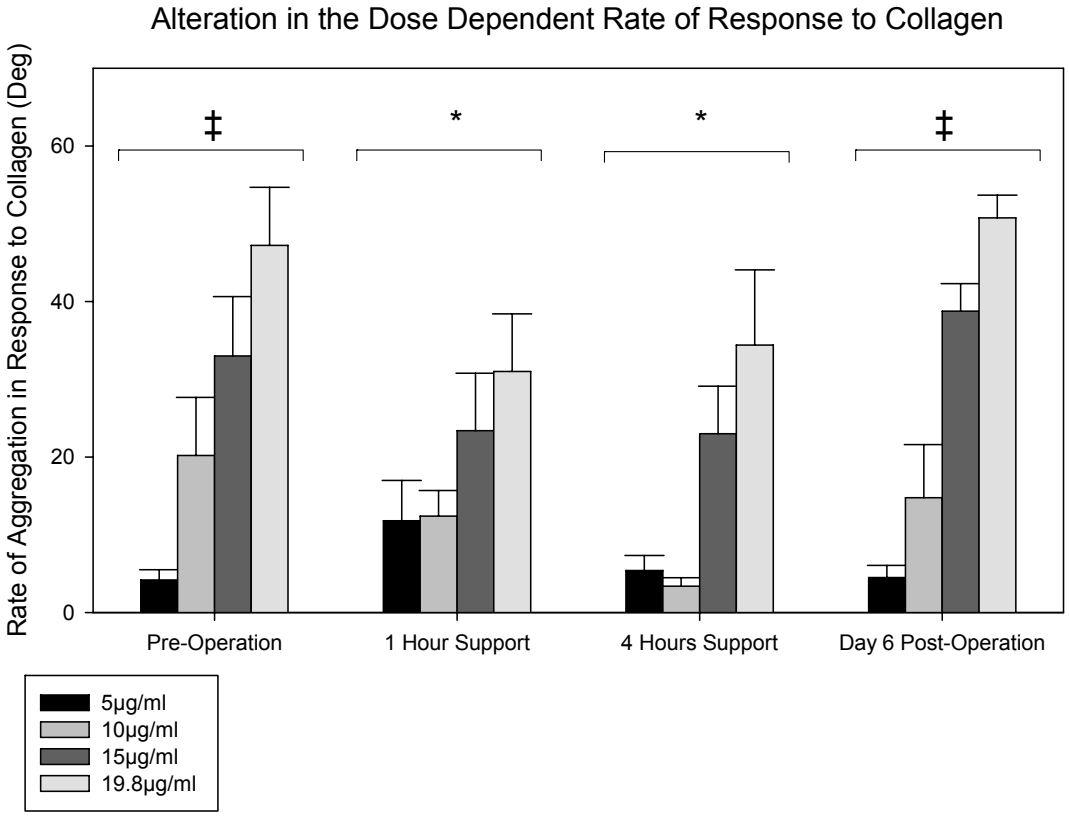

Figure 2.19. Change in Dose Dependency of Rate of Response to Collagen - ‡ indicates all values statistically significant from one another ($p<0.05$). * indicates loss of significant difference between 5µg/mL and 10µg/mL and loss of significant difference between 15µg/mL and 19.8µg/mL.

Platelets were not shown to respond to the coating material of the pump surface at any time point. An example of the response to cuvettes coated with MPC in comparison to a typical response to collagen is shown in figure 2.20. The slight drift decreasing over time is thought to be due to hydration of the MPC coating.

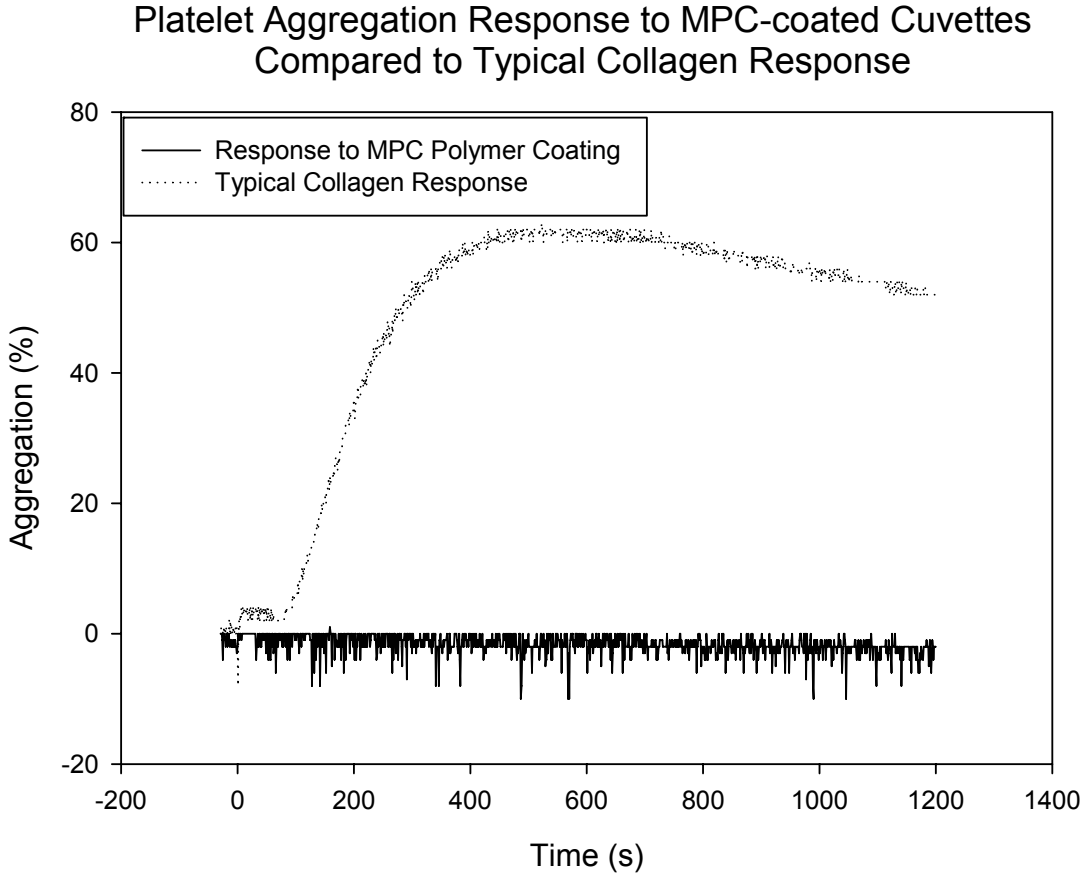

Figure 2.20. Platelet Aggregation Response to MPC-coated Cuvettes. Platelets are shown not to aggregate in response to an MPC-coated surface. A typical response to soluble collagen is shown as a reference.

2.4.2 Microparticle Populations. Microparticle populations, measured by flow cytometry in platelet poor plasma, were analyzed as a potential measure of blood trauma induced by ventricular assist devices. Additionally MPs have been theorized to contribute to thrombosis through exposure of active tissue factor on

their surfaces; they have been shown to incorporate into growing thrombi in vivo [30] possibly providing an additional source of tissue factor to propagate thrombogenesis. No statistically significant differences were seen in the microparticle population as a function of days post operation, although there appears to be a graduate increase with exposure time to the pump (figure 2.21).

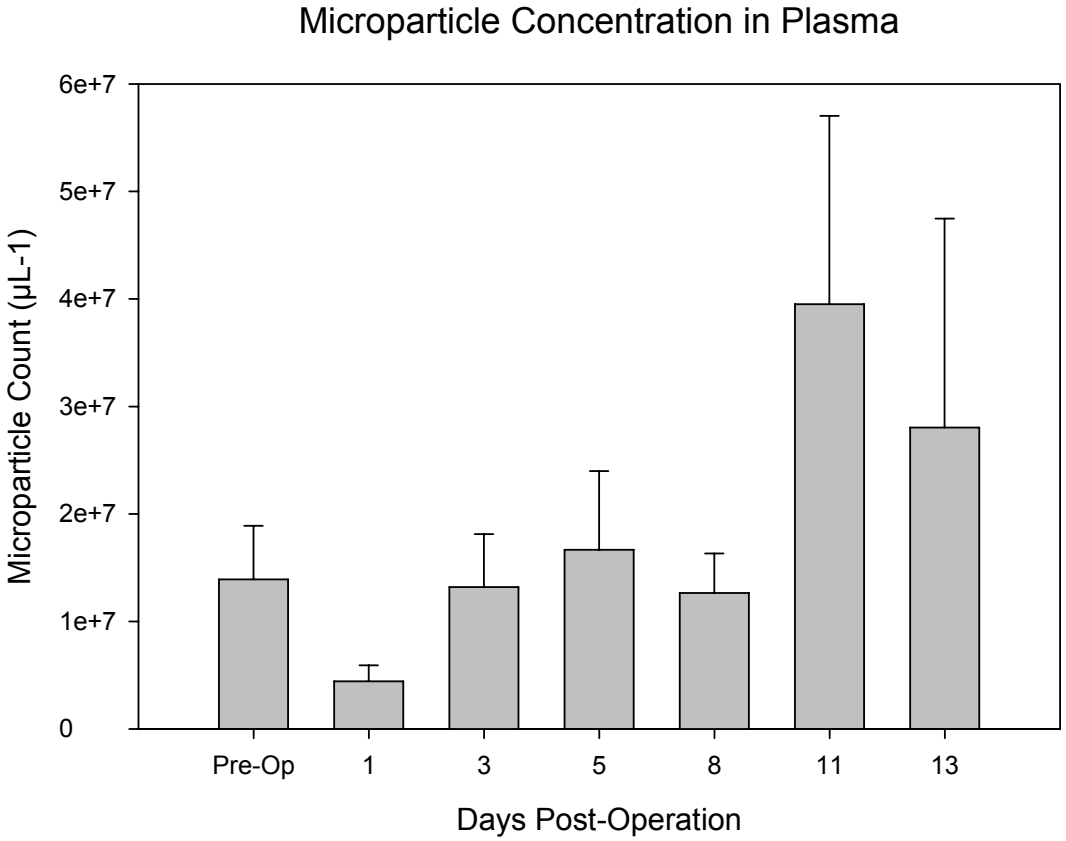

Figure 2.21. Microparticle Concentrations as a Function of Days Post-Implantation. There were no statistically significant differences among any of the time points.

2.4.3 Von Willebrand Factor Analysis Results. VWF multimer analysis was performed as detailed in section 2.2.11 and the results are shown in figures 2.22 and 2.23. The larger molecular weight multimers are shown at the top of the gel. All of the calves plasma samples exhibited decreased overall multimeric content

24 hours after surgery (as indicated by the lighter density of the column). Between the third and fifth post-operative days, multimeric appearance returned to normal. The normal appearance of VWF in calves is in contrast to what is typically observed in humans where a loss of large molecular weight multimers is observed (see section 1.7 – Ventricular Assist Devices and Acquired Von Willebrand's Disease). Because of this unexpected result from plasma samples of calves on blood pump support, the multimer composition under various controlled shear stresses and exposure times in the viscometer were investigated. Figure 2.23 shows the results of the comparison.

At 12.3 dynes/cm2, human VWF experiences increasing degradation with time culminating at 40 minutes with complete loss of multimer composition. Alternately, bovine VWF experiences minimal degradation at up to 20 minutes. The degradation of bovine VWF at 40 minutes is comparable to the degradation of human VWF at 10 minutes. At a higher shear stress of 54.2 dynes/cm2, degradation occurs at an increased rate, therefore shorter times were studied. These results indicate that bovine VWF is more resistant to shear stress induced degradation when compared with human VWF.

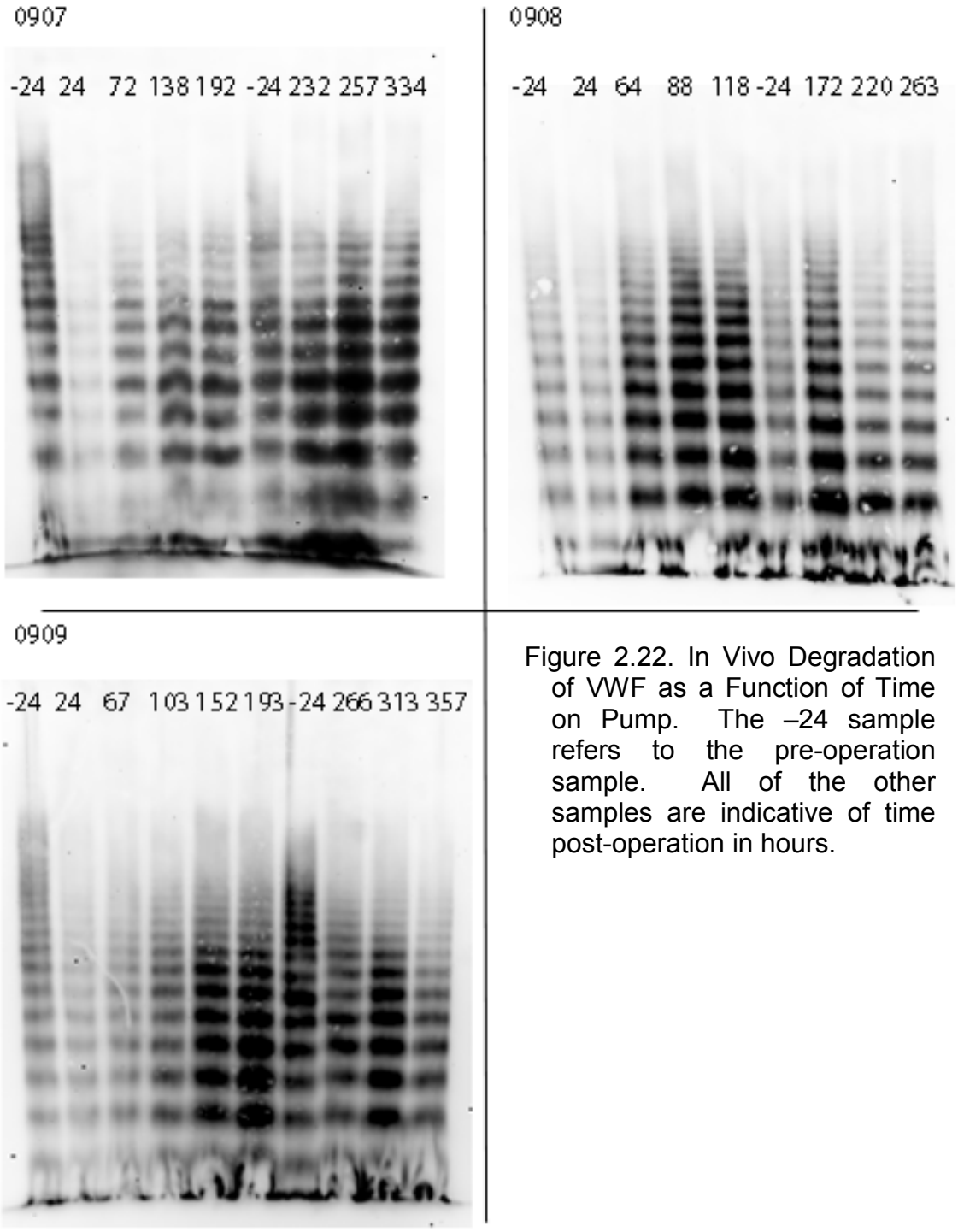

Figure 2.22. In Vivo Degradation of VWF as a Function of Time on Pump. The –24 sample refers to the pre-operation sample. All of the other samples are indicative of time post-operation in hours.

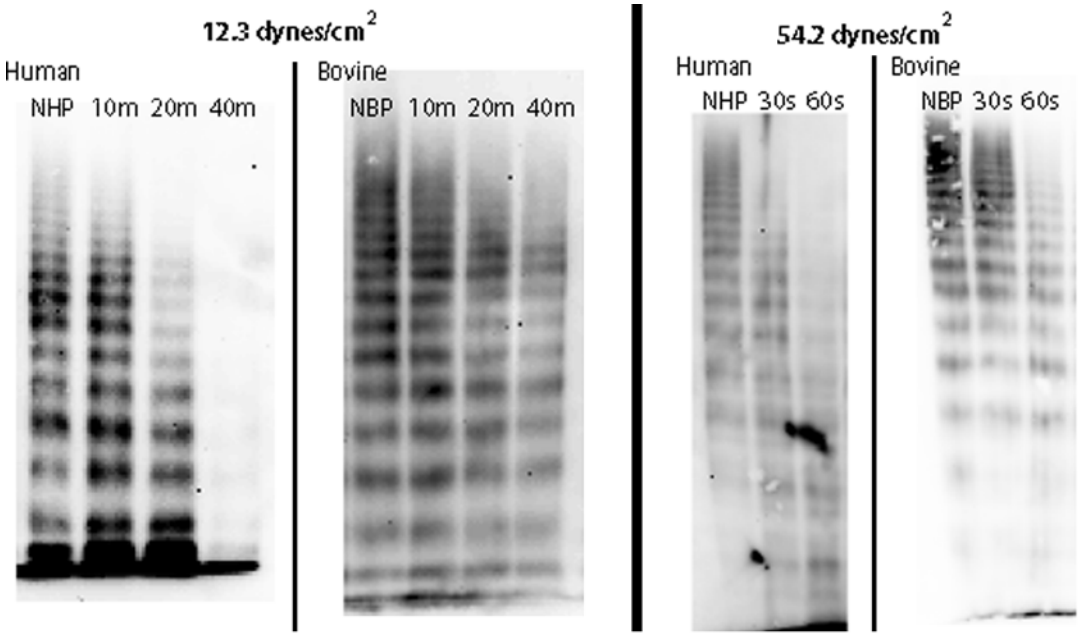

Figure 2.23. In Vitro Degradation of Human and Bovine VWF in response to Shear Stress. NHP is normal human plasma. NBP is normal bovine plasma. The sample titles refer to the exposure duration in seconds (s) and minutes (m). There are stark differences in the rate of degradation of VWF between bovine and human in response to shear stress.

2.4.4 Shear Stress Estimation within Secondary Flow Path. An area within the pump that was observed from the implant studies to be prone to thrombosis was the secondary flow path around the rotor. Examples of such thromboses are shown in figure 2.7 in section 2.3.4. The thrombi are primarily white, suggesting that they are primarily composed of platelets and were formed under high shear stresses, rather than being heavily fibrinaceous with entrapped red cells and thus red in color.

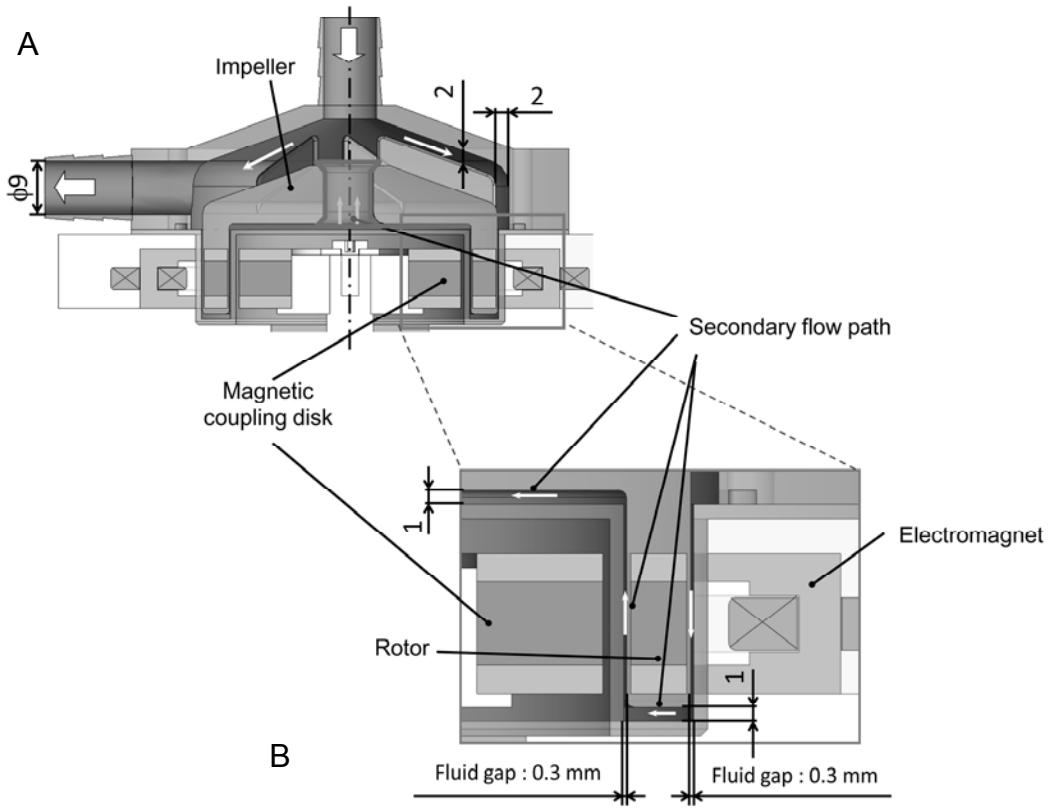

Figure 2.24. The Secondary Flow Path. A cross-section of the secondary flow path (B) of the pump head (A) is highlighted. Arrows shown in B indicate the direction of flow in the four distinct sections of the secondary flow path – one arrow per section. All measurements given are in millimeters.

The secondary flow area in the pump is designed to minimize thrombus by providing a washout region so that activated elements of the blood do not build up within the pump. However, little is known of the characteristic flow that develops within this region, specifically the local shear conditions. The shear stress environment of the pump head, and specifically within the secondary flow path (figure 2.24), has not been characterized in the investigational pump used in this study. In effort to provide insight, first-order analysis, a relatively simplified approach was undertaken, using estimated geometries and flow profiles. A previously published study of a pump similar to the one used in this study, which

had been scaled based on the Reynolds Number, concluded that at 2000 rpm the flow can be simplified as Couette type flow (figure 2.25) [82]. This study was performed in the same lab using a precursor to the design used here. For all flow areas, it was assumed the flow is only due to the velocity of the rotor – flow due to pressure gradients or centrifugal pumping were neglected. This permits a conservative lower-bound estimate of the shear forces based on RPM measurements.

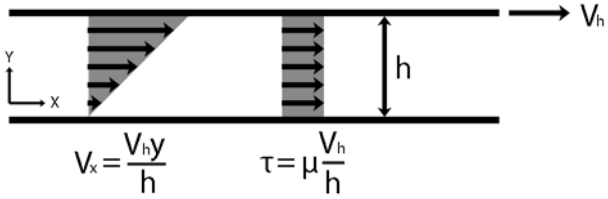

Figure 2.25. Couette Flow. Flow between two parallel plates one of which moves at velocity (V_h) results in constant shear stress

Because the flow through the secondary flow path can be simplified to Couette type flow, the primary determinants of shear stress are the gap height and the wall velocities, which is the product of the angular velocity and the radial position. The flow profile is described by the first equation in figure 2.25 [80], where V_x is the velocity in the x direction and V_h is the velocity of the moving wall at height h. Shear stress in Couette flow is relatively constant and given by the second equation in figure 2.25, where τ is the shear stress and μ is the viscosity. The viscosity of bovine whole blood is assumed to be 4.8 cP [83].

From this analysis, the highest shear stresses will be in the outer most face of the secondary flow path where the fluid first enters the secondary flow path. The gap is minimized at 0.3mm and the radial position on the rotor is maximized at R_r = 25.3mm. The highest rotations per minute (RPM) used in this study were 2300 RPM. The lower bound estimate of shear stress a packet of

fluid would experience as it moves through the secondary flow path is shown in figure 2.26. In two areas of the secondary flow path, the shear stress was independent of radial position characterized by constant shear stress with position through the secondary flow path. Whereas the other two areas will vary with the radial position due to the dependence of the upper plate velocity on radial position in that specific geometry, which is similarly characterized by decreasing shear stress. The calculated shear stresses are elevated from what would normally be experienced within the vasculature.

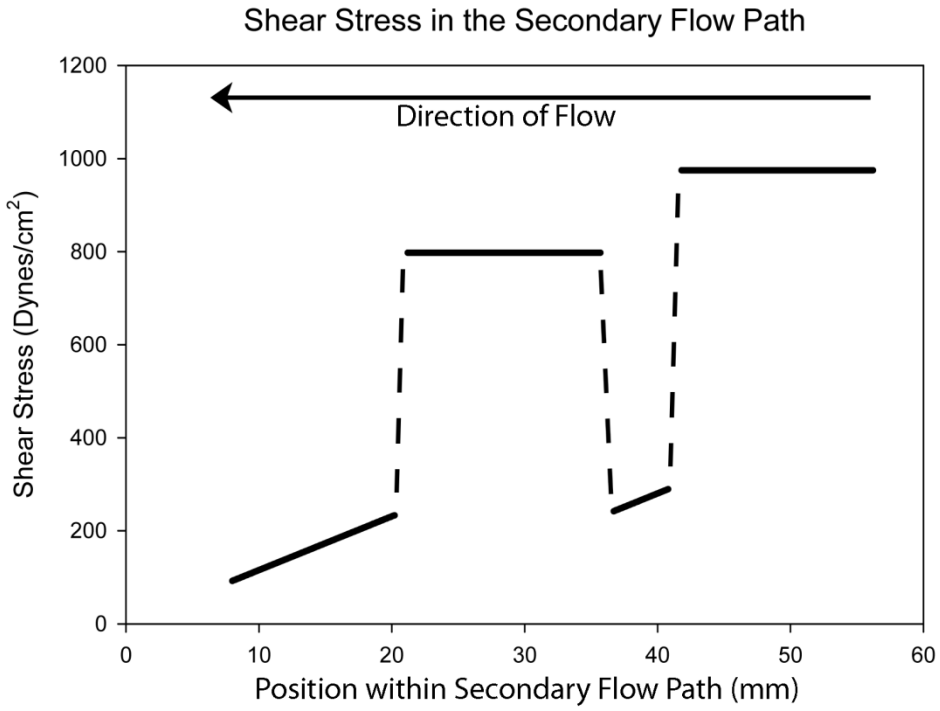

Figure 2.26. Shear Stress approximation within the Secondary Flow Path. Shear stresses calculated are shown as solid lines, whereas areas of complex flow are shown as dashed lines. Shear stresses are calculated at the maximum RPM used for this set of experiments (2300 RPM).

2.5 Discussion

The three main barriers to effective treatment with ventricular assist devices, as discussed in chapter 1, are: infection control, device longevity, and

hemostatic complications. The causes of infection and methods to mitigate those causes are being addressed in a multifaceted way, including decreased size of and ultimately elimination of the percutaneous lead and reduced pump size allowing for implantation in the pericardial space. Furthermore, the newest generation of devices could theoretically last indefinitely, with few moving parts and no sites for physical wear. Contrary to these two well-defined and understood barriers stands the problem of hemostatic complications including bleeding and thromboembolic complications, which are not well defined or understood.

Recent studies have demonstrated increased gastrointestinal bleeding is likely due to the loss of the larger molecular weight fraction of VWF (acquired VWD.) Additional studies have begun to evaluate hemostatic complications in animal models before pump designs begin implantation in humans. However, an evaluation of the animal models ability to reflect what has seen clinically has not been assessed. With recent clinical studies, it is now possible to begin evaluating the animal model, which is the primary concern of this chapter.

Two major hemostatic complications associated with ventricular assist device therapy include device originated thromboembolic complications and device-associated bleeding. The ability of the animal model to parallel these complications was assessed in this study. Of particular interest were markers of coagulation, platelets reactivity, and VWF degradation. *In vivo* experiments require very significant effort; these experiments were conducted as part of a large team in Tokyo, Japan. Dr S Takatani led experimental efforts. Dr E

Nagaoka led surgical and recovery efforts with the assistance of lab personnel. I worked as part of the lab personnel and conducted the experiments directly related to this thesis. From this experience, I learned the difficulty in planning, performing, and evaluating results from in vivo experiments. While these feasibility studies will continue to be necessary, they require a large amount of effort and, at least for the purposes of this thesis, they may not be the most suitable methodology to evaluate perturbations to the hemostatic system.

2.5.1 Anticoagulant and Antiplatelet Therapy. Patients on various third-generation devices frequently receive both an anticoagulant, such as coumadin (an inhibitor of vitamin k dependent coagulation factor synthesis) and antiplatelet therapy – usually aspirin, which irreversibly inhibits cyclooxygenase and the thromboxane dependent pathway of platelet aggregation. However, bovine typically receive only heparin, as is the case in this study, or heparin in combination with Coumadin; in some instances no anticoagulant/antiplatelet agent is administered [64]. Heparin enhances the function of antithrombin III in scavenging thrombin produced in the coagulation pathway. The lack of a specific antiplatelet therapy in bovine feasibility studies may be responsible for some of the increased thromboembolic complications.

2.5.2 Surgery and Thrombosis. The surgery to implant ventricular assist devices causes major tissue trauma, which results in an increased hemostatic/thrombotic response. This response to trauma may complicate the thrombotic response elicited by the pump directly. A study with mock implantations in a bovine animal model indicated effects of surgery persist

approximately 17 days post operation [73]. Therefore, it is thought, the transient changes could be both a function of surgery and the implantation of the pump.

2.5.3 Infection and Thrombosis. Infection has been definitively linked to thrombosis. Blood infection is one of the primary causes of disseminated intravascular coagulation (DIC). DIC leads to the formation of circulating microthrombi in the presence of highly active fibrinolysis and coagulation cascade. Infection is a common problem with ventricular assist devices. This device, being place extracorporeally, is particularly susceptible to infection. It has large diameter percutaneous tubing carrying blood both to and from the pump, which is positioned on the back of the animal. The large surface area of the percutaneous tubing increases the potential for infection. However, this device is an acute experiment and the pump is not intended for long-term support. Patients would not leave the hospital with this device in place; it is intended for bridge-to-bridge, bridge-to-decision, or bridge-to-recovery type applications. Careful and frequent cleaning of the wound site post-surgery could mitigate some of these problems.

2.5.4 Comparison of Bovine model with Clinical Observations. A number of hemostatic studies have been tacked on to feasibility studies, and the results of feasibility studies with respect to intrapump thrombus formation have influenced pump designs. However, it remains unclear how predictive the thromboembolic complications with bovine are in relation to what will be seen clinically in humans.

2.5.4.1 Aggregation response to ADP and Collagen. A previously published report [75] highlighted some of the differences in platelet aggregation response

among species. From those previously published studies it is apparent that bovine consistently responded to ADP and collagen but to a lesser degree compared to humans at the same agonist concentrations.

While the species differences in response exist, consistency in functional alterations caused by device placement may indicate sufficiently similar response to ventricular assist devices for inter-species extrapolation. As reported above, any changes in platelet aggregation observed in bovine implanted with the MedTech Dispo were not persistent. All of the changes observed could be due to the surgery (the tissue trauma or the anesthesia) or the blood may become acclimatized to the conditions of the pump after a short time frame. In the late term of the study, which may still have some lingering effects from surgery, any effect seen in the very near term has abated. The absence of a change in platelet response to ADP and collagen is in agreement with previously published results in humans by Klovaite et al conducted a mean of 151 days post-implantation [44]. While Klovaite et al did not note an impaired functional response to ADP or collagen, they did note an impaired VWF-dependent platelet aggregation in patients implanted with the HMII. They noted the effect was both associated with the plasma (when combined with normal platelets) and with platelets (when combined with normal plasma). They theorized this could be due to VWF degradation product interference with platelet receptors for VWF.

There are several means for assessing impaired VWF activity. Bovine response to ristocetin, a VWF dependent aggregation agonist, has proved inconsistent and frequently results in fibrin formation at higher concentrations.

This assay was not performed in our studies. Instead, the presence of bovine VWF was assessed by gel multimer assay.

2.5.4.2 VWF Degradation. The 24-hours on pump support sample showed decreased overall VWF concentrations evidenced by consistently lighter bands at this time point. After this decrease, multimeric content returned to normal while on pump support. This was an unexpected result when compared with what has been reported clinically in humans; this finding prompted studies directly comparing the shear stress degradation rates of human and bovine plasma. These studies found markedly decreased degradation of VWF in bovine plasma compared to human plasma.

The most likely cause of the overall loss of all multimers of VWF in bovine at 24-hours post-implantation is consumption of VWF in the hemostatic and/or thrombotic response to the surgery. VWF plays a critical role in both normal hemostatic function and in shear-related platelet-platelet aggregation leading to thrombosis. The subsequent return to a normal multimeric VWF is distinctly different from what has been reported clinically. As shown, multimers of VWF can be degraded due to shear forces, but only for longer exposure times. This suggests that bovine VWF may be more resistant to shear stress induced degradation compared with humans. The resistance of bovine VWF to degradation may protect bovine from bleeding diatheses, but may also predispose them to thromboembolic events on these devices. The reasons underlying the resistance to degradation are currently unknown.

It is concluded because of this difference in degradation, incidences of pump-derived thrombosis and thromboembolism in bovine animal models may not be predictive of pump performance in humans.

The difference in degradation of VWF between the bovine animal model and what has been demonstrated clinically is of the utmost importance when assessing hemostatic changes as a result of ventricular assist device placement in a bovine animal model and extrapolating to what would be expected in humans. The degradation of VWF results in several clinically relevant complications including gastrointestinal bleeding (see section 1.7). Conversely, the lack of degradation of VWF could result in increased thromboembolic complications due to the pivotal role of VWF in platelet aggregation under high shear stresses such as those within ventricular assist devices.

2.5.4.3 Thromboembolic complications. Thromboembolic complications (as presented in section 2.3.6 Necropsy Results) were seen in all experiments and included kidney and liver infarcts likely resulting from emboli originating from the pump. Furthermore, intrapump thrombosis was seen in all experiments, providing a possible nidus from which emboli formation occurs. Given the established role of VWF in platelet thrombus formation at high shear stresses it is hypothesized that these thromboembolic complications stem from the continued presence of HMW VWF, and may be less important in humans. A study comparing control animals to implant animals found no kidney infarcts in the control animals but as many as 5 infarcts were observed in otherwise uneventful implant animals [73].

Furthermore, the geometry of the secondary flow path where the thromboembolic complications are likely to have originated results in decreased flows and intermittently increased shear stresses as a packet of fluid moves through the secondary flow path. This could result in areas where platelets have increased interaction with one another, particularly the converging, moderate shear stress regions. The gap sizes in the pump are smaller than areas of the vasculature where platelet thrombi have been known to occlude the lumen such as in coronary or stenosed vessels. In the case of vessel stenosis, pathophysiologically elevated shear stresses are achieved followed by sudden deceleration and formation of recirculation eddies or stagnation zones. This has been shown to result in the activation of platelets, formation of microparticles and thrombi, which can subsequently embolize [34]. The combination of narrow spaces, high shear stresses upstream, and sudden deceleration creates zones that are conducive for thrombus formation. Furthermore, the lower bound shear stress estimate calculated in section 2.4.4, will be elevated when a more representative, and therefore more complex, flow system is considered.

2.5.4.4 Microparticles. Microparticles can be derived from all cell types, but most circulating microparticles are platelet-derived [26]. Microparticles were hypothesized to increase on pump support. However, they were not observed. This may be due to the fact that microparticles *in vivo* have a very short half-life. Previous studies in mice [21] and rabbits [60] have shown platelet-derived microparticle life spans of 30 minutes and 10 minutes respectively. This could result in a diminished accumulation of microparticles *in vivo*. In addition, with on-

going thrombosis, microparticles have been shown to incorporate and aid in propagation of growing thrombi *in vivo* [30]. The increased rate of microparticle production could be counter-balanced by increased consumption due to on-going thrombosis, which was demonstrated with increased circulating active hemostasis markers (section 2.3.5).

2.6 Conclusions

The most important finding of this study is the difference in VWF degradation in bovines and humans. It is clear that this result has implications for thromboembolic events as well as later bleeding complications. In feasibility studies thromboembolic events may result in changes to pump design to reduce likelihood of these complications later, but this trade off is not weighted against bleeding complications that are likely to occur clinically – particularly the increased gastrointestinal bleeding seen in this patient population that are not reflected in the bovine animal model. Careful consideration must be made when weighing what changes will yield meaningful results and not result in increased complications. Bleeding complications and thromboembolic complications are two sides to the same coin with protective overcompensation in one causing problematic responses in the other.

CHAPTER 3

IN VITRO EVALUATION OF VARIOUS ROTARY PUMP DESIGNS

In the previous chapter, we investigated a new type of heart assist pump *in vivo* in a bovine animal model. Such a study has severe limitations associated with determining the specific properties of the flow device and the extent to which such a device might be effective in man. Firstly, while the whole animal model is useful for determining the ability of the pump to operate under conditions that are necessary to support life, there is no adequate animal model that precisely parallels the cardiovascular behavior of humans. The bovine model is not optimal for the comparison of thromboembolic and bleeding complications associated with varied pump designs; in fact our previous studies suggested that bovine VWF may behave quite differently than the human protein in response to mechanical stress. Secondly, such studies are very expensive, even those conducted over a period of two weeks. And even in that period of time, numerous episodes, including thrombosis, pump stoppage, infection and even death occurred. Thus, an alternate methodology was developed for testing pump characteristics that is cheaper, more reliable and utilizes human blood.

In this chapter, we have designed an *in vitro* loop to evaluate a range of blood responses to three different pump designs. These designs included two experimental third-generation (non-contact bearing) designs and one commercially available second-generation design (contact bearing) design. This study eliminated the need for interspecies extrapolation because the comparisons were made using human blood. The design of the testing

minimized the effect of donor variability by using the same donor blood for each pump design.

3.1 Introduction

In vitro experiments with ventricular assist devices primarily focus on pumping ability, including such measures as head pressure-flow rate curves (termed H-Q curves) and the effect of the pump on blood trauma or damage. A defining parameter for a heart assist pump is that the pumps produce a low level of hemolysis or free hemoglobin in the blood in response to recirculation through an in vitro loop. Rarely are more sophisticated methods developed that would test the effect of the pump on the various hemostatic and thrombotic parameters in the blood. And never are such measures used to assist in the design of next generation pumps. This chapter is an effort to develop a methodology that would not only assess a pump's characteristic behavior with respect to hemostatic/thrombotic activation of blood parameters, but also to compare the behavior of several different pump types with the long range goal of becoming an effect tool for future design of such pumps.

3.2 Materials and Methods

The effect of 3 different ventricular assist device designs on human blood was evaluated in an *in vitro* flow loop. Human blood from the same donor was used in all three pumps tested to minimize the influence of donor variability. Platelet and coagulation related measures were of primary interest. This study design allows for better comparison of hemostatic complications induced by varied pump designs that would be more easily controlled and ideally more

clinically relevant than studies in the bovine animal model. The increased relevance would be due to the differences among animal species such as, the differences in rates of VWF degradation in response to elevated shear stresses, as demonstrated in chapter 2 of this thesis. These findings contrast to other clinical studies with patients receiving these devices and the pervasiveness of complications due to acquired VWD in patients receiving the new continuous-flow assist devices (see section 1.7 Ventricular Assist Devices and Acquired Von Willebrand's Disease).

3.2.1 Ventricular Assist Devices. The three pump designs tested were: a commercially available axial VAD with contact bearings (HeartMate II, Thoratec, Pleasanton, CA); an experimental miniaturized axial pump without contact bearings (corporation information confidential – hereafter referred to as axial VAD); and an experimental centrifugal pump without contact bearings (corporation information confidential – hereafter referred to as centrifugal VAD). The HeartMate II (HMII) is the only currently FDA-approved VAD available to heart failure patients. It is used here for comparison to what is currently available. The two experimental VADs represent advancement to third generation devices without contact bearings. The axial VAD is miniaturized to aid in expansion of patient population to which this therapy is available and decrease the implantation time to reduce the risk of infection and surgical complications. The centrifugal VAD has lower operational speeds, with the intent of decreased shear stress profiles and presumably decreased blood trauma.

All pumps were run at 4L/min and the corresponding RPM displayed in Table 3.1. Resistance was adjusted with flow restrictors to achieve and maintain the desired flow rate. Flow rate was directly measured with a transonic flow probe (Transonic Systems Inc, Ithaca, NY).

Table 3.1: Pump RPM values

Pump	RPM
HMII	10,000
Axial VAD	18,000
Centrifugal VAD	2,800

3.2.2 In Vitro Flow Loop. Healthy normal volunteers donated 240 ml of whole blood. Blood was collected by venipuncture in heparin anticoagulant (5U/L final concentration). Baseline samples were separated and the remaining 220 ml was used to prime the flow loop. A port in the flow loop (figure 3.1) was utilized to both fill the loop and collect samples. The loop was maintained at 37oC with a temperature-regulated air jacket for the duration of the experiment. After the loop was primed, a jump-start of the pump (quickly turned on then off again) helped dislodge any bubbles trapped within the pump (not visible). The prime sample was collected prior to starting the pump. Once the RPM and flow rate of the pump were stabilized, samples were collected at 0, 2, 5, 10, 20, 40 and 60 minutes after stabilization. Additionally, baseline and drain samples were incubated at 37ºC for 4 hours after the end of the flow loop testing to examine

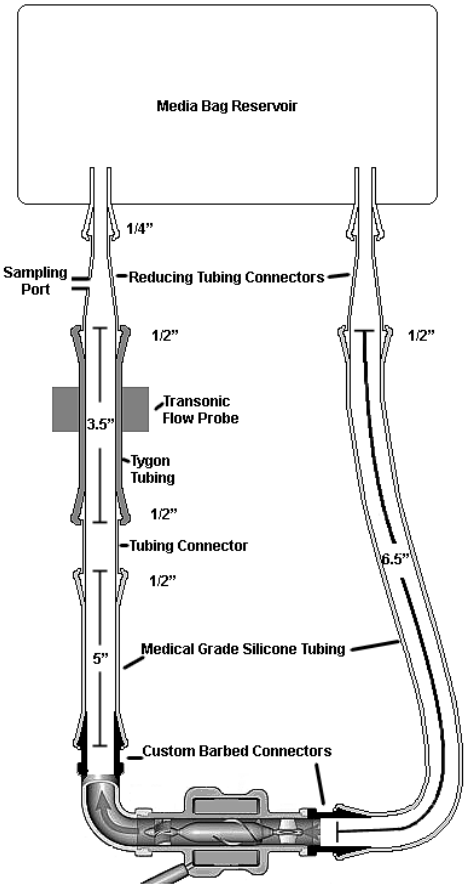

Figure 3.1 Schematic of Flow Loop. The design of the flow loop with the HMII is shown. Minor alterations were necessary for the different diameters of the connectors of the axial and centrifugal VADs.

any increase in expression or production of procoagulant factors that might be produced by synthetic activity of blood cells.

3.2.3 Blood Donors. Blood from six donors was used for each of the pumps for a total of 18 trials (n=6 per pump). Blood donations were performed in accordance with IRB approval. The order of the pumps selected for each donor was randomized. Donor demographics are detailed below in table 3.2.

Table 3.2:Donor Demographics

Age (years)	27 ± 5
Sex	
-Male	3 (50%)
-Female	3 (50%)
Racial Profile	
-Caucasian	3 (50%)
-Asian	2 (33%)
-Persian	1 (17%)
Weight (lbs)	138 ± 11

3.2.4 Hemolysis. Hemolysis is the current gold standard for comparing blood trauma among multiple pumps. The free hemoglobin (freeHb) was determined by QuantiChrom, a colorimetric hemoglobin assay kit (BioAssay Systems, Cat# DIHB-250). Hemolysis can be compared directly using free hemoglobin or through the use of the normalized index of hemolysis (NIH). The normalized index of hemolysis is a measure of the change in the mass of free hemoglobin in grams (ΔfreeHb) per 100L of blood pumped through the loop and given by the following equation [24]:

$$NIH(g/100L) = \Delta freeHb \; x \, V \; x \frac{100 \; x \; Hct}{100} \; x \frac{100}{Q \; x \; T} \qquad \text{(Eq 3.1)}$$

where V is the volume of the loop in liters, $\Delta freeHb$ is the change in plasma free hemoglobin (g/L) over the selected sampling time, Hct is the hematocrit (the volume proportion of erythrocytes in whole blood), Q is the flow rate in liters/minute, and T is the sampling time in minutes.

3.2.5 Platelet-Rich Plasma Particulate Size Distribution. The size distribution of particulates in platelet-rich plasma was measured from 0.68 - 12μm with a Multisizer 3 coulter counter (Beckman Coulter, Brea, CA). The coulter counter measures the size distribution of particles in suspension using the Coulter Effect. As particles flow through a charged aperture they change the electrical resistance within the microchannel of the aperture. This change in resistance results in voltage spikes which are correlated to size.

Coulter counters allow for the rapid analysis of the size distributions of large populations of particles. However, this methodology is limited at the low range due to electrical/vibrational interference and particulates within the sample diluent. To minimize electrical and vibrational interference, the instrument was placed on a benchtop spatially isolated from all other major equipment. To minimize diluent particulate, the sample diluent was filtered with a 0.1 μm polyvinylidene fluoride (PVDF) syringe filter (Millex, Cat#SLV033RS).

The size distribution of platelet-poor plasma particulates (including platelets, microparticles, and cell debris resulting from apoptosis or membrane shedding) was given as a histogram. In figure 3.2, the average of 10 baseline samples is shown. This was used to delineate the platelet population from the microparticles and cell debris, which was low in all baseline samples. In figure 3.2, greater than 90% of the population had an effective diameter between 1.6-4.0 μm. This was defined as the platelet population. Cell debris resulting from blood trauma was defined as particles with diameters below 1.6 μm.

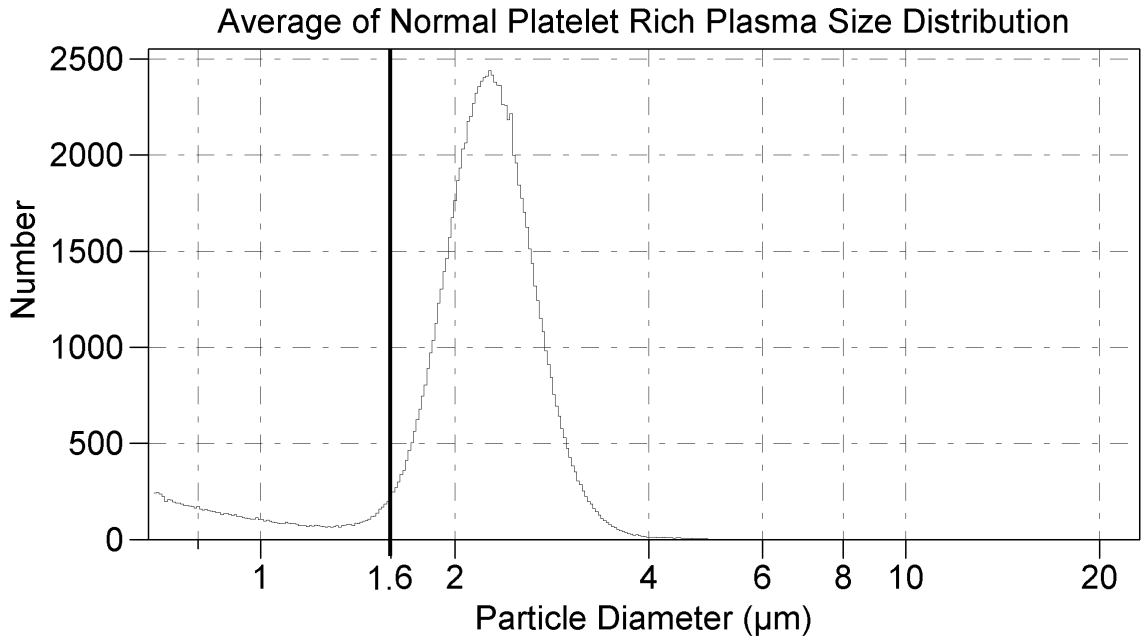

Figure 3.2: Baseline PRP Population Size Distribution. Microparticles are defined as events below 1.6 µm whereas platelets are the population between 1.6 and 4 µm.

3.2.6 Platelet Population Analysis. Platelet populations were analyzed at the University of Chicago flow cytometry facility. Populations were determined from whole blood samples with no additional processing to minimize inadvertent activation. The entire platelet population was stained with mouse anti-human CD41a antibody directly conjugated to a fluorescein isothiocyanate (FITC) fluorochrome (Beckton Dickinson, Cat# 340929, clone HIP8). This antibody has been demonstrated to bind to both resting and activated platelets equally [14]. In order to detect activated platelets, the cells were labeled with mouse anti-human CD62P antibody directly conjugated to a phycoerythrin (PE) fluorochrome (Beckton Dickinson, Cat# 555524, clone AK-4). The concentration of antibody used to stain the samples was determined specifically for this application.

The following isotype controls were chosen based on manufacturer recommendation and used at the same concentration as the antibody: Mouse IgG1 FITC (Beckton Dickinson, Cat# 349041) and Mouse IgG1κ PE (Beckton Dickinson, Cat# 555749). Counting gates were set by comparing stained samples with their respective isotype control at all time points. After staining, samples were fixed with 1% paraformaldehyde at 4˚C and kept on ice until analysis. Test samples were made up as shown in table 3.3 for each sampling time point.

Stopping gates were set to obtain 10,000 platelet events on all samples. AccuCount Ultra Rainbow Fluorescent Particles 5.0-5.9μm in diameter (SpheroTech, Cat# ACURPF-50-10) were included in the CD62P test sample for quantification of platelet population concentrations ([P], cells per μL). The beads have a wide range of fluorescence, therefore they must be excluded with

Table 3.3. Sample Staining Outline

Test Sample	FITC Isotype	CD41a Ab	PE Isotype	CD62P	Beads
FITC Control	X				
CD41a Sample		X			
PE Control		X	X		
CD62P Sample		X		X	X

Boolean (NOT(Beads)) operators when gating (Boolean gating not shown in figure). The population concentrations are determined by:

$$[P] = \frac{E_t E_p}{N_p V_t} \qquad \text{(Eqn 3.2)}$$

where Et is the number of events in the test sample, Ep is the number of AccuCount Fluorescent particle events, Np is the lot specific number of particles per 50 µL, and Vt is the volume of test sample initially used.

Gating populations for analysis are detailed in figure 3.3. Using the FITC vs. SSC scatter plot, the entire platelet population is delineated. CD62P expression, a measure of platelet activation, can be examined using the PE vs. SSC scatter plot with each population examined independently. Furthermore, individual platelets can be discriminated from platelets associated with increased granularity (events not within the individual platelet sub-population). The increase in granularity may be due to the presence of white blood cell associated platelets or increases in circulating microthrombi.

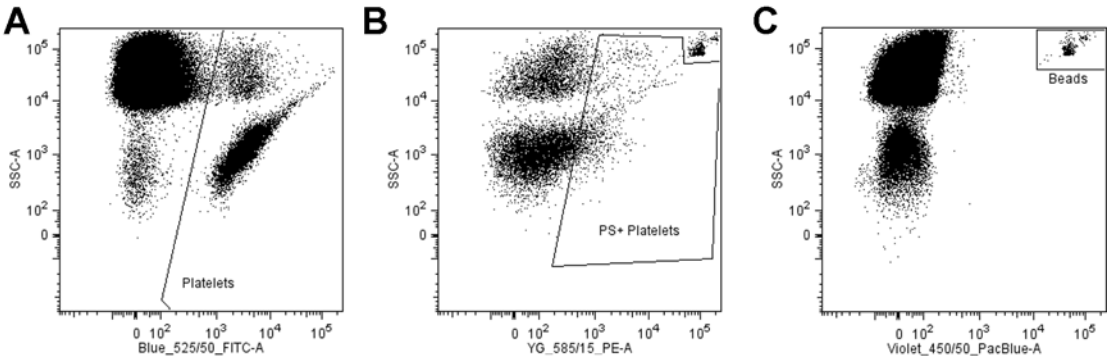

Figure 3.3 – Population Gating for Flow Cytometry – The entire platelet population (A) is labeled with FITC conjugated anti-CD41a antibody. P-Selectin expression (B) is labeled with PE conjugated P-Selectin antibody. For quantification, “Beads” (D) at a known concentration were included.

3.2.7 Von Willebrand Factor Multimer Analysis. Von Willebrand factor multimer analysis was conducted as previously described in section 2.2.11.

3.2.8 Deposit Observation. Upon completion of the experiment, the remaining blood in the loop was filtered through a 400 μm screen. Each pump was back-flushed with phosphate buffered saline (PBS) followed by a cleaning protocol. All cleaning materials were also passed through the screen. Any deposits found in the screen were removed with forceps and placed in PBS until the completion of the cleaning protocol whereupon they were fixed in 10% formalin. Brightfield images were taken of the deposits.

3.2.9 Coagulation Based Assays. Coagulation based assays were preformed at the College of New Jersey (Ewing, NJ). Prothrombin fragment was measured with a commercially available ELISA kits (Enzygnost F1+2, Siemens Healthcare Diagnostics Inc., Deerfield, IL). Tissue factor antigen was measured with a commercially available kit (IMUBIND® Tissue Factor ELISA, American Diagnostica Inc., Stamford, CT). All kits were performed according to manufacturer protocol.

3.2.10 Statistical Analysis. Statistical significance between groups was determined with analysis of variance (ANOVA). Since the blood from the same donor was used on all three pumps, repeated measures (RM) ANOVA was used on the total hemolysis and cell debris data. In both ANOVA and RM ANOVA, Student Newman-Keuls (SNK) post-hoc test was used to compare groups. Peaks in the percent P-selectin positive platelets were compared to the percentage at time 0 with paired t-tests. Also, the initial and final percent P-

selectin positive platelets were also compared with paired t-tests. In all statistical methods, $p<0.05$ was considered statistically significant. Data is presented as mean ± SD in the text and mean ± SEM in the figures.

3.3 Results

3.3.1 Plasma Free Hemoglobin as an Indicator of Blood Trauma. Hemolysis is the most commonly used standard measure for blood trauma. In our studies, the plasma free hemoglobin values were determined for each time point studied. The initial value for free hemoglobin (time 0) was subtracted from all plasma free hemoglobin values in order to measure specifically increases in free hemoglobin as a direct result of the pump (small values of hemoglobin may be released by the blood draw and loop priming). Figure 3.4 shows the increase in plasma free hemoglobin over time for each pump. Linear regression analysis was performed on each pump as a function of time and the slopes of the regression lines (subsequently referred to as rates of hemolysis) were compared.

Among the three pumps analyzed in this study, the centrifugal VAD induced the least amount of hemolysis over time. The centrifugal VAD had both the lowest rate of hemolysis and the lowest total hemolysis. The rates of hemolysis were 2.455 ± 3.010 mg/dL/min, 0.907 ± 0.565 mg/dL/min, and 1.889 ± 0.742 mg/dL/min for Axial VAD, centrifugal VAD and HMII, respectively. The rates of hemolysis were significantly different between the centrifugal VAD and axial VAD ($p=0.003$) and between the centrifugal VAD and HMII ($p=0.036$) (Figure 1).

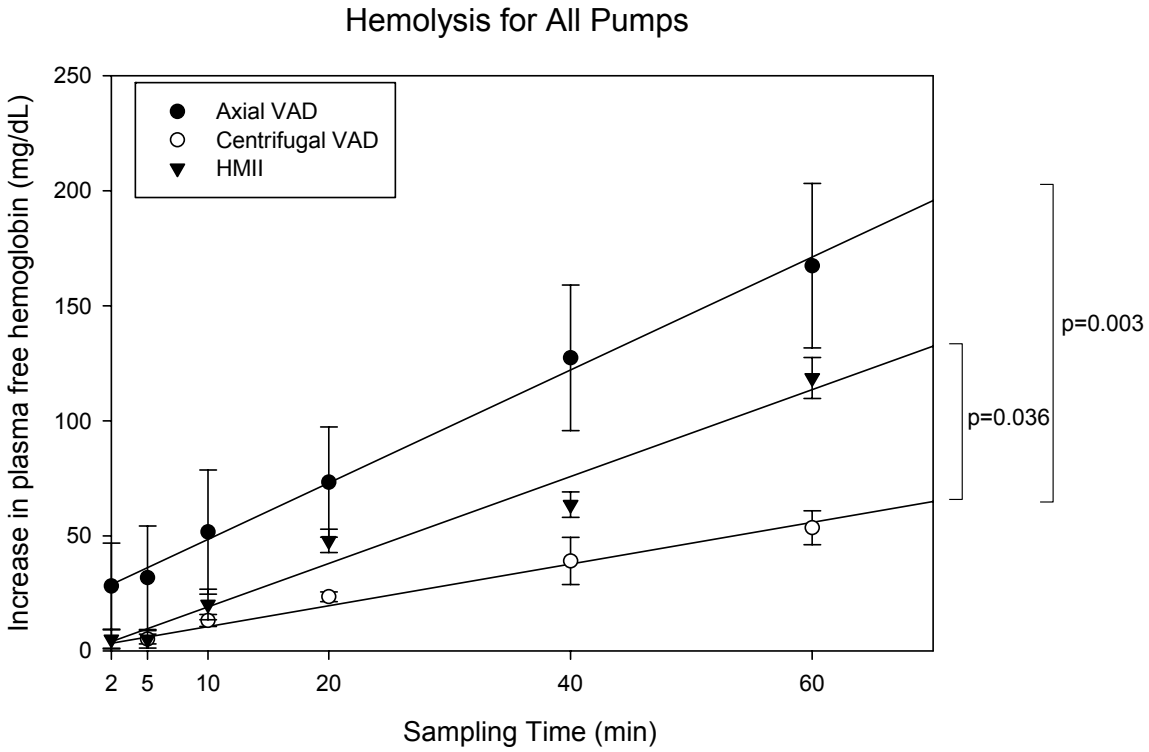

Figure 3.4. Increase in Plasma Free Hemoglobin Over Time. Data is presented as mean ± SEM. (Note: Axial VAD n=6, Centrifugal VAD n=5, HMII n=6)

The total hemolysis induced by the pump over the course of the experiment was calculated for each pump as:

$$Total\ Hemolysis = freeHb_{t=60} - freeHb_{t=0} \qquad \text{Eqn 3.3.}$$

There was a statistically significant difference between the axial VAD and centrifugal VAD total hemolysis (167.4 ± 87.6 vs. 53.5 ± 16.4 mg/dL, p=0.006) and between the centrifugal VAD and the HMII total hemolysis (53.5 ± 16.4 mg/dL vs. 118.6 ± 21.8 mg/dL, p=0.027).

The normalized index of hemolysis (N.I.H.) was calculated for each experimental run. Figure 3.5 shows the N.I.H. for each sample time and pump. N.I.H. is a measure of the change in the mass of free hemoglobin (grams) per 100L of blood pumped through the loop. The N.I.H. equation includes the

donor's hematocrit, the flow rate, and the circulation time and allows for a normalized comparison of pumps. As seen in the figure, the centrifugal VAD resulted in significantly lower N.I.H. that either of the two pumps. All pumps showed higher values of this parameter at short times with values decreasing with increasing circulation times.

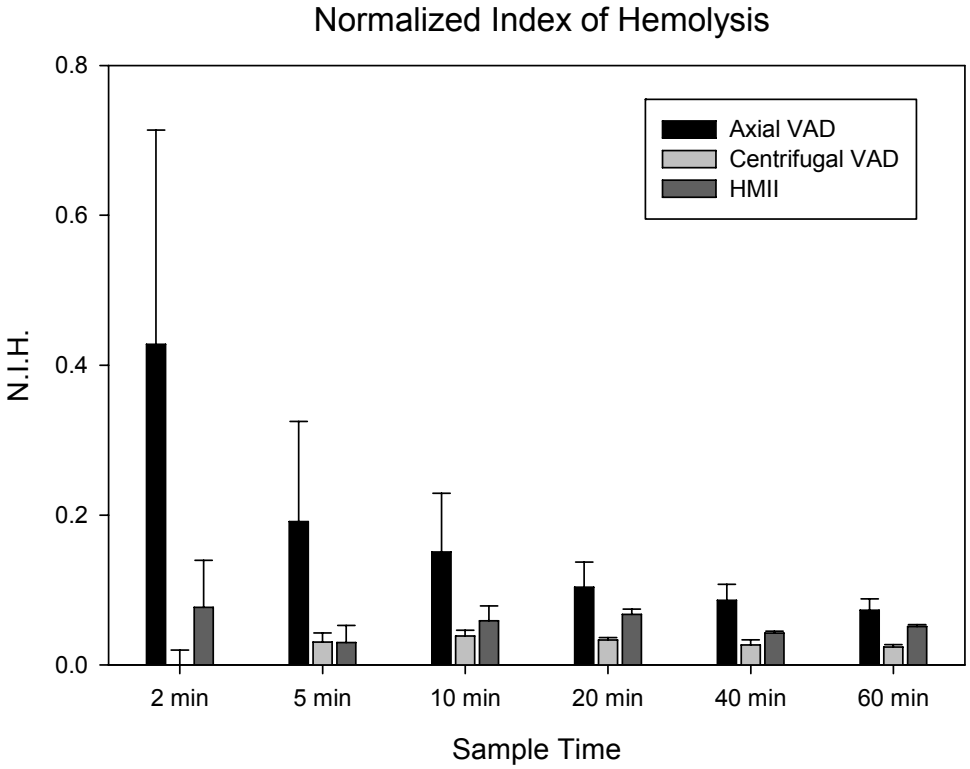

Figure 3.5. N.I.H. for Each Pump Over Time. Data is presented as mean ± SEM. (Note: axial VAD n=6, centrifugal VAD n=5, HMII n=6)

3.3.2 Platelet Activation Analysis Results. The total platelet concentration and platelet activation due to the pump were determined by flow cytometric analysis. The total platelet concentration was measured to evaluate loss of platelets due to possible microaggregate formation, accumulation within the pump/loop, or lysis. P-selectin (CD62P) is expressed by activated, degranulated platelets.

The total platelet concentration was not statistically significantly different at any of the time points as shown in figure 3.6. There was no difference observed among the various pumps.

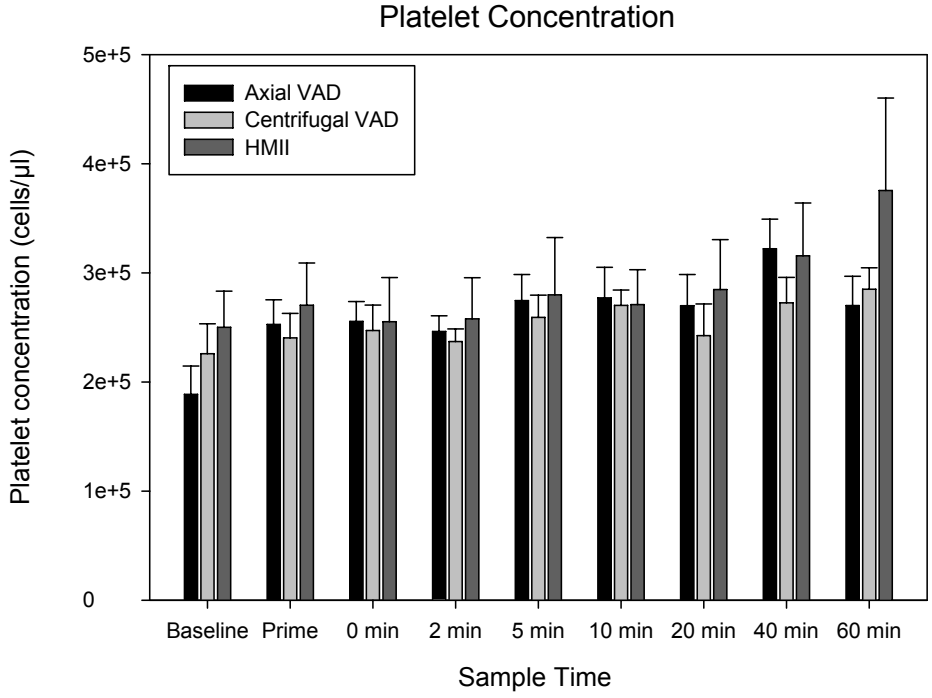

Figure 3.6. Platelet Concentration Over Time. Data is presented as mean ± SEM. (Note: axial VAD n=6, centrifugal VAD n=6, HMII n=6)

The results of the platelet activation analysis are shown in figure 3.7. This figure shows the percentage of P-selectin positive platelets over time. Thebaseline, prime and zero time points did not differ from one another indicating minimal activation due to the blood draw, the flow loop priming, and initiation of the pump.

Within the first two minutes of running the axial VAD, platelets went from a resting state of 5.5% to 11.3% P-selectin positive. The platelet activation peaked at 10 minutes. There was a significant increase from time 0 to 10 minutes (5.5 ± 3.6 vs. 11.6 ± 8.0%, p=0.03). By the end of the experiment (time 60), there was no significant difference with time 0 (5.6 ± 4.2 vs. 5.5 ± 3.6%, respectively).

No statistically significant changes in platelet activation were observed between the centrifugal VAD and the HMII. In the centrifugal VAD results, a small peak in the percent P-selectin positive platelets occurred at 20 minutes but it was not significant (4.6 ± 2.6% for time 0 vs. 6.3 ± 3.4% at 20 minutes). In addition, there was no significant difference between the time 0 and time 60 sample (4.6 ± 2.6 vs. 4.1 ±2.5%, respectively). The percentage of P-selectin positive platelets for the HMII did not show a peak over the course of the experiment, and there was no significant difference between the start and stop of the experiment (5.5 ± 3.1 vs. 3.6 ± 2.0%, respectively).

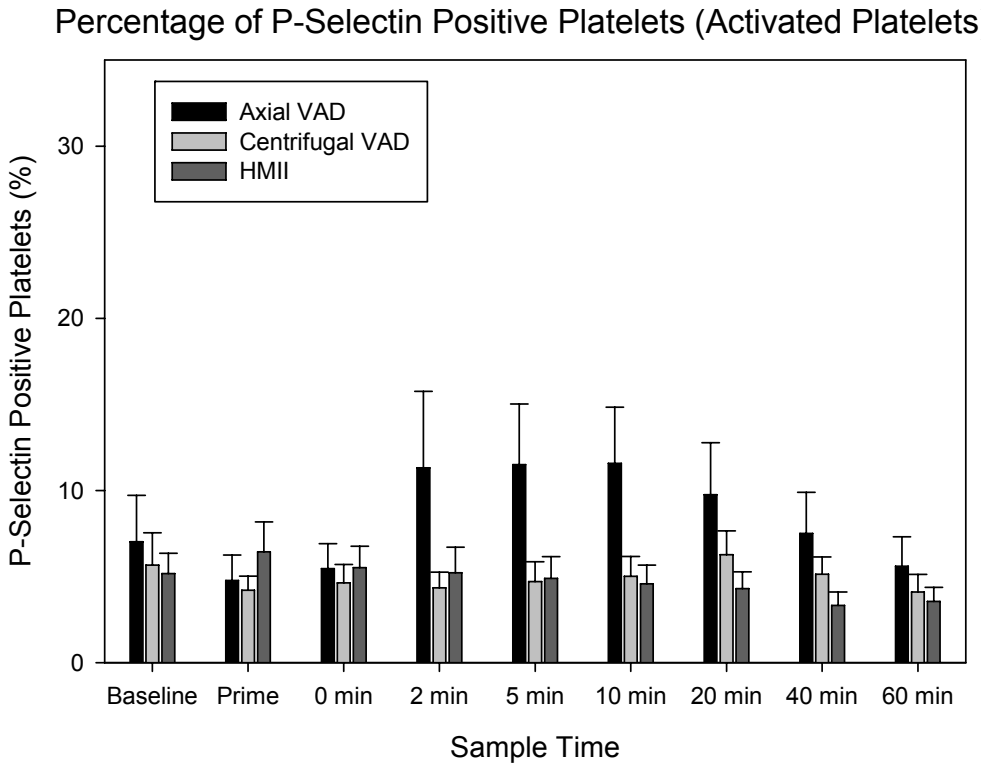

Figure 3.7. Change in Percent of Platelet Population that is P-selectin Positive Over Time. Data is presented as mean ± SEM. (Note: MVAD n=6, HVAD n=6, HMII n=6)

3.3.3 Platelet-rich Plasma Size Analysis Results. The size distributions of particulates in platelet-rich plasma were acquired using the Multisizer 3 Coulter Counter. These experiments allowed for assessment of changes in the size distribution of cellular components and accumulation of cellular debris and microparticles (MPs) as a result of the pump. As described in the methods, platelets were defined as the population peak between 1.6 μm and 4 μm and cell debris resulting from microparticle formation, shear stress-induced rupture, or membrane shedding was defined as counts below 1.6 μm.

The cell debris counts were quantified for each sampling time and each pump as a measure of blood cell trauma. In all three pumps, the cellular debris counts increased with time (Figure 3.8). Cell debris at time 0 was subtracted

from the cell debris at the end of the experiment (60 minutes) to determine the total amount of debris caused by the pump. There was a statistically significant difference in cell debris caused by the axial VAD when compared to the centrifugal VAD (188,000 vs. 54,400 counts respectively, p=0.047); however, there was no difference between the centrifugal VAD and the HMII or between the axial VAD and the HMII. The rates of cell debris formation (slopes of the linear regressions) did not differ significantly among the pumps.

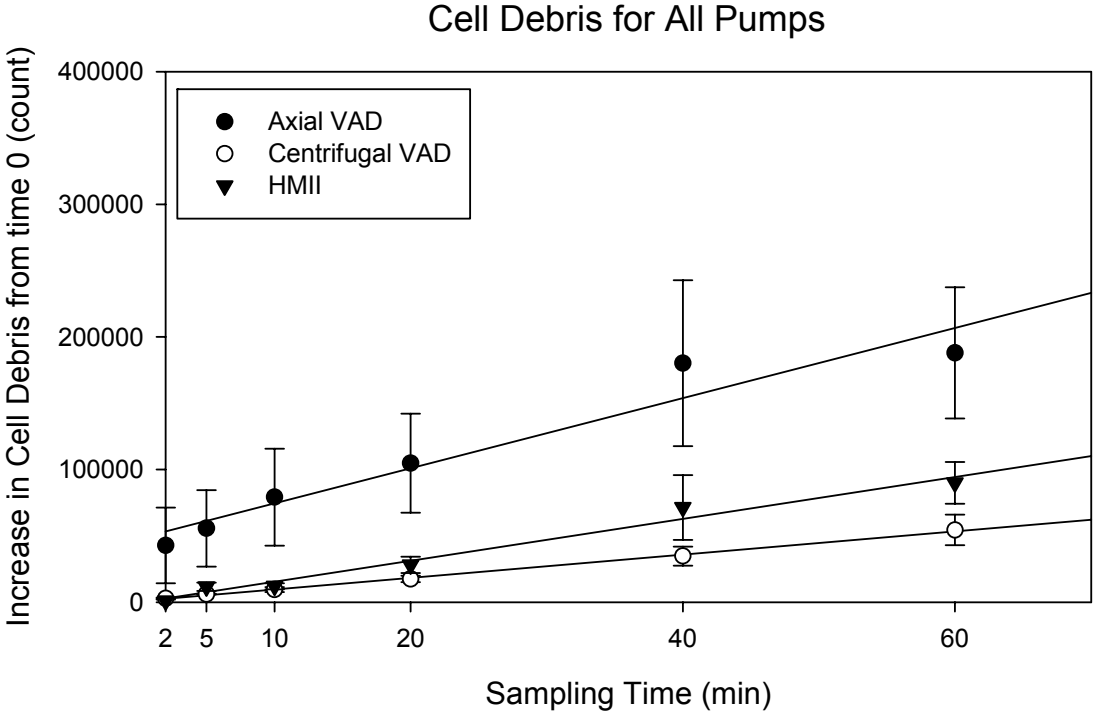

Figure 3.8. Increase in Cell Debris (particles < 1.599 µm) Over Time. Data is presented as mean ± SEM. (Note: axial VAD n=6, centrifugal VAD n=5, HMII n=5)

3.3.4 Von Willebrand Factor Multimer Analysis. VWF multimer molecular weight analysis by western blotting is a definitive method for demonstration and characterization of the composition of the VWF molecule and can to used diagnostically to determine the various types of von Willebrand's disease (vWD).

It allows for clear demonstration of multimeric composition; typically the large molecular weight multimers are required for normal hemostatic function.

The centrifugal VAD, HMII, and axial VAD all demonstrated increased degradation of large molecular weight multimers at the 10 and 60-minute time points. The axial VAD consistently demonstrated greater loss when compared to the centrifugal VAD and HMII; this difference is most evident at the 60-minute time point. The gels from all 6 donors are shown in Figure 3.9.

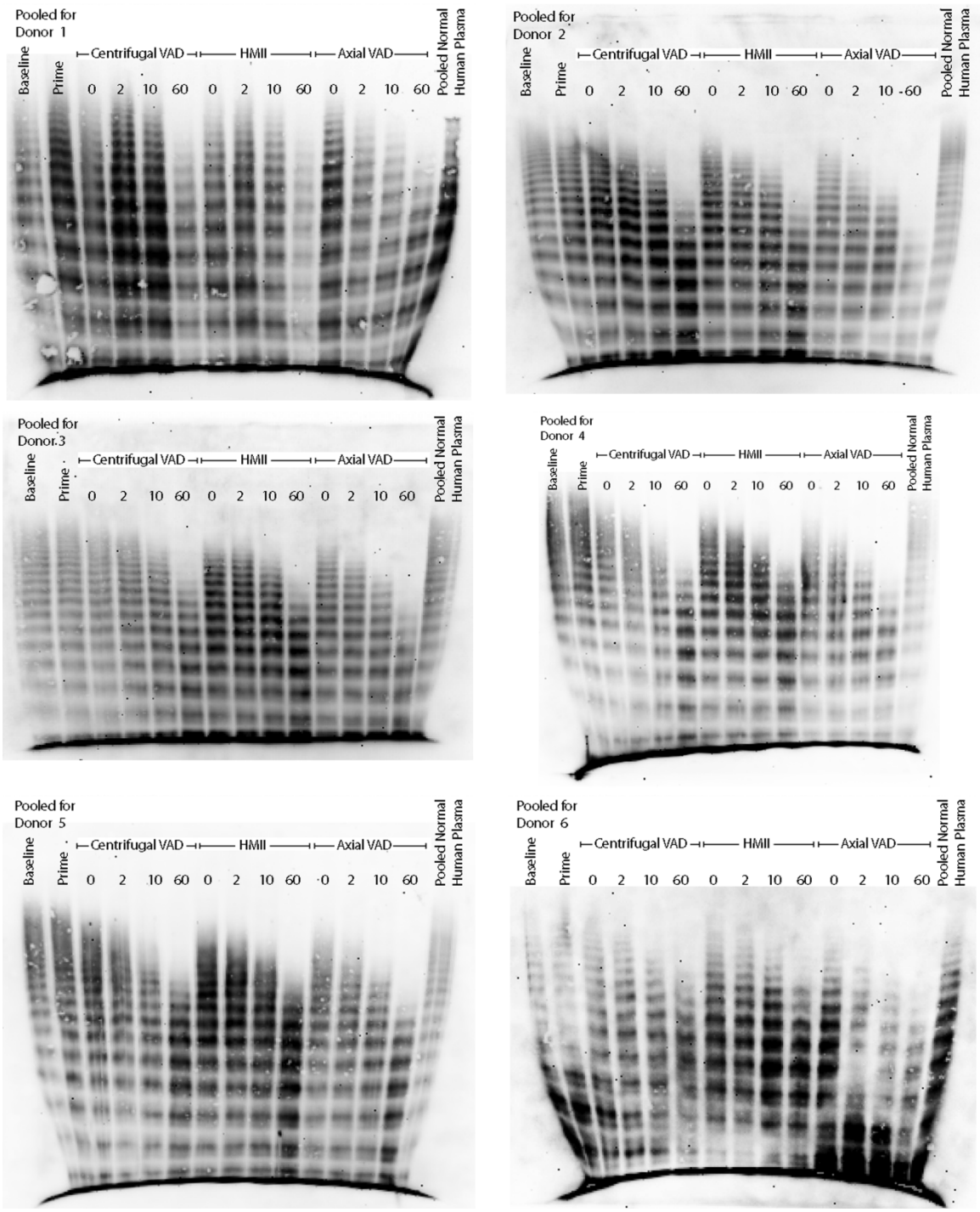

Figure 3.9. VWF Multimer Gels for All Donors. Higher molecular weight multimers are towards the top of the gels. Over time all pumps exhibit VWF degradation. The axial VAD exhibits more degradation than the other two, particularly evident at 60 minutes.

3.3.5 Observation of Deposit Formation. As part of the pump cleaning protocol, all cleaning materials were passed through a 400μm screen. This allowed for the observation of deposits formed within the pump or tubing at the end of the experiment. In one instance the centrifugal VAD had a small deposit in the pump. The HMII showed deposits in 4 of the 6 experiments, mostly associated with the pump. In one experiment with the HMII (donor 1), not all deposits that were observed were recovered. No deposits were observed in any of the axial VAD experiments. The deposit observations are summarized in Table 3.4. Example images of recovered deposits are shown in Figure 3.10.

Table 3.4. Observation of Deposits by Experiment and Location

	Centrifugal VAD	HMII	Axial VAD
Donor 1		Pump*	
Donor 2		Pump, Tubing	
Donor 3	Pump		
Donor 4		Pump	
Donor 5		Pump	
Donor 6			

- "Pump" indicates thrombus was recovered after back-flushing pump with PBS.
- "Tubing" indicates thrombus was recovered from interior surface of tubing.
- * Indicates instances where not all deposits that were observed were recovered

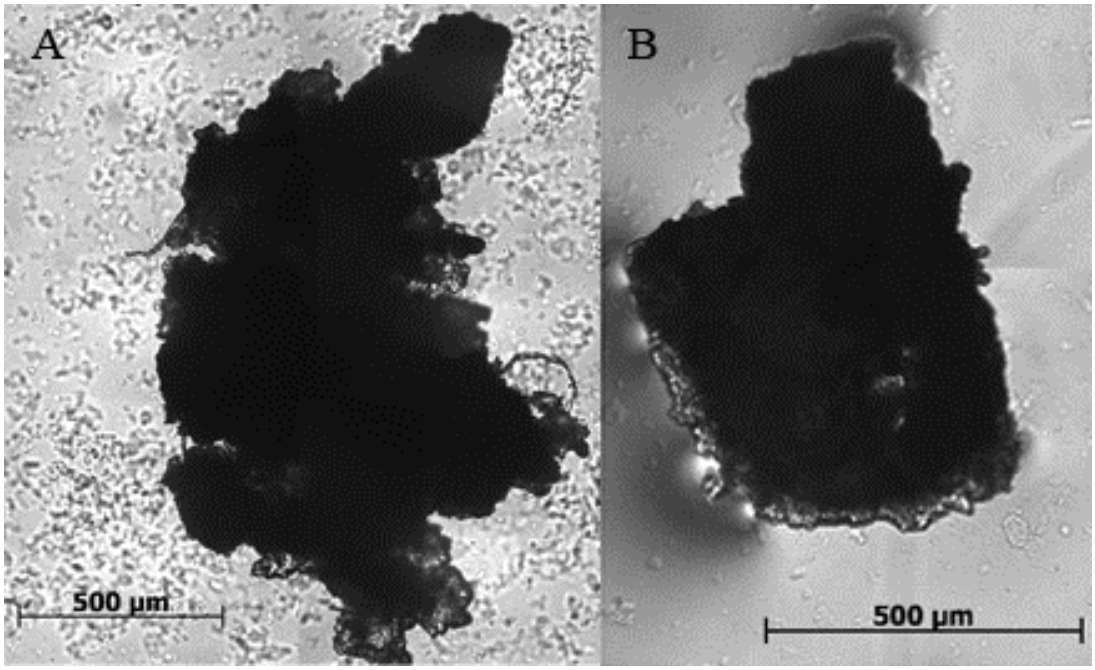

Figure 3.10. Images of deposits. These deposits were found in the pump/loop at the end of the experiment. (A) Deposit found in HVAD run. (B) Deposit found in a HMII run.

3.3.6 Coagulation Based Assays. Thromboembolic and bleeding events are pathophysiologic responses rooted in the hemostasis system. It is unclear whether these adverse events are primarily regulated by platelets or coagulation. For this reason, coagulation was evaluated within this system.

The conversion of prothrombin to thrombin is the point at which both the extrinsic and intrinsic coagulation cascades merge into the common pathway. Thrombin has many functions in hemostasis, including cleavage of fibrinogen to form fibrin, activation of FV and FVIII zymogens to form active coagulation enzymes, and activation of platelets (for details see section 1.6.1). As such, it is central to coagulation; however, it has a very short half-life before inhibition by antithrombin, which is enhanced by heparin, the anticoagulant used in this study.

Because of this surrogates of thrombin formation are necessary. Prothrombin fragment 1+2 (PT frag) is the inactive by-product of the conversion of prothrombin to thrombin.

PT frag was not found to increase over the course of the experiment for any of the pumps studied as shown in figure 3.11. However, when incubated for an additional three hours (four hours total from the start of the experiment) a statistically significant increase was seen for the HMII from 193.2 ± 114.4 for the baseline (4 hours) sample to 909.8 ± 431.6 for the drain (4 hours) sample as shown in figure 3.12. No statistically significant difference was observed with either third generation experimental VAD.

Tissue factor is the main endogenous initiator of the extrinsic pathway and generally sequestered within cells or the vessel wall separated from flowing blood. The presence of tissue factor within the plasma results in a hypercoagulable state which would result in a predisposition to thrombosis, a common complication of VAD therapy. Tissue factor was not increased at any time throughout the experiment or upon incubation, which would allow for increased production and expression (figures 3.13 and 3.14).

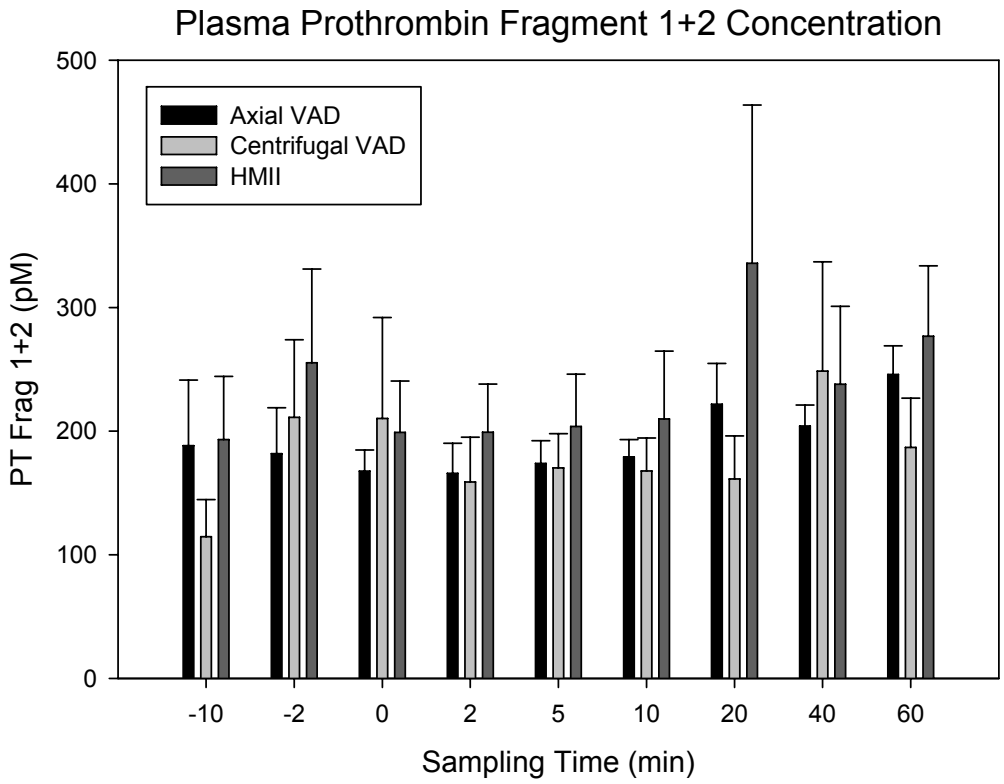

Figure 3.11. Prothrombin Fragment Concentration. PT frag was not found to vary over the course of the experiment.

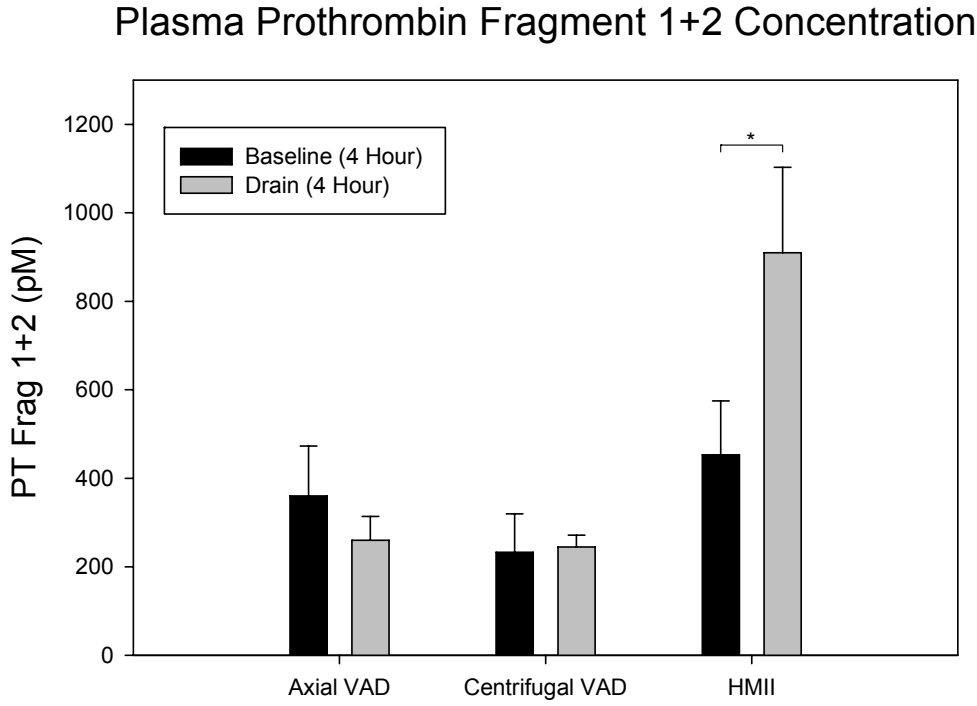

Figure 3.12. Prothrombin Fragment Concentration after Incubation. PT frag was statistically significantly increased for the HMII after incubation for 3 hours after the termination of the experiment, four hours from the start.

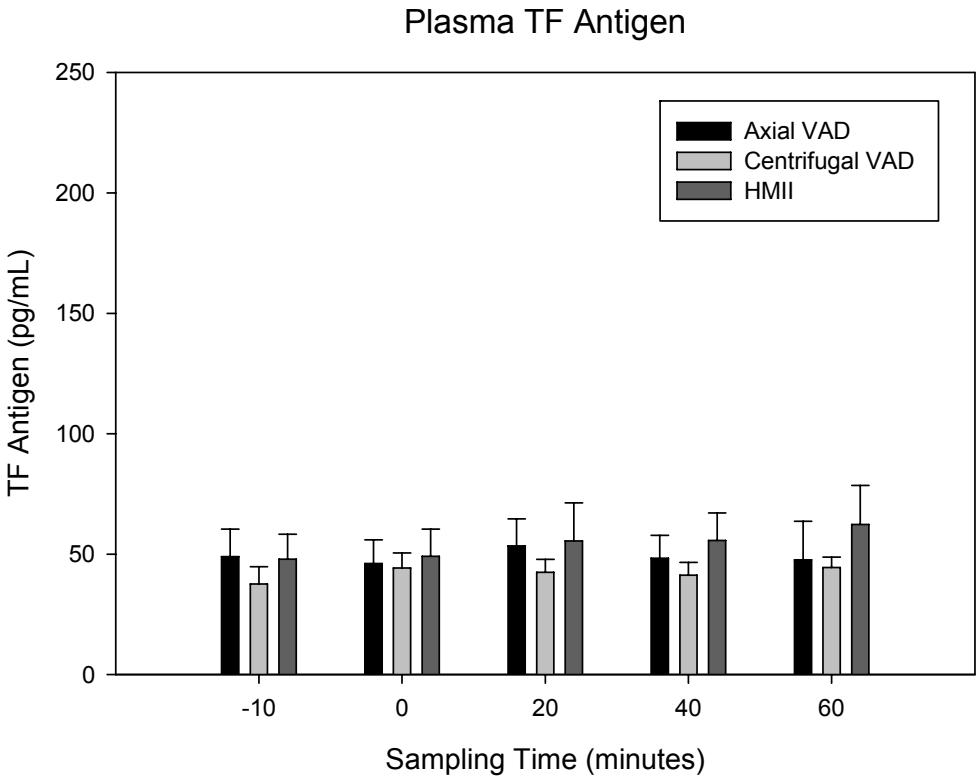

Figure 3.13. Tissue Factor Antigen. Tissue factor antigen was not found to change with any of the pumps studied.

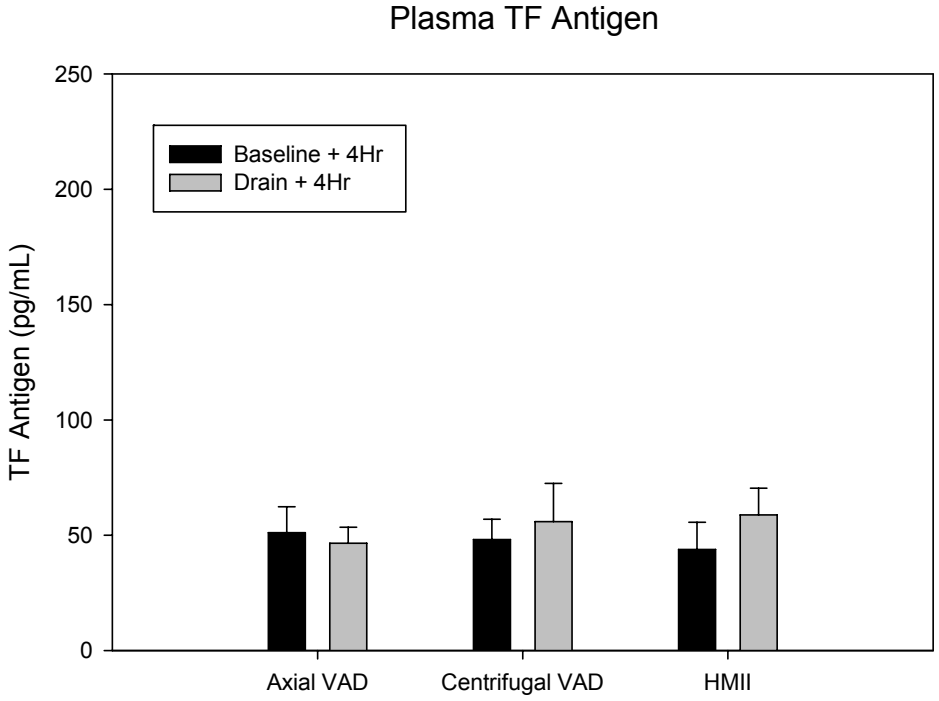

Figure 3.14. Tissue Factor Antigen Production. Tissue factor was not found to be unregulated as a result of the blood trauma caused by the pumps studied.

3.4 Discussion

This study shows that it is possible to stratify pump designs with regards to various hemostatic effects using direct comparison *in vitro* testing as summarized in table 3.5. The presence of deposits is likely indicative of increased thromboembolic complications. The HMII had the most instances of deposit formation. The HMII has several surfaces that could allow deposit formation. There are the contact bearings that are separated by a thin film of fluid in normal operations and the flow stators, which jut into the flowstream to straighten flows to and from the rotor. The secondary flow path of the centrifugal VAD could provide a low flow region with pathophysiologic shear stresses for activation of platelets and formation of a deposit. However a deposit in this region would most likely be released later in the washing procedure than was observed in this experiment. It is likely that it would be dislodged later in the washing procedure due to the small gap, which trapped air during the priming procedure and necessitated the jump-start.

Interestingly, despite increased p-selectin expression at early time points, no deposits were found in the axial VAD. This may be due to the combination of the high flow rate through the pump and this particular pumps distinct compact size and straightforward design allowing for adequate washing of all the surfaces to prevent deposition. Another possible explanation for the lack of deposition of platelets in the axial VAD could be the greater extent of VWF degradation. In the gel results, the greater extent of VWF degradation was most evident at the 60-

minute time point, which consistently showed fewer higher molecular weight bands (refer to section 3.3.4 and figure 3.9).

The increased degradation of VWF in the axial VAD may provide some additional protection against thrombus formation. As previously discussed, VWF is central to platelet thrombus formation, particularly at the high shear stresses characteristic of the pump environment. VWF is most active at the higher molecular weights multimers. This could mean that despite increased activation of platelets as measured by P-Selectin expression, aggregates are unable to form due to lack of HMW VWF.

Table 3.5. Summary of Results

	Centrifugal VAD	**HMII**	**Axial VAD**
Plasma Free Hemoglobin Assay	Lowest Rate of Hemolysis	Intermediate Rate of Hemolysis	Highest Rate of Hemolysis
Platelet Activation	No Significant Change	No Significant Change	Significant Increase *
Platelet Size Analysis	Lowest Rate of Cell Debris Formation	Intermediate Rate of Cell Debris Formation	Highest Rate of Cell Debris Formation
vWF Multimer Analysis	Degradation Increased with Time	Degradation Increased with Time	Degradation Increased with Time
Deposit Observation	1 of 6 runs	4 of 6 runs	0 of 6 runs
Coagulation	No Activation	Activation after 4 Hours	No Activation

Furthermore, previous studies have demonstrated the functional deficit in VWF-dependent platelet aggregation is associated with a change in both the platelets and plasma VWF (figure 3.15) [44]. The authors theorized VWF degradation products could inhibit HMW VWF activity. The combined result of axial pump's increased degradation of HMW VWF with the absence of deposits within the pump further support the hypothesis put forward in chapter two that degradation of HMW VWF in the absence of a bleeding diathesis may be protective against thrombotic events.

The results of these studies seem to indicate that thromboembolic and bleeding complications may be primarily due to platelet mediated responses. There was no up regulation of plasma tissue factor and no production of thrombin during the course of the experiment. Furthermore, the production of thrombin

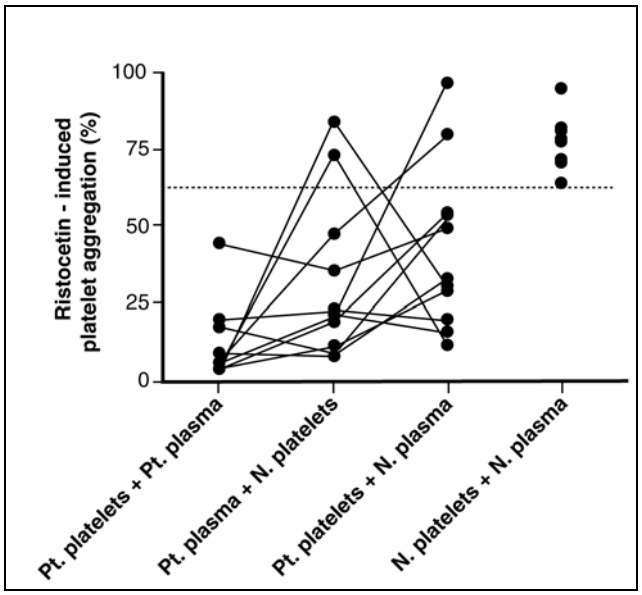

Figure 3.15. Inhibitory Effects of aVWD Associated with Platelets and Plasma. The Inhibitory effects of VADs associated acquired VWD are associated with both the patient's platelets (Pt. platelets) and the patient's platelets (Pt. plasma) in comparison to normal platelets/plasma (N. platelets and N. plasma).

that was observed after incubation may be due to the aggregation of platelets observed as evidenced by deposit formation (see section 3.3.5). Coagulation requires the positive feedback of the initial production of thrombin to amplify the production of enzymes necessary to amplify the coagulation response [57]. The additional time may have allowed thrombin conversion to proceed sufficiently for detection without resulting in the coagulation amplification. The inability to produce the amplification response may be due to the action of heparin and anti-thrombin III inhibiting thrombin.

These experiments, when compared to the *in vivo* experiments presented in chapter 2, were cheaper, faster, had fewer confounding factors, and can easily be expanded. While *in vivo* experiments will continue to be necessary, with these methodologies hemostatic effects may now be able to influence the design phase prior to beginning the arduous task of in vivo feasibility studies. Furthermore, the hemostatic effects observed in these experiments may be more reflective of what would be clinically relevant. Finally, more direct comparisons of pump designs are possible with such methodologies.

.

CHAPTER 4

SUMMARY AND FUTURE STUDIES

This thesis consists of two separate sets of experiments both directed at evaluating hemostatic/thrombotic complications induced by ventricular assist devices. The first set was integrated into feasibility studies performed in Tokyo, Japan. These experiments proved to be typical of in vivo experimentation in general and the interpretations of the findings were confounded by several complicating factors, which made conclusive analysis difficult. In general, these experiments were technically difficult, required significant man-hours (including 24-hour monitoring) and encountered numerous complications including infection, thromboembolic/bleeding complications and device malfunctions. While in vivo studies are absolutely necessary for the longer term evaluation of such pumps and will continue to be so, they are not particularly suitable for the evaluation of hemostatic variables that may play a role in pump behavior due to differences elucidated in chapter two of this thesis. An alternative methodology to evaluate pump design and elucidate hemostatic and thrombotic effects were developed and discussed in chapter three of this thesis. These experiments can easily be expanded to address specific questions and can be utilized more easily in the pump design process related to such variables.

4.1 Future Studies

The results of this thesis can be built upon with additional experimentation. The focus of future studies can be broken down into specific areas – assessment of additional commonly used animal models for ventricular assist devices; further

characterization of VWF degradation; additional assays and pump designs for further comparisons of pumps and elucidation of pump related pathologies.

4.1.1 Assessment of Additional Animal Models. Because animal models are already commonly used in feasibility studies, which will continue to be necessary, including hemostatic compatibility studies onto them would be beneficial. Most current studies are done in bovine animal models, although ovine animal models are also used. Evaluation of the ovine model for similar changes in platelet reactivity, specifically the presence of aVWD, is a necessary precondition to using these animals for hemostatic compatibility studies.

4.1.2 VWF Degradation. Further characterization of the degradation of VWF in response to shear stress, specifically at shorter time intervals and higher shear stresses more relevant to VADs, would aid in the design process. Additional characterization of the mechanisms of degradation under the ultrahigh shear stress, short contact times environment of the pump is needed. Little is currently known about whether the degradation is purely mechanical or mediated through enzymatic mechanisms – perhaps ADAMTS13 regulated. However, it could be due to a preferential consumption of HMW VWF, which could be examined by evaluation of the antigenic concentration of VWF within the *in vitro* experimental setup. Further characterization of the mechanisms of degradation could provide some insight into possible treatments for acute bleeding complications associated with VAD therapy. If increased degradation rates are indeed regulated by ADAMTS13, inhibition of ADAMTS13 would likely boost HMW VWF concentrations quickly because VWF is secreted constitutively. Finally,

additional measures of the “activity” of VWF could be added to the battery of assays run with the *in vitro* pump experiment; these would include the ristocetin cofactor assay, which measures agglutination of platelets in a VWF dependent manner, and the collagen binding assay, which measures the ability of VWF to bind collagen in an ELISA-type assay.

4.1.3 Additional *In Vitro* Studies. This experimental setup allows for easy expansion of the array of assays to address specific questions and allows for additional comparisons between designs. In light of the results presented in this thesis, the effect of pump designs on platelet function warrants additional study; whereas, additional study of the coagulation effects may not yield fruitful results. Additional characterization of microparticles with respect to their cellular origin could provide insight into which blood cells are predominantly being affected by the high shear stress environment. Furthermore, microparticles not only have potential biological activity which could be transferred to more benign surfaces, but also could impose a physical burden on the microvascular system if produced in large quantities; therefore, further characterization is warranted. These types of study could provide additional insights with clinical relevance due to the nature of the experimental design, as previously discussed.

4.2 Summary of Results and Implications

In the bovine animal model, a statistically significant increase in microparticle populations was not demonstrated. This could be due to the short half-life of microparticles *in vivo* (effective removal mechanisms). The *in vitro* study demonstrated microparticle formation might be a measure of blood trauma

presuming sufficient accumulation for detection. Additional studies are needed, preferably using clinical samples. Moreover, the reactivity of microparticles formed as a result of VAD therapy needs to be characterized. As previously discussed, microparticles have been shown to participate and propagate thrombosis *in vivo* and a number of reactive species have been demonstrated on microparticles including adhesive receptors/ligands. Microparticles could induce a hypercoagulable state, resulting in increased incidences of thromboembolic events. Additional studies are required and warranted based on initial studies.

This thesis has elucidated the ways in which the bovine animal model is insufficient for studying hemostatic alterations as a result of ventricular assist devices. Specifically, in the bovine animal model, VWF is not degraded *in vivo*, as has been demonstrated in humans. This could potentially explain decreased gastrointestinal bleeding events discussed previously, as discussed. Furthermore, the exact mechanism that protects bovine VWF from shear degradation is not yet characterized and could offer therapeutic hope for patients suffering from acquired VWD related bleeding complications. While both the bovine and human genes encoding for VWF precursors have been sequenced, and locations of differences noted [40], the functional impact of these differences has yet to be characterized.

Hemostasis is a complex balance between bleeding and thrombosis; any change in one direction could have implications for the other. Much of the recent studies demonstrating the presence of aVWD in patients with VADs have focused on the increased bleeding potential; however, if the aVWD were

corrected, it could result in increased thromboembolic events, such as thrombotic stroke. For patients using VADs as bridge-to-transplant, a thrombotic stroke nullifies eligibility for transplantation, resulting in a shift in patient status to destination therapy. In light of these findings, aVWD, in the absence of a bleeding diathesis, may not be as deleterious as previously thought.

Due to the insufficiency of the bovine animal model, a series of in vitro experiments to evaluate potential hemostatic complications as a result of basic design were developed to demonstrate alternative methodologies to compare pump designs. While these experiments do not alleviate the need for feasibility studies in animal models, they do provide a cheaper and more suitable method for evaluating potential hemostatic complications and making comparisons among designs. This methodology eliminates the need for interspecies extrapolation; increases the available assays and baseline values for comparison; and allows for direct comparison between designs using the same donor blood. Furthermore, because of the setup of these experiments, it is possible to expand and customize the assay set to address specific questions, which have not been addressed previously.

Finally, this study also demonstrated that most of the thrombotic complications are likely associated with the platelet side of the coagulation – as opposed to the coagulation side. This indicates that patients may respond more favorably to reduced antiplatelet over anticoagulation reduced therapy, particularly in the presence of bleeding complications. This result does not provide evidence for elimination of anticoagulation because of the short

experiment time in contact with artificial surfaces in the *in vitro* experiments compared to the long implant time with artificial surfaces in patients. It does provide some early basis to begin retrospective clinical studies with respect to the relative efficacy of anticoagulation versus antiplatelet therapy. That is to say, a retrospective analysis might be designed to stratify patients based on relative strength of anticoagulation and/or antiplatelet therapy to see if bleeding or thrombotic complications are increased or decreased in relative frequency.

BIBLIOGRAPHY

1. Alba, A.C. and Delgado, D.H., *The future is here: ventricular assist devices for the failing heart.* Expert Rev Cardiovasc Ther, 2009. 7(9): p. 1067-77.
2. Baldauf, C., et al., Shear-induced unfolding activates von Willebrand factor A2 domain for proteolysis. J Thromb Haemost, 2009. 7(12): p. 2096-105.
3. Biro, E., et al., Human cell-derived microparticles promote thrombus formation in vivo in a tissue factor-dependent manner. J Thromb Haemost, 2003. 1(12): p. 2561-8.
4. Boilson, B.A., et al., Device therapy and cardiac transplantation for end-stage heart failure. Curr Probl Cardiol, 2010. 35(1): p. 8-64.
5. Borchiellini, A., et al., Quantitative analysis of von Willebrand factor propeptide release in vivo: effect of experimental endotoxemia and administration of 1-deamino-8-D-arginine vasopressin in humans. Blood, 1996. 88(8): p. 2951-8.
6. Born, G.V., Aggregation of blood platelets by adenosine diphosphate and its reversal. Nature, 1962. 194: p. 927-9.
7. Brun-Hansen, H.C., Kampen, A.H., and Lund, A., *Hematologic values in calves during the first 6 months of life.* Vet Clin Pathol, 2006. 35(2): p. 182-7.
8. Cannegieter, S.C., Rosendaal, F.R., and Briet, E., Thromboembolic and bleeding complications in patients with mechanical heart valve prostheses. Circulation, 1994. 89(2): p. 635-41.
9. Crow, S., et al., Acquired von Willebrand syndrome in continuous-flow ventricular assist device recipients. Ann Thorac Surg, 2010. 90(4): p. 1263-9; discussion 1269.
10. Crow, S., et al., Gastrointestinal bleeding rates in recipients of nonpulsatile and pulsatile left ventricular assist devices. J Thorac Cardiovasc Surg, 2009. 137(1): p. 208-15.
11. Crow, S., et al., Comparative analysis of von Willebrand factor profiles in pulsatile and continuous left ventricular assist device recipients. Asaio J, 2010. 56(5): p. 441-5.
12. Davi, G. and Patrono, C., *Platelet activation and atherothrombosis.* N Engl J Med, 2007. 357(24): p. 2482-94.
13. Del Conde, I., et al., Tissue-factor-bearing microvesicles arise from lipid rafts and fuse with activated platelets to initiate coagulation. Blood, 2005. 106(5): p. 1604-11.
14. Delgado, A.V., et al., Antibodies against human cell receptors, CD36, CD41a, and CD62P crossreact with porcine platelets. Cytometry B Clin Cytom, 2003. 56(1): p. 62-7.
15. Deng, M.C., et al., Destination mechanical circulatory support: proposal for clinical standards. J Heart Lung Transplant, 2003. 22(4): p. 365-9.
16. Diamant, M., et al., Elevated numbers of tissue-factor exposing microparticles correlate with components of the metabolic syndrome in

uncomplicated type 2 diabetes mellitus. Circulation, 2002. 106(19): p. 2442-7.
17. Dolgin, M. and New York Heart Association. Criteria Committee., *Nomenclature and criteria for diagnosis of diseases of the heart and great vessels*. 9th ed. 1994, Boston: Little Brown. xiv, 334 p.
18. Dowling, R.D., et al., *The AbioCor implantable replacement heart.* Ann Thorac Surg, 2003. 75(6 Suppl): p. S93-9.
19. Fang, J.C., Rise of the machines--left ventricular assist devices as permanent therapy for advanced heart failure. N Engl J Med, 2009. 361(23): p. 2282-5.
20. Feys, H.B., et al., Thrombotic thrombocytopenic purpura directly linked with ADAMTS13 inhibition in the baboon (Papio ursinus). Blood, 2010. 116(12): p. 2005-10.
21. Flaumenhaft, R., *Formation and fate of platelet microparticles.* Blood Cells Mol Dis, 2006. 36(2): p. 182-7.
22. Frazier, O.H., et al., Right ventricle-sparing left ventricular resection and replacement with a continuous-flow rotary blood pump: an in vivo experiment. Tex Heart Inst J, 2010. 37(3): p. 276-9.
23. Gachet, C., *ADP receptors of platelets and their inhibition.* Thromb Haemost, 2001. 86(1): p. 222-32.
24. Garon, A. and Farinas, M.I., *Fast three-dimensional numerical hemolysis approximation.* Artif Organs, 2004. 28(11): p. 1016-25.
25. Gensch, C., et al., Late-breaking clinical trials presented at the American Heart Association Congress in Chicago 2010. Clinical Research in Cardiology, 2011. 100(1): p. 1-9.
26. George, J.N., et al., Isolation of human platelet membrane microparticles from plasma and serum. Blood, 1982. 60(4): p. 834-40.
27. George, J.W., Snipes, J., and Lane, V.M., *Comparison of bovine hematology reference intervals from 1957 to 2006.* Vet Clin Pathol. 39(2): p. 138-48.
28. Goldberg, L.R., *Heart failure.* Ann Intern Med, 2010. 152(11): p. ITC61-15; quiz ITC616.
29. Goldstein, D.J., Oz, M.C., and Rose, E.A., *Implantable left ventricular assist devices.* N Engl J Med, 1998. 339(21): p. 1522-33.
30. Gross, P.L., et al., Leukocyte-versus microparticle-mediated tissue factor transfer during arteriolar thrombus development. J Leukoc Biol, 2005. 78(6): p. 1318-26.
31. Guyton, A.C., Hall, J.E. Textbook of medical physiology. 11 Ed. 2006, Philadelphia, PA: Elsevier Saunders. xxxv, 1116 p.
32. Hayes, H.M., et al., Management options to treat gastrointestinal bleeding in patients supported on rotary left ventricular assist devices: a single-center experience. Artif Organs, 2010. 34(9): p. 703-6.
33. Heilmann, C., et al., Acquired von Willebrand syndrome in patients with ventricular assist device or total artificial heart. Thromb Haemost, 2010. 103(5): p. 962-7.

34. Holme, P.A., et al., Shear-induced platelet activation and platelet microparticle formation at blood flow conditions as in arteries with a severe stenosis. Arterioscler Thromb Vasc Biol, 1997. 17(4): p. 646-53.
35. Hoshi, H., et al., Disposable magnetically levitated centrifugal blood pump: design and in vitro performance. Artif Organs, 2005. 29(7): p. 520-6.
36. Hoshi, H., Shinshi, T., and Takatani, S., *Third-generation blood pumps with mechanical noncontact magnetic bearings.* Artif Organs, 2006. 30(5): p. 324-38.
37. Hubbell, J.A. and McIntire, L.V., Platelet active concentration profiles near growing thrombi. A mathematical consideration. Biophys J, 1986. 50(5): p. 937-45.
38. Jackson, S.P., *The growing complexity of platelet aggregation.* Blood, 2007. 109(12): p. 5087-95.
39. Jackson, S.P., Nesbitt, W.S., and Kulkarni, S., *Signaling events underlying thrombus formation.* J Thromb Haemost, 2003. 1(7): p. 1602-12.
40. Janel, N., et al., Comparison of the 5'-flanking sequences of the human and bovine von Willebrand factor-encoding genes reveals alternation of highly homologous domains with species-specific Alu-type repeats. Gene, 1995. 167(1-2): p. 291-5.
41. Jarvis, G.E., *Platelet aggregation: turbidimetric measurements.* Methods Mol Biol, 2004. 272: p. 65-76.
42. Johnson Jr, C.A., et al., Platelet Activation in Ovines Undergoing Sham Surgery or Implant of the Second Generation PediaFlow Pediatric Ventricular Assist Device. Artif Organs, 2011.
43. Keuren, J.F., et al., Microparticles adhere to collagen type I, fibrinogen, von Willebrand factor and surface immobilised platelets at physiological shear rates. Br J Haematol, 2007. 138(4): p. 527-33.
44. Klovaite, J., et al., Severely impaired von Willebrand factor-dependent platelet aggregation in patients with a continuous-flow left ventricular assist device (HeartMate II). J Am Coll Cardiol, 2009. 53(23): p. 2162-7.
45. Lahpor, J.R., *State of the art: implantable ventricular assist devices.* Curr Opin Organ Transplant, 2009. 14(5): p. 554-9.
46. Leiderman, K. and Fogelson, A.L., Grow with the flow: a spatial-temporal model of platelet deposition and blood coagulation under flow. Math Med Biol, 2010. 28(1): p. 47-84.
47. Leung, L. and Nachman, R., *Molecular mechanisms of platelet aggregation.* Annu Rev Med, 1986. 37: p. 179-86.
48. Lietz, K. and Miller, L.W., *Destination therapy: current results and future promise.* Semin Thorac Cardiovasc Surg, 2008. 20(3): p. 225-33.
49. Lin, P.J., *Reviewing the Reality: why we need to change.* European Heart Journal Supplements, 2005. 7(Supplement E): p. E15-E20.
50. Litwak, K.N., et al., Retrospective analysis of adverse events in preclinical ventricular assist device experiments. Asaio J, 2008. 54(4): p. 347-50.
51. Lloyd-Jones, D., et al., Heart disease and stroke statistics--2010 update: a report from the American Heart Association. Circulation, 2010. 121(7): p. e46-e215.

52. Loehr, L.R., et al., Heart failure incidence and survival (from the Atherosclerosis Risk in Communities study). Am J Cardiol, 2008. 101(7): p. 1016-22.
53. Makris, M., *Gastrointestinal bleeding in von Willebrand disease.* Thromb Res, 2006. 118 Suppl 1: p. S13-7.
54. Malehsa, D., et al., Acquired von Willebrand syndrome after exchange of the HeartMate XVE to the HeartMate II ventricular assist device. Eur J Cardiothorac Surg, 2009. 35(6): p. 1091-3.
55. Mallat, Z., et al., Elevated levels of shed membrane microparticles with procoagulant potential in the peripheral circulating blood of patients with acute coronary syndromes. Circulation, 2000. 101(8): p. 841-3.
56. Meyer, A.L., et al., Acquired von Willebrand syndrome in patients with an axial flow left ventricular assist device. Circ Heart Fail, 2010. 3(6): p. 675-81.
57. Monroe, D.M. and Hoffman, M., *What does it take to make the perfect clot?* Arterioscler Thromb Vasc Biol, 2006. 26(1): p. 41-8.
58. Mueller, J.P., et al., The CentriMag: a new optimized centrifugal blood pump with levitating impeller. Heart Surg Forum, 2004. 7(5): p. E477-80.
59. Nieuwland, R., et al., Cell-derived microparticles generated in patients during cardiopulmonary bypass are highly procoagulant. Circulation, 1997. 96(10): p. 3534-41.
60. Rand, M.L., et al., Rapid clearance of procoagulant platelet-derived microparticles from the circulation of rabbits. J Thromb Haemost, 2006. 4(7): p. 1621-3.
61. Rogers, J.G., et al., Chronic mechanical circulatory support for inotrope-dependent heart failure patients who are not transplant candidates: results of the INTrEPID Trial. J Am Coll Cardiol, 2007. 50(8): p. 741-7.
62. Rose, E.A., et al., Long-term use of a left ventricular assist device for end-stage heart failure. N Engl J Med, 2001. 345(20): p. 1435-43.
63. Sadler, J.E., *Biochemistry and genetics of von Willebrand factor.* Annu Rev Biochem, 1998. 67: p. 395-424.
64. Saeed, D. and Fukamachi, K., In vivo preclinical anticoagulation regimens after implantation of ventricular assist devices. Artif Organs, 2009. 33(7): p. 491-503.
65. Sakariassen, K.S., Bolhuis, P.A., and Sixma, J.J., Human blood platelet adhesion to artery subendothelium is mediated by factor VIII-Von Willebrand factor bound to the subendothelium. Nature, 1979. 279(5714): p. 636-8.
66. Savage, B., Saldivar, E., and Ruggeri, Z.M., Initiation of platelet adhesion by arrest onto fibrinogen or translocation on von Willebrand factor. Cell, 1996. 84(2): p. 289-97.
67. Schalm, O.W., *Veterinary hematology*. 2.ed. ed. 1965, Philadelphia: Lea & Febiger. 664 s.
68. Siedlecki, C.A., et al., Shear-dependent changes in the three-dimensional structure of human von Willebrand factor. Blood, 1996. 88(8): p. 2939-50.

69. Skipwith, C.G., Cao, W., and Zheng, X.L., Factor VIII and platelets synergistically accelerate cleavage of von Willebrand factor by ADAMTS13 under fluid shear stress. J Biol Chem, 2010. 285(37): p. 28596-603.
70. Slaughter, M.S., Long-term continuous flow left ventricular assist device support and end-organ function: prospects for destination therapy. J Card Surg, 2010. 25(4): p. 490-4.
71. Slaughter, M.S., et al., Advanced heart failure treated with continuous-flow left ventricular assist device. N Engl J Med, 2009. 361(23): p. 2241-51.
72. Slaughter, M.S., et al., HeartWare miniature axial-flow ventricular assist device: design and initial feasibility test. Tex Heart Inst J, 2009. 36(1): p. 12-6.
73. Snyder, T.A., et al., Platelet activation, aggregation, and life span in calves implanted with axial flow ventricular assist devices. Ann Thorac Surg, 2002. 73(6): p. 1933-8.
74. Solen, K.A., et al., Markers of thromboembolization in a bovine ex vivo left ventricular assist device model. Asaio J, 1994. 40(3): p. M602-8.
75. Soloviev, M.V., Okazaki, Y., and Harasaki, H., *Whole blood platelet aggregation in humans and animals: a comparative study.* J Surg Res, 1999. 82(2): p. 180-7.
76. Someya, T., et al., Development of a disposable maglev centrifugal blood pump intended for one-month support in bridge-to-bridge applications: in vitro and initial in vivo evaluation. Artif Organs, 2009. 33(9): p. 704-13.
77. Tan, K.T., et al., Clinically apparent atherosclerotic disease in diabetes is associated with an increase in platelet microparticle levels. Diabet Med, 2005. 22(12): p. 1657-62.
78. Thompson, K.A., et al., Review article: the new concept of interventional heart failure therapy--part 1: electrical therapy, treatment of CAD, fluid removal, and ventricular support. J Cardiovasc Pharmacol Ther, 2010. 15(2): p. 102-11.
79. Tominaga, R., Harasaki, H., and Golding, L.A., Blood coagulability and hematological changes in calves with chronic centrifugal biventricular bypass pumps. J Surg Res, 1994. 56(1): p. 13-9.
80. Truskey, G.A., Yuan, F., and Katz, D.F., *Transport phenomena in biological systems*. 2004, Upper Saddle River, N.J.: Pearson/Prentice Hall. xxi, 793 p.
81. Uriel, N., et al., Acquired von Willebrand syndrome after continuous-flow mechanical device support contributes to a high prevalence of bleeding during long-term support and at the time of transplantation. J Am Coll Cardiol, 2010. 56(15): p. 1207-13.
82. Watanabe, N., et al., Quantification of the secondary flow in a radial coupled centrifugal blood pump based on particle tracking velocimetry. Artif Organs, 2005. 29(1): p. 26-35.
83. Windberger, U., et al., Whole blood viscosity, plasma viscosity and erythrocyte aggregation in nine mammalian species: reference values and comparison of data. Exp Physiol, 2003. 88(3): p. 431-40.

84. Zhang, X., et al., Mechanoenzymatic cleavage of the ultralarge vascular protein von Willebrand factor. Science, 2009. 324(5932): p. 1330-4.